INVESTIGATION OF COPPER DEPOSITION ON STEEL IN MOLTEN COPPER CHLORIDE

By

RION DSOUZA

A Thesis Submitted in Partial Fulfillment of the Requirements for the Degree of

Master of Applied Science

in

Mechanical Engineering

University of Ontario Institute of Technology

Faculty of Engineering and Applied Science

Oshawa, Ontario, Canada

ABSTRACT

Hydrogen is considered as the most prominent candidate for clean energy generation. The Copper Chloride (Cu-Cl) cycle has been chosen as an effective cycle for production of hydrogen due to its comparatively lower operating temperatures and cost. While most materials subjected to the molten Cu-Cl environment are bound to corrode, stainless steel (SS) materials are coated with a layer of copper. This thesis study is primarily aimed at understanding the phenomenon of copper deposition on steel and also investigating the possibility of using this layer as a protective barrier against corrosion. Experiments are conducted with SS material being tested in molten Cu-Cl at 500^0C for different immersion durations. Sol-gel coating methods are also tested for their ability to withstand the harsh Cu-Cl environment. Results show that, both the substrate and the copper coatings obtained, disintegrate as the immersion duration in molten Cu-Cl is increased. The sol-gel coating method also fails owing to its high porosity levels. It is concluded that since the iron in steel has more affinity towards chloride ions, it most likely reacts with molten copper chloride to form iron chloride thus leading to the formation of copper layer on its surface. This layer of copper is weak and discontinuous and cannot be construed to behave as a protective barrier against corrosion.

Keywords: Hydrogen; Cu-Cl cycle; corrosion; stainless steel; copper deposition; sol-gel coating

ACKNOWLEDGEMENTS

First and foremost I would like to acknowledge and extend my heartfelt gratitude to both my supervisors, Prof. Dr. Ibrahim Dincer and Prof. Dr. Ghaus Rizvi for believing in me and giving me this ever so valuable opportunity of pursuing research. Dr. Ibrahim Dincer has always been an inspiration to me and many others, with the way he conducts himself and also by his ebullient nature. His ability to propel his students to the limit in order to bring out the best in them and make them realize their true potential is a trait that not many possess. Although he has achieved a lot in science, his passion and enthusiasm to pursue more is of great motivation to all his students and fellow researchers. Dr. Ghaus Rizvi has also been a driving force to me throughout my research. His ability to impart the right suggestions, wisdom and guidance has been extremely beneficial throughout my journey. I would like to take this opportunity to wish both Dr. Ibrahim Dincer and Dr. Ghaus Rizvi the best in their future endeavours.

The efforts and guidance provided to me by Dr. Calin Zamfirescu, throughout my voyage as a master's student, was extremely helpful and for this I express my sincere appreciation and gratitude to him. Dr. Calin never seized to amaze me with his ideas about science and in general the world. I would also like to thank Mr. Mudit Nijhawan who helped me get acquainted with the lab and also made sure that my transition to being a researcher was smooth.

I would like to thank Dr. Larry Pershin and Sal Boccia from University of Toronto for their assistance with the SEM and EDX analysis of my samples. Dr. Larry was very welcoming and readily accepted me into his lab and made sure that I had all the resources needed for my work at UofT. I would also like to thank Mr. Peter Kahr at UOIT for his assistance with the fabrication of my samples. The assistance provided by Mr. Burak Yuzer and Mr. Ghassan Chehade towards coating of my samples via the Sol-gel method was instrumental in my work and for this I extend my sincere appreciation to them. The assistance received from Shuja Azhar, my predecessor in this work is also highly appreciated. Finally I would like to thank all the members of CERL and the ACE 3030 lab for their valuable support, both direct and indirect, and wish them all the success in the future.

Last but not the least I would like to thank my loving parents for their constant encouragement and support. They have brought me up with good values and for this I will remain ever so grateful to them.

TABLE OF CONTENTS

LIST OF FIGURES

LIST OF TABLES

NOMENCLATURE

A	Area (m^2)
D	Density (kg/m^3)
F	Faraday's constant (96485.33 C/mol)
i	Diffusion current (A)
i_L	Limiting diffusion current (A)
P	Power (W), Pressure (kPa)
n	No. of transferred electrons
t	Time (s)
R	Gas constant (kJ/kmol-K)
T	Absolute temperature (K)
V_a	Over voltage (V)
V_c	Concentration potential (V)
V_T	Combined potential (V)
w	Weight (kg)

Greek Letters

α	Transfer coefficient
β	Half-cell constant
Δ	Difference
η	Efficiency

Acronyms

AAS	Atomic Absorption Spectroscopy
Al_2O_3	Aluminum Oxide (Alumina)
APS	Air Plasma Spraying
ASTM	American Society for Testing and Materials
CERL	Clean Energy Research Laboratory
CS	Carbon Steel
CPR	Corrosion Penetration Rate
Cu-Cl	Copper Chloride
$Cu\text{-}Cl_2$	Cupric Chloride

CVD	Chemical Vapour Deposition
CYSZ	Ceria Yttria Stabilized Zirconia
DEA	Di-ethanolamine (DEA)
EBC	Environmental Barrier Coatings
EDTA	Ethylene Diamine Tetra Acetic acid
EDX	Energy Disperse X-ray Spectroscopy
EIS	Electrochemical Impedance Spectroscopy
EMIM	1-Ethyl-3-methylimidazolium
EMF	Electro Motive Force
FCEV	Fuel Cell Electric Vehicles
FTIR	Fourier Transform Infrared Spectroscopy
HCl	Hydro-Chloric Acid
HVOF	High Velocity Oxygen Fuel
ITV	Immersion Test Vessel
MCS	Medium Carbon Steel
MCrAlY	M= Nickel, Cr= Chromium, Al= Aluminum, Y=Yttrium.
Ni-Cr	Nickel Chromium
OECD	Organization for Economic Cooperation & Development.
PPE	Personal Protective Equipment.
PSZ	Partially Stabilized Zirconia
PVD	Physical Vapour Deposition
SBF	Simulated Body Fluid
SEM	Scanning Electron Microscopy
SHS	Super Hard Steel
SS	Stainless Steel
UOIT	University of Ontario Institute of Technology
XRD	X-Ray Diffraction
YSZ	Yttria Stabilized Zirconia

CHAPTER 1: INTRODUCTION

1.1 Hydrogen as an energy carrier

Clean energy generation has been at the forefront of ideas in many countries across the world. Extensive research is being carried out in order to determine methods for reducing carbon emissions. Efforts are also being made to clean up the existing carbon footprint in the Earth's atmosphere. Wind, solar, hydro and geothermal energies have been identified as the main contributors for clean energy generation. However, the intermittent nature and seasonal variability severely limits the usefulness of clean energy sources. This results in an inconsistency in the production of energy and therefore there is a need to store the energy produced from clean/renewable sources and nuclear sources. Lately, scientists have identified Hydrogen as the most clean and prominent energy carrier as it is abundantly available in our environment. Hydrogen fuel is a zero-emission fuel when burned with oxygen. Although it is just being introduced in the market as a transportation fuel, many countries and industries are working towards safe, clean and economical hydrogen production and distribution for widespread use such as in treating metals, producing fertilizers, fuel cell electric vehicles (FCEVs) etc.

One of the most challenging aspects of employing hydrogen as a clean energy carrier comes from being able to efficiently extract it from compounds such as water, hydrocarbons and other organic matter. Producing hydrogen from renewable energy sources is the best method considered for supplying the energy requirements of hydrogen society. Sustainable development involves a stream of energy resources which are readily available at reasonable costs and has either minimal or zero adverse effects on its surroundings. Hydrogen can also be produced from a variety of feedstock consisting of various types of fossil resources, such as natural gas and coal, as well as renewable resources, such as solar, wind, etc. Currently, steam reforming i.e combining high-temperature steam with natural gas to extract hydrogen, accounts for the majority of the hydrogen produced .

Dincer and Acar (2015) studied various methods for the production of hydrogen and inferred that hydrogen produced from nuclear waste heat is the cleanest. Figure 1.1 illustrates the possible methods of hydrogen production.

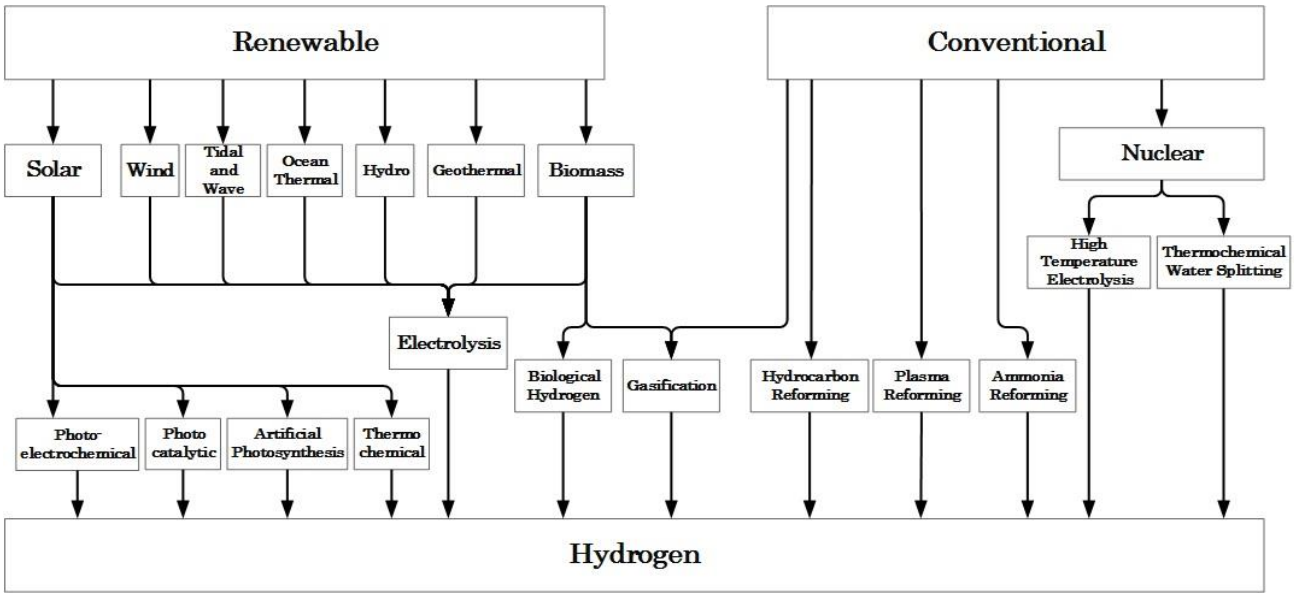

Fig. 1.1 Various renewable and nuclear sources based hydrogen production methods (Adapted from Bicer, 2015)

Numerous solar thermochemical water-splitting cycles (nearly 300) have been investigated for hydrogen production, each with different sets of operating conditions, engineering challenges, and hydrogen production opportunities. Two examples of thermochemical water splitting cycles, the "direct" two-step cerium oxide thermal cycle and the "hybrid" copper chloride cycle, are illustrated in Figure 1.2. Typically direct cycles are less complex with fewer steps, but they require higher operating temperatures compared with the more complex hybrid cycles (U.S Dept. Of Energy, 2015)

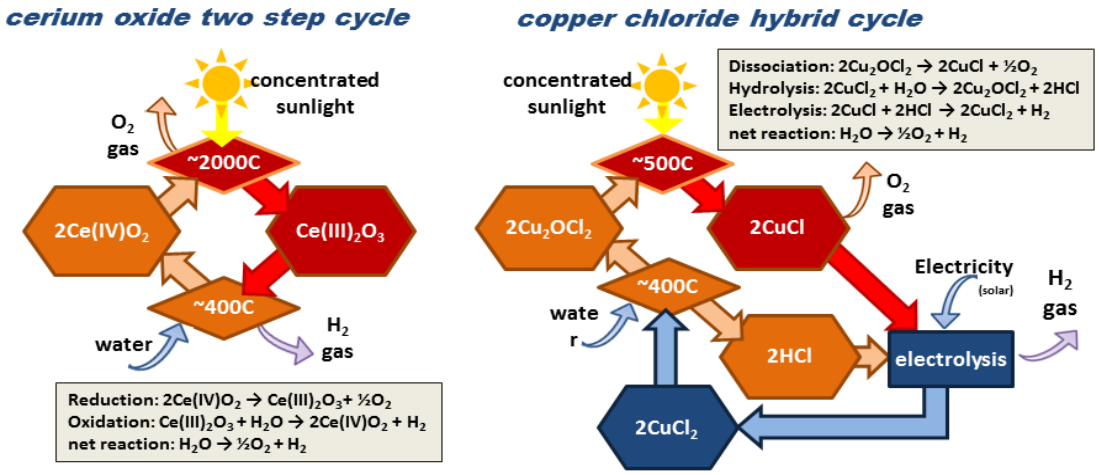

Fig. 1.2 Examples of thermochemical water splitting cycles (Adapted from U.S Department Of Energy,2015)

1.2 The Cu-Cl Cycle

To produce hydrogen on a large scale, an efficient cycle is required. Amongst the various thermo-chemical cycles, Cu-Cl cycle requires less heat input and it works on a relatively lower maximum temperature (500^{o}C) (Lewis et al., 2009). The four step Cu-Cl cycle splits water into oxygen and hydrogen by a sequence of reactions in a closed internal loop.

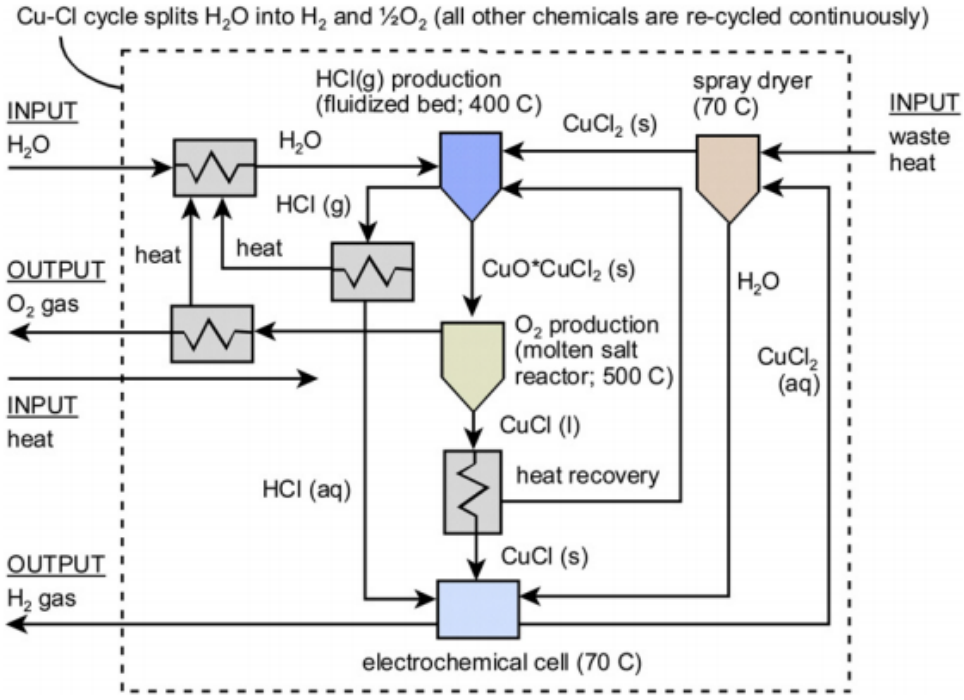

Fig. 1.3 Schematic of the four step Cu-Cl cycle (Naterer et al., 2010)

Table 1.1 – Reaction steps of Cu-Cl cycle (Naterer et al., 2010)

Step	Reaction	Temperature Range (^{o}C)
1	2 CuCl (aq) + 2HCl (aq) ⟶ H_2 (g) + 2$CuCl_2$ (aq)	<100 (electrolysis)
2	$CuCl_2$ (aq) ⟶ $CuCl_2$ (s)	<100
3	2 $CuCl_2$ (s) + H_2O (g) ⟶ $CuO*CuCl_2$ (s) + 2HCl (g)	400
4	$CuO*CuCl_2$ (s) ⟶ 2CuCl (l) + ½ O_2	500

At first, Cu-Cl reacts with HCl to produce cupric chloride (Cu-Cl_2) and hydrogen gas (H_2) (Magali et al., 2009). The aqueous Cu-Cl_2 is then converted into a solid by drying it. Then it is sent to a fluidized bed reactor where waste heat, input water and solid Cu-Cl_2 is combined together to produce HCl and copper oxychloride (CuO*Cu-Cl_2) (Magali et al., 2009). In a molten salt reactor,

$CuO*Cu\text{-}Cl_2$ is decomposed to yield molten cuprous chloride (Cu-Cl) and oxygen. The only inputs in this cycle are water and heat. Other chemicals are recycled and reused, thereby, keeping them in a close internal loop. The highest temperature in a Cu-Cl cycle is at the molten salt reactor i.e 500 degree Celsius.

1.3 Thesis Motivation

The use of hydrogen as a clean energy generation medium has captivated the attention of countries across the globe. Hydrogen is a benign entity with no adverse environmental effects. This has prompted for an increase in its use as a fuel. However, major hindrances are encountered during the production of hydrogen through the Cu-Cl cycle. The corrosion of materials subjected to the harsh Cu-Cl environment at designated temperatures is a major impediment in the scientific progress of creation of large scale Cu-Cl plants. Edwin (2012), Kaveh (2014) and Shuja (2016) conducted experiments on different materials by immersing them in a Cu-Cl bath at 500^0C under inert conditions and tested them for their integrity. Samples made up of different materials and shapes were coated with a wide range of protective coatings and were tested in molten Cu-Cl for their ability to resist corrosion within the harsh Cu-Cl environment. Shuja (2016) also conducted tests with Stainless steel materials coated with MCrAlY (M= Nickel, Cr= Chromium, Al= Aluminum, Y=Yttrium) and Yttria Stabilized Zirconia (YSZ) by the physical vapour deposition (PVD) method. Results showed that, even in this case the coatings were unable to adhere to the surface. However, Scanning Electron Microscopy (SEM) and Energy Dispersive X-ray spectroscopy (EDX) results for these tests indicated that the layer of coating was replaced with a continuous layer of copper which is a motivation for the current research. Hence this thesis is focused on the replication of the continuous copper layer coating and investigating the possibility of using it as a protective barrier against corrosion.

1.4 Thesis Objectives

Experiments carried out on ceramic coated Stainless Steel samples in molten Cu-Cl by Shuja (2016) showed that the protective coating layer was replaced with a uniform and continuous layer of copper. Hence the main aim of this thesis is to investigate the possibility of formation of such layer of copper and test it for its ability to behave as a protective barrier against corrosion for different immersion durations.

The specific objectives of this thesis study are as listed below:

- To test Stainless Steel and Carbon Steel samples in molten Cu-Cl at 500^0C and replicate the formation of the copper layer coating. It was previously observed that a layer of copper a coating was formed on the surface of steel materials immersed in molten Cu-Cl. This formation was a cause for investigation and hence the first step in this thesis study is to replicate the formation of this layer.
- To investigate the formation of copper coatings on the surface of the steel substrate. This objective aims at deducing the cause of formation of copper on the surface of steel substrates immersed in molten Cu-Cl. A thorough analysis of the conditions and the chemical reactions leading to this formation is to be investigated.
- To test the effects of immersion durations on the behavior of the copper coating. Upon replication of the copper layer formation it is necessary to test this layer at different immersion durations and temperature in order to have an understanding of its behavior at varying conditions. Hence this objective aims at observing the behavior of the copper coating for varying inputs of temperature and time.
- To analyze the strength and uniformity of the copper layer obtained. This objective aims at deducing the strength of the copper layer formed for different immersion durations in order to determine its ability to behave as a protective coating. The coating's ability to avoid disintegration, during prolonged exposure to molten Cu-Cl is to be tested.
- To coat metal samples with protective coatings such as Alumina (Al_2O_3) and Yttria Stabilized Zirconia (YSZ) via the sol-gel method and test the efficiency of the coatings in molten Cu-Cl at 500^0C. In this case the sol-gel coating method is observed for its porosity levels and also tested for its ability to behave as corrosion barrier in the harsh Cu-Cl environment. The performance of the sol-gel method as compared to other conventional coating methods like High velocity Oxygen Fuel (HVOF) method and Air Plasma Spraying (APS) method is to be recorded.
- To analyze SEM and EDX results of the samples, post immersion and determine the strength and uniformity of the copper layer obtained, interpretation of these results in terms of the copper layer's ability to behave as a protective coating layer against corrosion. Further, the integrity of the substrate is to be analyzed.

CHAPTER 2: BACKGROUND AND LITERATURE REVIEW

The purpose of this section is to have a thorough review of the past work that has been done in relation to the formation of copper deposits on steel materials in the presence of molten salts. Although not much work has been carried out in this field, efforts are being made to include a conglomeration of all related research that follow similar principles. The different types of coatings investigated as well as Sol-gel coating method is described in detail in the following sections.

2.1 Background

The following subsections provide an introduction of the corrosion theories and the factors leading to disintegration of materials in corrosive environments. A preliminary understanding of these phenomena becomes imperative in order to interpret the tests and findings observed in this thesis study. Further, a thorough review of the work leading to this research has also been mentioned. The different coating methods used and the results obtained have been discussed.

2.1.1 Corrosion

Corrosion is basically defined as the deterioration of materials due to their chemical interaction with the environment. Deteriorative mechanisms are different for different material types. In metals, there is actual material loss either by dissolution or by the formation of non-metallic scales or films. Ceramic materials are relatively resistant to deterioration which usually occurs at high temperatures. Polymers are mainly associated with the term degradation as the mechanisms and consequences differ from those of metals and ceramics (Callister, 2006).

2.1.2 Corrosion Electrochemistry

In metallic materials, the corrosion process is generally electrochemical, wherein the transfer of electrons takes place from one chemical species to another through a chemical reaction. Metal atoms lose electrons in a reaction named as oxidation reaction. The site at which oxidation takes place is called the anode and hence oxidation is may be referred to as anodic reaction. The electrons generated from metal atoms that are oxidized must be transferred to and become part of another chemical species. This reaction is termed as reduction reaction.

The following is an example of oxidation and reduction reactions:

$$Fe \longrightarrow Fe^{2+} + 2e^{-} \text{ (Oxidation)} \quad (2.1)$$

$$2H^{+} + 2e^{-} \longrightarrow H_2 \text{ (Reduction)} \quad (2.2)$$

$$Fe + 2H^{+} \longrightarrow Fe^{2+} + H_2 \text{ (Overall Reaction)} \quad (2.3)$$

2.1.3 Cell Potentials

It is observed that not all metals oxidize to form ions with the same degree of ease. For example, if copper and iron electrodes are connected electrically with both being in their ionic solution of 1M concentration, the reduction reaction will occur in the copper electrode at the expense of oxidation in the iron. Cu^{2+} ions will electrodeposit as metallic copper on the copper electrode, while iron corrodes at the other end of the cell and enters the electrolytic solution as Fe^{2+} ions. The half-cell reactions are represented as follows:

$$Fe \longrightarrow Fe^{2+} + 2e^{-} \text{ (Oxidation)} \quad (2.4)$$

$$Cu^{2+} + 2e^{-} \longrightarrow Cu \text{ (Reduction)} \quad (2.5)$$

However, when zinc and iron electrodes are connected electrically with both electrodes being in their ionic solution of 1M concentration, the zinc in this case acts as the anode and undergoes oxidation and the iron acts as cathode and undergoes reduction. The overall electrochemical reaction is as follows:

$$Fe^{2+} + Zn \longrightarrow Fe + Zn^{2+}$$

For all combinations of electrodes an electric potential will be generated between the two half cells and its magnitude can be determined by connecting a voltmeter in the external circuit. The potential difference between the electrodes is the driving force that causes the redox reactions. The standard EMF series provides data on different electrodes stating their ability to oxidize or reduce for different electrode combinations.

2.1.4 Rate of Corrosion

The rate of corrosion or corrosion penetration rate (CPR) may be defined as the thickness loss of material per unit time. The CPR is given by the following relation:

$$\mathrm{CPR} = \frac{87.6\mathrm{w}}{\mathrm{DAt}} \qquad (2.6)$$

where, w is Weight loss in (mg), D is the density in g/cm^3, A is area of the specimen (inch^2) and t is the exposure time (hr), CPR is corrosion penetration rate (mm/year)

2.1.5 Kinetics of Corrosion

The kinetics of corrosion provides an understanding of the concept of corrosion rates. The following are the different terminologies used to determine the rate of corrosion

2.1.5.1 Polarization

Polarization can be defined as the change in the standard electrode potential resulting from a net current. Its magnitude is quantified in terms of overvoltage. Overvoltage, V_a, is a measure of polarization with respect to the equilibrium or standard potential of an electrode. The net oxidation and reduction processes occur at the interface between the electrode and the electrolyte, which results in a displacement of the electrode potentials from their equilibrium potentials. This deviation from is called Polarization.

2.1.5.2 Activation Polarization

Electrochemical reactions consist of a series of steps that occur in a particular order between the electrode and the electrolyte. Activation polarization refers to electrochemical reactions that are controlled a particular step in the sequence of reactions that occur at the slowest rate. The term activation is used in this type of polarization since an activated energy barrier is associated with this slowest, rate limiting step. The relationship between the current density (i) and overvoltage for activation polarization is:

$$\mathrm{Va} = \pm\beta \log \frac{\mathrm{i}}{\mathrm{io}} \qquad (2.7)$$

where V_a is overvoltage, β and i_o are constants for a particular half-cell.

2.1.5.3 Concentration Polarization:

This type of polarization exists when the reaction rate is limited by diffusion in the solution. For example, in a hydrogen evolution reduction reaction, at low reduction rates the distribution of hydrogen ions adjacent to the electrode surface is relatively adequate. At very high reduction rates the region adjacent to the electrode surface will become depleted of hydrogen ions. When the reduction rate is increased further, a limiting rate will be reached that is obtained by the diffusion

rate of hydrogen ions to the electrode surface. This limiting rate is the limiting diffusion current density i_L. The equation for this type of polarization, considering no activation polarization, is:

$$\mathrm{Vc} = 2.3 \frac{RT}{nF} \log\left(1 - \frac{i}{i_L}\right) \quad (2.8)$$

Where V_c is concentration polarization, n is no. of transferred electrons, R is gas constant, F is Faraday's constant, T is absolute temperature.

2.1.5.4 Combined Polarization:

Both activation and concentration polarization usually occurs at an electrode. Activation polarization occurs at lower reaction rates whereas concentration polarization occurs at higher reaction rates. The total polarization is the sum of activation and concentration polarization.

$$V_T = \mathrm{Va} + \mathrm{Vc} \quad (2.9)$$

2.1.6 Corrosion Prevention Methods

Several methods may be used for corrosion prevention based on their stated application. Some of these methods are enlisted below:

- Cathodic protection.
- Use of non-corrosive materials (such as alloys)
- Corrosion inhibitors.
- Plating.
- Corrosion resistant coatings.

As the environment in a Cu-Cl cycle is harsh and enclosed, creation of an artificial protective environment may not be feasible. The use of cathodic protection may also not be advisable as the current needed for cathodic protection may interfere with the Cu-Cl leading to varying results. Corrosion inhibitors may also react with the Cu-Cl to form undesirable compounds. However using non-corrosive materials and corrosion resistant coatings are plausible solutions for mitigating the level of corrosion in a Cu-Cl environment.

2.1.7 Corrosion Resistant Coatings

Corrosion resistant coatings protect metals against degradation due to oxidation or exposure to environment. The coatings act as a barrier that shield the underlying base metal from the corrosive environment. Metallic and ceramic coatings can be used for corrosion prevention. Metallic coatings

can be grouped as cathodic coating and anodic coding. In relation to steel, Silver, Nickel, Chromium and Lead are cathodic while Zinc and Cadmium are anodic in most environments.

2.1.8 Coating Methods

Various methods can be used to apply coatings on a substrate. Thermal sprays, physical vapour deposition (PVD), chemical vapour deposition (CVD) and paint applications are some methods used to apply coating. PVD and CVD are very highly expensive and are not readily available, whereas, paints cannot withstand high temperatures. The thermal spray methods are the most economical and efficient methods for this application. Gas turbine blades and boiler tubes are coated using thermal spray method in order to prevent corrosion (Pan et al., 2016). The coating methods are selected mainly based on factors such as porosity, density, bond strength and coating cost etc.

2.1.9 Thermal Spraying

Thermal spray method is a coating method in which a semi molten material is sprayed onto the substrate at a high temperature and large impact velocity. Coating material is usually melted using electric means or by the combustion of fuels. Metals, ceramics, alloys and plastics are the coating materials that are usually used for spraying. The quality of the coating is evaluated by its bond strength, porosity level and surface finish. The coating quality can be increased with the increase of particle velocity. The various types of thermal spray methods used are as follows:

- Air Plasma Spraying (APS)
- High velocity oxy-fuel coating spraying (HVOF)
- Detonation spraying
- Wire arc spraying
- Flame spraying
- Warm spraying
- Cold spraying

As the coating methods used in the thesis study leading to this research were HVOF and APS, a brief of these 2 methods has been explained in the following sections:

2.1.9.1 Air Plasma Spraying

The mechanism of APS is shown in the Figure 2.1. Plasma spay is produced by subjecting a gas to a high intensity electromagnetic field to a point up to which the ionized gaseous substance becomes

increasingly conductive. The coating powder is injected in line with the plasma through a port which makes the powder melt. This mixture is then made to strike the surface of the substrate at a high temperature and impact velocity. During plasma spraying, the particles travel at a velocity of 150-300 m/s. The porosity level of ceramic coatings with plasma sprays are 1-2% and the bond strength lies between 21-41 MPa (Vidal et al., 2016). This molten powder sticks to substrate and subsequently solidifies to form a strong coating layer. The APS method can generate temperature up to 16000K (Metco, 2016).

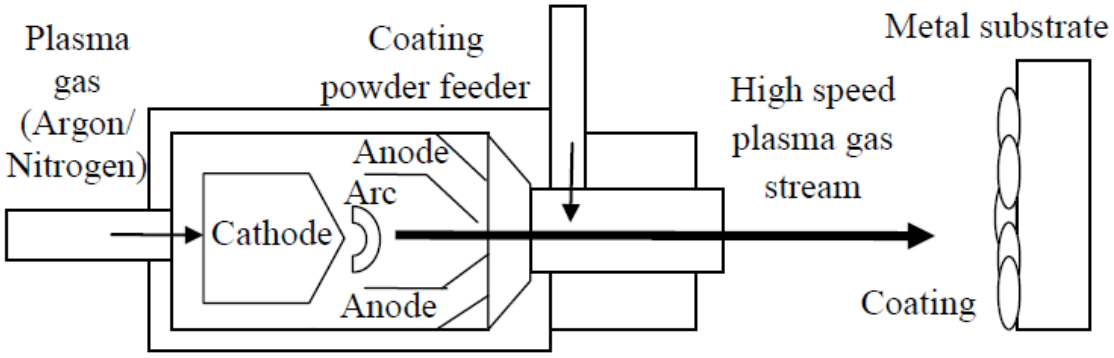

Fig. 2.1 Air plasma Spray System (Modified from Edwin, 2012)

2.1.9.2 High Velocity Oxy-fuel

HVOF is another thermal spraying method which involves melting of a coating powder and spraying it onto the substrate material. In this case a high temperature, high pressure gas is produced by combustion of fuel with oxygen. Molten or semi-molten powder combined with the high pressure gas is accelerated through a nozzle and impinged on the surface of the substrate where it gets solidified, forming a smooth coated layer with a lamellar structure (Mahesh et al., 2007). The HVOF method is cost effective, flexible and has a superior quality of coating (Stokes and Looney, 2014). The porosity for coatings with HVOF method is less than 2% and its bond strength lies between 48-62 MPa (Vidal et al., 2016).

As this method has higher particle impact velocity and lower particle temperature when compared to the air plasma spray method, the coatings produced in this case have higher density, bond strength and toughness (Li et al., 2016) Schematic of the HVOF thermal spray gun is shown in Figure 2.2.

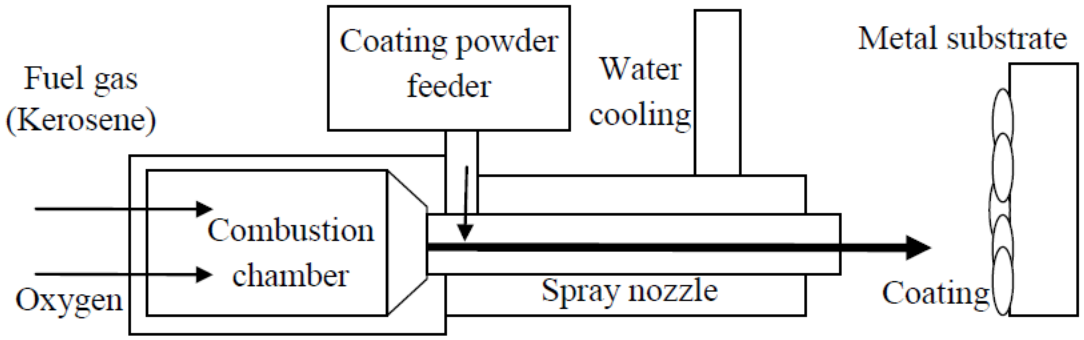

Fig. 2.2 HVOF Thermal Spray System (Modified from Edwin, 2012)

2.1.10 Evaluation of Coatings

Edwin (2012) tested different materials for their corrosion resistance capacity when immersed in copper chloride at 500 degree Celsius. Inconel 625 and Super Austenitic stainless steel (AL6XN) were used as base metals. Diamalloy 4006 was used as bond coat. A ceramic coat of YSZ and alumina were used as secondary top layers. The base metals were tested with different combinations of bond and secondary top layer coatings. The coatings were sprayed using the thermal spray method and coin shaped samples were used for testing.

Fig. 2.3 Coin shaped sample geometry by Edwin (2012)

Inconel 625 is known to have a high nickel content and hence was expected to behave strongly against corrosion. The secondary top layers were added as a shield to protect the base layer from coming in direct contact with the molten Cu-Cl whereas the bond coats were added to improve the adhesive strength between the base metal and secondary top layer coatings. The bond coats also served as dual purpose coatings to protect the base metal from corroding.

The Table 2.1 indicates eleven sets of combinations of base metal, adhesive coatings and top later coatings were tried and tested by Edwin (2012)

Table 2.1 Coating combinations tested by Edwin (2012).

Sr. No.	Samples	Abbreviation
1	Bare (Uncoated) Inconel 625	In625
2	Bare (Uncoated) Stainless steel AL6XN	SS
3	Inconel 625 coated with Diamalloy 4006 coating	InDi
4	Stainless Steel AL6XN coated with Diamlloy 4006 coating	SSDi
5	Inconel 625 coated with Diamalloy 4006 and YSZ coatings	InDiYS
6	Inconel 625 coated with Diamalloy 4006 and Alumina coatings	InDiAl
7	Stainless Steel AL6XN coated with Diamlloy 4006 and YSZ coatings	SSDiYS
8	Stainless Steel AL6XN coated with Diamlloy 4006 and Alumina coatings	SSDiAl
9	Inconel 625 coated with YSZ coatings	InYS
10	Stainless Steel AL6XN with YSZ coatings	SSYS
11	Stainless Steel AL6XN with Alumina coatings	SSAl

Upon completion of the tests it was observed that none of the coatings were able to adhere to the base metals at elevated temperatures. This phenomenon was observed due to the high porous nature of thermal spray coatings and also presence of sharp edges in the samples. As expected, the Inconel 625 outperformed Austentic stainless steel in terms of corrosion and Diamalloy 4006 and YSZ coating provided better corrosion protection than alumina (Al_2O_3 $3TiO_2$) to the base metal. It was also observed that the bare portions of the SS samples wherein coatings fell off were covered with deposits of copper (Edwin 2012)

Kaveh (2014) investigated the performance of different coatings on samples immersed in molten Cu-Cl. As the prime focus was to determine the coating performance, the original base metal (Inconel 625) was replaced by a rather inexpensive metal i.e mild carbon steel was selected as the base metal. Further, the geometry of the samples was also modified to incorporate more curved surfaces whilst eliminating the presence of any sharp edges. This was done to ensure better coating adherence to the surface of the base metal. Bullet shaped samples with a threaded hole at the center were fabricated and coated using the thermal spray method.

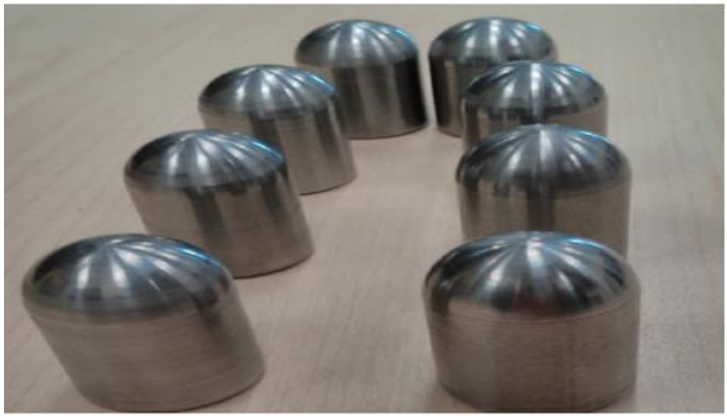

Fig. 2.4 Bullet shaped sample geometry by Kaveh (2014).

Kaveh (2014) studied the performance of YSZ coatings in molten Cu-Cl while using Diamalloy 4006 and Superhard Steel 9172 as bond coats. The Table 2.2 indicates the six sets of combinations of base metal, bond coats and top later coating were tried and tested by Kaveh (2014)

Table 2.2 Coating combinations tested by Kaveh (2014).

Sr. No.	Sample Name	Abbreviation
0	Bare (uncoated) medium carbon steel – 1045	Mild
1	Medium carbon steel (1045) coated with YSZ coating	YSZ
2	Medium carbon steel (1045) coated with Diamalloy 4006 and YSZ coating	Dia + YSZ
3	Medium carbon steel (1045) coated with SHS 9172 coating	SHS
4	Medium carbon steel (1045) coated with Diamalloy 4006	Dia
5	Medium carbon steel (1045) coated with SHS 9172 and YSZ coatings	SHS + YSZ

The results showed that the YSZ coatings were unable to withstand the conditions in the molten Cu-Cl owing to the high porosity in the coatings. The coating thickness was also found to be insufficient. The combination of Diamalloy and YSZ was tested for 48 hours and was observed to have a better corrosion resistance. The YSZ layer was delaminated but the layer of Diamalloy remained intact. Similar results were obtained when Superhard steel 9127 was employed as a bond coat.

In addition to the coatings employed by Kaveh (2014), Shuja (2016) included Aluminium Oxide as a secondary top layer of ceramic. Shuja (2016) also modified the geometry of the samples to include curved surfaces on both ends of the metal samples. This was done to avoid presence of

any sharp edges as it was previously inferred that cracks developing at any sharp edges would progress to other areas as well.

Fig. 2.5 Sample geometry with both sides rounded Shuja (2016)

The Table 2.3 indicates the seven sets of combinations of base metal, bond coats and top later coatings were tested by Shuja (2016)

Table 2.3 Coating combinations tested by Shuja (2016)

Sr. No.	Combination details	Abbreviation
0	Medium Carbon Steel (1045) – (Uncoated)	MCS
1	Medium Carbon Steel (1045) coated with Diamalloy 4006 - bond (YSZ top)	MCSDiYS
2	Medium Carbon Steel (1045) coated with SHS - bond (Al_2O_3 top)	MCSHSAl
3	Medium Carbon Steel (1045) coated with Diamalloy 4006	MCSDi
4	Medium Carbon Steel (1045) coated with SHS - bond coat (YSZ top)	MCSHSYS
5	Medium Carbon Steel (1045) coated with Bond Diamalloy 4006 (top Al_2O_3)	MCSDiAl
6	Medium Carbon Steel (1045) coated with SHS-9172	MCSHS

The results from the tests showed that the SHS coating combinations (SHS, SHS+YSZ, SHS+Al_2O_3) were unable to withstand the high temperature Cu-Cl environment, i.e all the SHS coating combinations were unable to adhere to the substrate. The high porous nature of the coatings led to the penetration of Cu-Cl, causing it to react with the substrate. Both YSZ and Alumina were unable to shield the underlying SHS bond coat and the metal substrate. In contrast the coating combinations of Diamalloy 4006 (Diamalloy, Diamalloy+YSZ, Diamalloy+Al_2O_3) performed much better than the SHS coating combinations. The portions of coats that were left adhered to the surface was a lot more compared to the SHS coating combinations. Deposits of copper were formed in regions where the molten Cu-Cl reacted with the metal substrate. It was inferred that thermal spray and HVOF coating methods were highly porous in nature and produced inefficient coatings.

2.2 Literature Review

Srinivasan et al. (1988) studied the formation of copper deposits on steel articles dipped in acid copper sulphate solution through galvanic displacement. The copper deposits obtained were porous and non-adherent. A suitable complexing agent was added to the solution in order to obtain clear and adherent deposits of copper on steel. The effect of immersion time on the thickness of the deposit and the potential-time behavior of the steel electrode with and without the incorporation of complexing agent was studied. The effect of temperature on potential-time behavior was also reported.

The range of conditions under which the reactions were to occur in order to obtain adherent, bright and reasonably continuous coatings on more active base metals were framed as follows:

- The electrolyte had to dissolve the base metal without the formation of oxides, insoluble salts or other products which would hinder contact with the surrounding ions.
- Attack of the base metal by the electrolyte had to be non-vigorous, resulting in a suitable substrate or lattice on which the depositing metal could develop a continuous structure.
- The deposition rate on the noble metal ion had to be regulated such that its lattice structure would be filled in as orderly a fashion as possible.
- The driving force (EMF) had to be sufficiently low to meet the above requirements.

The immersion deposit of copper formed on steel from simple acidic copper solutions were fragile and non-adherent. Direct copper plating of steel from acid sulphate solution using allyl thiourea as the inhibitor was studied. The displacement of copper on steel from sulphate solutions was also reported. Bright adherent copper deposit on steel was obtained using copper sulphate, ethylene diamine tetra acetic acid and wetting agent.

The experimental setup included mild steel samples that were mechanically finished to mirror finish. The samples were degreased with trichloroethylene electro cleaned in alkali and washed with water. Later, they were pickled in 10% v/v hydrochloric acid at a temperature of 313K for one minute. Initial experiments were carried out by the incorporation of various complexing agents such as ethylene diamine tetra acetic acid (EDTA), glycine, di-ethanolamine (DEA), tartaric acid, in copper sulphate and sulphuric acid electrolyte. Of them, tartaric acid was found to be very effective in producing smooth, adherent and bright coatings on steel substrates. Hence, further experiments were carried out using copper sulphate (100 g/l), sulphuric acid (35 g/ 1) and tartaric

acid (80 g/l) in distilled/deionized water. The prepared panels were weighed, and immersed in the copper solution for 1 to 8 minutes, washed well, dried and reweighed. The weight loss due to pickling was taken into account in determining the amount of copper deposited by chemical displacement. Experiments were conducted with and without the incorporation of complexing agent. The adhesion of the coating was tested.

Their results showed that the deposition rate of copper was almost constant in the solution having no complexing agent but the deposit is non-adherent and flaky. Addition of a complexing agent increased the rate of copper deposition resulting in a smooth, adherent and bright copper deposit. The main reactions taking place during the immersion deposition of copper on steel were as follows

$$Fe + Cu^{2+} \longrightarrow Fe^{2+} + Cu \quad (2.10)$$

$$Fe + 2H^{+} \longrightarrow Fe^{2+} + H_2 \quad (2.11)$$

The poor adhesion of copper was due to evolution of hydrogen gas. However addition of the complexing agent suppressed the evolution of hydrogen gas on mild steel resulting in a stronger deposit of copper.

Based on the studies it was concluded that the conditions needed for obtaining a bright and adherent deposit of copper on steel were $CuS0_4$ 100 g/l, tartaric acid - 80 g/l, H_2S0_4 35 g/l with a temperature of 298 to 308K.

Saravanan et al. (2013) studied the nucleation of copper on mild steel dipped in copper chloride (Cu-Cl_2.$2H_2O$)–1-ethyl-3-methylimidazolium chloride [EMIM]Cl–ethylene glycol (EG) ionic liquid. Cyclic voltammetry and chronoamperometry methods were employed to successfully electrodeposit a copper layer on mild steel in a copper chloride (Cu-Cl_2.$2H_2O$)–1-ethyl-3-methylimidazolium chloride [EMIM]Cl–ethylene glycol (EG) ionic liquid. Testing of the surface was performed using SEM and X-ray diffraction techniques.

The experiment included an ionic liquid with the molar concentration of Cu-Cl_2_$2H_2O$–[EMIM]Cl–ethylene glycol was 1 : 1 : 2 which was prepared by the slow addition of a known weight of Cu-Cl_2_$2H_2O$ to a mixture of [EMIM]Cl and ethylene glycol at room temperature. This mixture was stirred profusely using a magnetic stirrer for about 2 hours until a uniform blend was obtained. The electrochemical measurements and experiments were carried out at ambient conditions. Cyclic voltammetry was employed using the three electrode electrochemical cell with platinum as the working electrode, platinum sheet as the reference electrode and saturated calomel electrode with a

Luggin capillary as the reference electrode. The voltammograms had scan rates varying from 25 to 100 mV/s. The electrodeposition experiments were carried out at a potential of -0.7 V. The surface structure of the electrodeposits were studied using the scanning electron microscope and the deposition size was assessed by an X-ray diffraction technique.

Their results obtained from their experimental analysis was as follows. Cu^{2+} reduced at a potential of about -0.186 V and the oxidation of Cu^{1+} occurred at +1.074 V. The anodic and the cathodic peaks displayed a linear dependence on the square root of the scan rate. Cu^{1+} reduced to Cu at -0.942 V and copper oxidized at +0.664 V. The electrodeposition of copper with acid sulphate solutions were bound to take place in the following 2 steps

$$Cu^{2+} + e^{--} \longrightarrow Cu^{+} \quad (2.12)$$

$$Cu^{+} + e^{--} \longleftrightarrow Cu \quad (2.13)$$

Sol-gel process can be described as the generation of an oxide network by continuous condensation reactions of molecular precursors in a high viscous medium. This process involves the transformation of monomers into a colloidal solution (sol) that behaves as the precursor for an integrated network (or gel) of either discrete particles or network polymers. There are basically two methods to prepare sol–gel coatings: the organic and the inorganic method. The inorganic method involves the building of networks through the formation of a colloidal suspension (usually oxides) and gelation of the sol (colloidal suspension of minute particles,1–100 nm) to form a network in continuous liquid phase. The organic approach usually begins with a solution of monomeric metal or metalloid alkoxide precursors in an alcohol or a low-molecular weight organic solvent. Of the two the organic method is the most commonly used method for sol-gel coating.

Viazzi et al. (2006) studied the synthesis by sol-gel route and characterization of Yttria Stabilized Zirconia coating for thermal barrier applications. Prominent work focused at developing sol-gel techniques, which were non-directional methods, to prepare, by suitable chemical modifications, nanocrystalline materials with a controlled morphology was carried out. The main advantage of this method was to reduce the crystallization temperature, to a much lesser degree than the conventional processes thus allowing the synthesis of reactive powders with nanometric particles size. The development of an alkoxide sol was optimized in order to obtain homogeneous YSZ films. The nature and quantity of binders was studied. Superalloys were then immersed in the so-gel and withdrawn at several controlled rates before being annealed at various temperatures. The films microstructures were investigated by using scanning electron microscopy. It was observed that the

combination of a slower withdrawal speed (17 cm/min) with a 3 wt.% content of Dibutyl phthalate allowed the most homogeneous and the thicker coatings. Moreover, SEM images indicated that the deposit was present all over the rough surface of the substrate and was composed of two morphologies: a YSZ thin covering film and a thicker discontinuous layer replicating the substrate topography.

The substrate used in this case was a Ni-based superalloy (Hastelloy X), covered by a NiCrAlY bondcoat, plasma sprayed under air. The roughness of the surface was essential to allow the adherence of the YSZ plasma sprayed top coat however the same was unusual for a sol-gel coating as the substrate wettability towards the sol was not a constant. The precursors used for the preparation of YSZ sol were zirconium (IV) propoxide ($Zr(OPr)_4$) , yttrium (III) nitrates hexahydrate and the solvent was 1-propanol. A complexing agent, acetylacetone (AcAc), was also used to reduce the zirconium alkoxide reactivity towards water and to avoid hydroxides formation. Layers were deposited by immersion of the substrates in the sols and were withdrawn at controlled speeds. The sample was then dried for a certain period at room temperature and later annealed thrice i.e for 2 hours at 950^0C followed by a half an hour step at 1150^0C and again 950^0C for 4 hours. Results showed that each deposit of YSZ cracked before and after the heat treatment. No difference was noticed with the different binders used. It was observed that the cracking phenomenon was also due to the sudden densification of the YSZ during annealing. It was concluded that optimization of the sol formulation would lead to the production of homogenous YSZ coatings by sol-gel route. This study was focused on the creation of an adequate chemical interface between NiCrAlY bond coat and subsequent thicker layers.

Masalski et al. (1999) investigated the Improvement in corrosion resistance of the 316l stainless steel by means of Al_2O_3 coatings deposited via sol-gel method. They prepared Two-, four- and six-layered Al_2O_3 coatings of the AISI 316 type stainless steel by means of the Sol-Gel method. Aluminium isopropoxide was used as the precursor. The coatings had a thickness of approximately 2 to 3 microns and had an uneven structure. The aluminium oxide coating was heated at temperature of 500^0C and remained stable within the period of 1000 hours exposition in the Ringer's solution.
For the experimental analysis crushed aluminium isopropoxide (500 g in quantity)was added in portions under continuous stirring into a boiling solution of 2.25 dm^3 of distilled water and 5 ml of concentrated nitric acid. Hydrolysis proceeded according to the following reaction

$$2\,[(CH_3)_2CHO]_3Al + (3+n)H_2O \longrightarrow Al_2O_3.nH_2O + 6\,(CH_3)_2\,CHOH \qquad (2.14)$$

The mixture was evaporated down to 1 dm^3 and was stirred continuously at high temperatures. 15±20 ml portions of concentrated nitric acid were added to clarify the solution. The acid was added mainly to reduce the pH value towards an increase in the sigma potential and to move away from the isoelectric point of the $Al(OH)_3.nH_2O$ colloid which reduced the agglomeration rate of particles. Upon cooling down to room temperature the solution was hardened to a colourless gel with around 15% of hydrated aluminium hydroxide in terms of anhydrous Al_2O_3. In order to obtain a proper solution to deposit coatings with 10% Al_2O_3, the original gel was combined with water in suitable ratios and the solution was vigorously mixed. The viscosity of the aluminium solution measured was about 8 centi poise. The Al_2O_3 coatings were deposited on the surface of steel ground with no. 600 emery paper by adopting of a thin liquid film being formed on the solid substrate. The sample was being immersed and pulled out of the solution at uniform speed perpendicular to the liquid surface. Finally the sample was cured at 500^0C for about 30 minutes.

Their results showed that the Al_2O_3 film mapped to the substrate quite well. Irregularities of the steel substrate after polishing with emery paper and scratched portion of the coating were clearly observed. The following conclusions were drawn from the data received.It was possible to obtain amorphous aluminium oxide coatings on stainless steel 316L using sol-gel method.The aluminum coating heated at 500^0C has an added advantage on the resistance to pitting corrosion, contrary to the heating process at 850^0C.EIS results proved that the aluminium oxide coatings were not decomposed when the coated samples were immersed in the ringer solution for 1000 hours.

Pourhashem et al. (2013) studied the double layer bioglass-silica coatings on 316L stainless steel by sol–gel method. In this research 45S5 bioglass- silica coatings on 316L stainless steel were formulated by the sol–gel method and were characterized by different techniques. According to X-ray diffraction (XRD) results, by sintering 45S5 bioglass at 600^0C for 5h, coatings containing both $Na_2Ca_2Si_3O_9$ crystalline phase and amorphous phase were obtained. Scanning electron microscopy (SEM) results showed that coatings prepared via appropriate sol aging and substrate preparations were free of any cracks. Potentio-dynamic polarization tests in simulated body fluid (SBF) showed that coatings improved the corrosion resistance of substrates significantly.

Two methods were used for surface preparation of stainless steel samples in order to compare the effects on coating properties: mirror polished substrates and substrates sandblasted with silica beads. The silica sol was prepared by adding tetraethyl orthosilicate to ethanol and HCl. Distilled water was then added to the solution and was then stirred at room temperature until a clear solution

was achieved. A 45S5 bioglass sol with chemical composition of 45 % by weight of SiO_2, 6 % by weight of P_2O_5, 24.5 % by weight of Na_2O and 24.5 percentage by weight CaO was pre pared by sol–gel process. Tetraethyl orthosilicate was added into 0.1 mol/L of nitric acid as catalyst at room temperature. The following chemicals were added sequentially and about one hour was given to each reagent to react thoroughly under constant agitation: thriethyl, sodium nitrate ($NaNO_3$) and calcium nitrate tetra hydrate ($Ca(NO_3)_2$ _ $4H_2O$) respectively. To allow completion of the hydrolysis reaction and achieving a clear sol, agitation was continued for one hour after the last addition.

The double layer coatings consisting of an intermediate silica layer and a top 45S5 bioglass layer was prepared by dipping the substrates into silica sol gel aged for 24 hours at room temperature with a withdrawal rate of 5cm/min followed by drying in an oven at 450^0C for 30 minutes. This process was repeated again followed by heat treating the sample at 600^0C for 5 hours.

Their results proved that the surface preparation of the substrates had significant effect on the coating properties. Bioglass-silica coatings exhibited a better electrochemical behavior as compared to the bare substrates. Further, in vitro behavior of coated substrates was considered during 30 days of immersion in SBF solution at 37°C via XRD ,SEM, AAS and the tests indicated the growth of apatite and calcium silicates on the surface of coated samples.

Adraider et al. (2012) studied the structural characterization and mechanical properties of alumina coatings on SS samples fabricated using the sol–gel technology and fibre laser processing. Alumina coatings were synthesized via a sol–gel method and deposited on stainless steel substrates by dip coating method. The coated substrates were then treated with pulsed ytterbium fibre laser radiation in continuous wave mode and with varies specific energies. The composition and the material structure of the coated surfaces after laser processing were studied using XRD, SEM and contact angle measurements, while the mechanical properties of modified surfaces were analyzed using nano-indentation. The results showed that the alumina xerogel films coated on the substrates were successfully converted into crystalline alumina ceramic coatings by the laser irradiation, the structure of coatings obtained were dependent on the irradiation conditions, with the increase of laser specific energy leading to the formation of initially ϒ- Al_2O_3 with increasing amounts of α- Al_2O_3 at higher energy. Nano-indentation results revealed that the laser processing resulted in significant improvement in hardness and Young's modulus of the alumina-coated surface and, at optimum, could achieve the mechanical properties at the same level as pure α-alumina ceramic, much higher than those of the as-dried xerogel coating.

The sol–gel alumina coatings were prepared using aluminium isopropoxide (98%) as the precursor agent, acetic acid as the catalyst, and a 4:1 mixture of distilled water and isopropanol as the solvent. The concentration was 0.75 mol for the precursor and 0.15 mol for the catalyst. The reaction system was stirred at 80^0C for several hours until the system became transparent, indicating that a colloidal alumina dispersion was formed. The alumina sol was then ready for coating the stainless steel substrate. The alumina films were deposited on the cleaned substrates via a dip-coating process with the same immersion and removal speed of 2.3 mm/s. The thickness of the alumina sol-gel coating that was obtained was approximately 3.5 μm.

Their results showed that the surface mechanical properties of stainless steel with alumina coating were enhanced using sol-gel coating technology in combination with subsequent fibre laser irradiation under continuous wave mode. It was also confirmed that the laser processing condition could be controlled to enhance the microstructure of the resultant alumina coating. The ATR-FTIR analysis and contact angle measurement proved the change of chemical composition and physical properties of the sol–gel alumina coatings after laser irradiation. The XRD analysis confirmed the conversion of alumina xerogel film into crystalline aluminium oxide in both ϒ- Al_2O_3 and α- Al_2O_3 under laser irradiation and the magnitude of crystalline phase rises with the rise in laser specific energy transferred onto the coated area. The SEM observation on the surface morphology of laser irradiated area displayed the traverse pattern left by laser scan and reflected the significant interaction of laser with the coated surface. Nano-indentation results confirmed that the mechanical properties of all substrates coated with alumina were improved substantially after laser irradiation in comparison with the as-dried coating without laser treatment.

2.3 Main Gaps in the Literature

The literature review mentioned in the above sections mainly focusses on corrosion resistant coatings, sol-gel coatings and the electrodeposition phenomena of copper on steel. It has been noticed that the phenomenon of copper deposition on steel immersed in molten Cu-Cl has not yet been studied or is mostly under explored. This may be attributed to recent developments in the Cu-Cl cycle for hydrogen generation. This research is mainly focused on the replication of copper layer formation on steel in molten Cu-Cl and testing it for its ability to behave as a protective barrier against corrosion. Further research may be conducted in order to quantify the strength of the copper

layer obtained. A mathematical model may also be generated in order to predict the behavior of copper layer with increasing immersion durations.

2.4 Problem Statement

A major obstacle facing the development of large scale industrial plants for hydrogen generation is to find materials that can sustain the corrosive Cu-Cl environment for prolonged durations. As of today, none of the existing materials are able to handle this environment without undergoing corrosion. A possible solution is to use special metals coated with metallic or ceramic coatings. Edwin (2012), Kaveh (2014) and Shuja (2016) conducted experiments on different metals coated with various corrosion resistant coatings, for their ability to resist corrosion in the Cu-Cl environment. However, none of the coatings were able to survive the tests. This was investigated to be due to the high porosity level in the coating methods used. Moreover, results obtained from Shuja (2016) showed that a strong and uniform layer of copper was being generated on the surface of the steel substrate which was being immersed in molten Cu-Cl. In this thesis study an attempt is made to replicate this copper layer formation and test it for its ability to behave as a protective barrier against corrosion. As this thesis study is limited to testing the integrity of the copper coating obtained for various immersion durations, no theoretical analysis has been performed. Further research on the behavior of this layer at different durations may be carried out by generating a mathematical model that incorporates the theories of corrosion and the data obtained from this research.

CHAPTER 3: EXPERIMENTAL APPARATUS AND PROCEDURE

In this chapter, the detailed explanation of experimental setup is presented. In addition, materials and devices used in the experiments are briefly described for better evaluation of the systems.

3.1 Experimental Apparatus

With relevance to ASTM G31, apparatus for immersion tests in molten chemical solutions has to consist of a heating entity enclosing the Immersion test vessel (ITV), a condenser, a scrubber, flowmeters for controlling the amount of oxygen and supports for test specimens. The Top cover of the immersion test vessel must have sufficient openings to accommodate the purge gas inlet and exits, sample insertion openings and openings for thermocouples. Monitoring devices such as J type thermocouples, gas flowmeters, temperature controllers and oxygen analyzers had to be installed. The entire setup had to be operating inside a fume-hood as per the safe operating procedures. Proper Personal Protective Equipment (PPE) had to be worn at all times during the immersion tests.

3.1.1 The Immersion Test Vessel

Previous experiments were conducted by using both a heating mantle and the immersion test vessel or by using heating tapes to heat the immersion test vessel. As heating tapes are expensive and burn out easily, standard Ni-Cr heating wire was used in order to heat the immersion test vessel. The following analysis provides a detailed explanation of the basis of selection of the Ni-Cr wire.

In order to obtain the heating value of the wire to be selected it was imperative to determine an optimum value for the resistance per inch or foot of the heating wire. The circumference of the immersion test vessel was found to be 17.3" and the height of the immersion test vessel was 6".Considering a gap of 6" between coils the total number of winds needed were 6"/0.25" = 24 coils. Hence the total length of the heating wire needed was 17.3" * 24 = 420" or 40'.
Considering line voltage of 100 V and current drawn to be 10 amps, the total resistance required for the heating wire $R = V^2/P$ was found to be equal to 10,000/1000 which is 12Ω.Therefore, the resistance per foot required for the heating wire obtained was 12/40 = 0.3 Ω/ft.

Ni-Cr heating wires, specifically 60-15 Ni-Cr (Chromel C-60 % Nickel and 15 % Chromium) electric resistance wires were best suited for moderate heating applications (Standard specification for wire for use in wire-wound resistors: B-267-90, 2001). Chromel C is an alloy which has an

operating temperature of 1030^0C and high electrical resistivity and excellent resistance to oxidation at medium to high temperatures. Chromel C is also relatively cheaper than Chromel A and is also most commonly used in heating elements, resistance windings and hot wire cutters. Hence it was selected as it best suited the requirements of the experiments planned for immersion tests. Ω·circ.mil/ft of Chromel C was obtained as 112. A circular mil is defined as the unit of area, equal to the area of a circle with a diameter of one mil (one thousandth of an inch). It corresponds to $5.067\times10-4$ mm².Therefore, considering the resistance per foot required for the heating wire as 0.3Ω/ft the circular mil required for the heating wire was 373. Hence diameter of the resistance wire was obtained to be 21.8 mil = 0.021 inches.Using this as the base specification an easy-to-form Nickel Chromium Alloy, 0.025"Diameter x 135 Feet Long, 1/4 lb. Spool heating wire was order from McMaster CARR. The heating wire was wound around the immersion test vessel with its two ends connected to copper wires which would thenceforth be connected to the external power supply. The steps involved in this process are as follows:

The immersion test vessel was initially placed on a table, attached rigidly with clamps. Next the Ni-Cr wire was wound firmly around the immersion test vessel while maintaining an outward force around it. This was done to ensure that the wire was in contact with the immersion test vessel throughout its circumferential periphery. The number of winds and total length of the heating wire was selected based on calculations mentioned earlier in this section**.**

Two turns of copper wire were wound at the top and the bottom of the immersion test vessel. A fairly thick wire was selected to ensure that wires stayed firm against the wall of the immersion test vessel i.e. without any slippage. Both ends of the heating wire were connected to the copper wires by coiling them uniformly around the copper wires, with the copper wires being at its core. The copper wires were held in place by using cable connectors and screws. The other ends of the copper wires were meant for connection to the external power supply. Efforts were taken to ensure that the length of the copper wires chosen was long enough to wind around the vessel as well as extend beyond it in order accommodate the power supply connections to the external circuit.

The copper wires were tightened by tightening the mounting screw and thus was held firmly against the immersion test vessel. It was important to orient the nut towards the user in order to accommodate for additional tightening of the copper wire. The Figures 3.1 depicts the winding patterns of the Ni-Cr heating wire and the copper wire around the immersion test vessel.

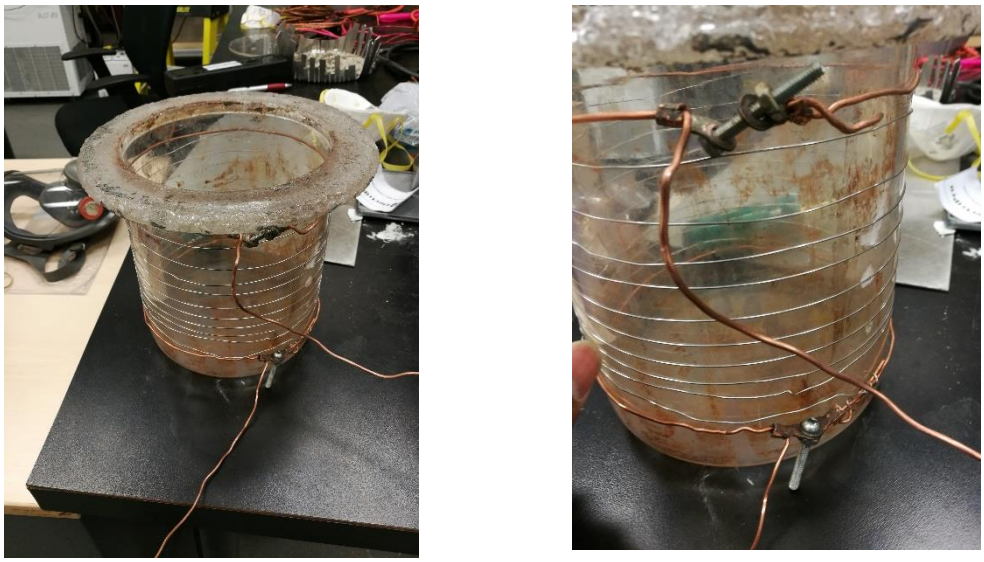

Fig. 3.1 Ni-Cr wound around the immersion test vessel

Upon testing it was observed that the winds of the heating wire quivered due to heating expansion which led to the neighboring winds coming in contact with each other thereby increasing the resistance of the wire. This was eliminated by adding ceramic beads throughout the length of the heating wires. The procedure mentioned earlier was employed to wind the heating wire, encapsulated by the ceramic beads, around the immersion test vessel.

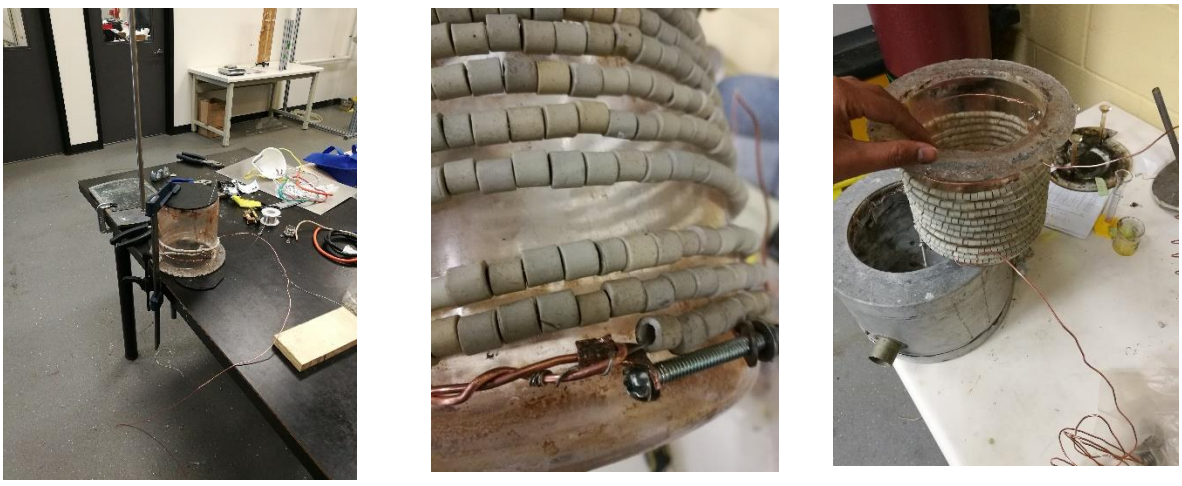

Fig. 3.2 Ni-Cr with ceramic beads wound around the immersion test vessel

A semi-solid cement slurry was prepared by using cement mix and water in the ratio 3:1. This mixture was prepared inside a bucket and was stirred vigorously for around 20 minutes using a

stirrer until a uniform mixture was obtained. The slurry was then pasted on the immersion test vessel which was wound with heating wires encapsulated by ceramic beads. The entire system was then left to cure for around 12 hours. This process ensured that the heating wires didn't quiver and were held firmly in place when connected to the external power supply.

Fig. 3.3 Cement slurry pasted around the immersion test vessel

The immersion test vessel was tested on its own for about an hour by connecting the two ends of the copper wire to the external power supply under close supervision. No complexities were observed during the testing and the required heating was achieved without any hindrances.

Fig. 3.4 Testing of the immersion test vessel

The immersion test vessel was next enclosed in a mantle which served as an enclosure for the heating wires and also as an insulator for preventing any heat loss. The mantle had a circular opening on its surface through which the 2 copper leads from the immersion test vessel were drawn

out for external connections. A third copper wire meant for ground connection was also fitted inside the mantle and was drawn out through the circular opening. Efforts were being made to ensure that none of metal entities of the immersion test vessel were in contact with the mantle. A junction box was then fitted rigidly to the circular opening. The three copper leads coming out of the mantle and into the junction box were then connected to the three leads of a standard electric cable. The other end of the electric cable was fitted into a standard 15 Amps cable plug meant for connection to the external power supply. The 3 copper leads and the 3 leads from the cable were connected together using screwed cable connectors and were subsequently taped with insulation tapes in order to meet the safety requirements.

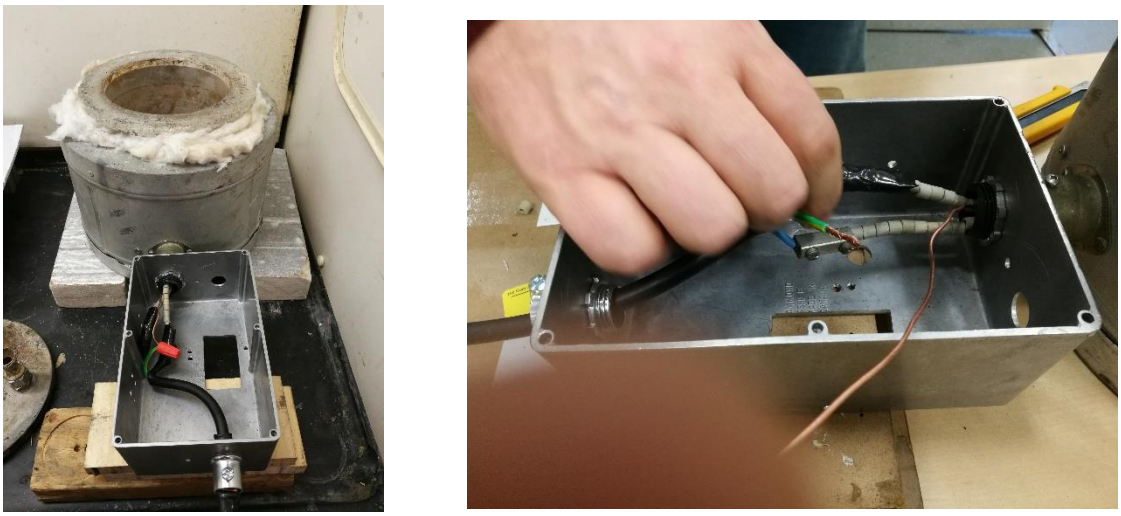

Fig. 3.5 Cable termination in the JB

3.1.2 The Condenser

The purpose of the condenser was to cool the Cu-Cl fumes coming out of the immersion test vessel before letting it into the scrubber. The condenser used was made up of fused quartz material and had a lid attached to it with three openings on the top. The first opening was to receive the gases coming out of the immersion test vessel. The second opening was to let off the gases into the scrubber once cooled. The third opening was used to insert a pressure gauge in order to continuously monitor the pressure levels inside the condenser. The temperature of the condenser was found to be slightly above room temperature.

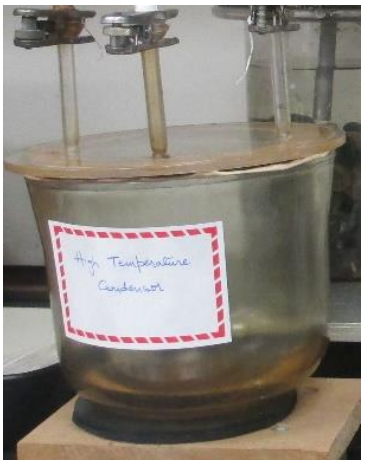

Fig. 3.6 The condenser

3.1.3 The Scrubber

The scrubber used in this experiment was made up of glass. It was fitted with a rubber cork at its top with 2 openings. One opening acted as an inlet in order to accept the already cooled gas coming out of the condenser and the second opening acted as an exhaust letting off the gases inside the fumehood. The purpose of the scrubber was to neutralize the gases coming out of the condenser before letting it out into the fumehood. The scrubber solution was prepared by adding 100 grams of sodium bicarbonate powder into 1 litre of water. The inlet pipe inside the scrubber was suspended in the scrubber solution at a distance close to the top surface of the scrubber solution. This was done to reduce the pressure head inside the system and prevent any back pressure.

Fig. 3.7 The Scrubber

3.1.4 Temperature Controller

Glas-col temperature controllers were used for measuring and controlling the temperature within the immersion test vessel. As Cu-Cl melts at 426^0C, the controller was set to a temperature of 500^0C. J type thermocouples were used to measure the temperature inside the test vessel. The temperature controllers are designed to shut off power supply when the temperature in the immersion test vessel measured by the thermocouples reaches the set temperature of the controller thus maintaining the temperature at the set value. The temperature was also raised in increments of 50 degree Celsius in order to avoid any damage to the heating vessel.

Fig. 3.8 The Temperature Controller

3.1.5 The Connecting Tube

The connecting tube is an integral part of the setup. It is made up of fused quartz and serves as a passage for transferring the Cu-Cl fumes along with the inert gas into the condenser. As it was in direct contact with the hot immersion test vessel the temperature of the connecting tube was relatively high compared to the condenser and the scrubber.

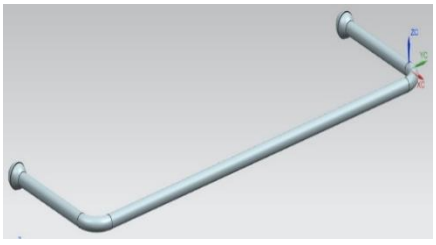

Fig. 3.9 The Connecting Tube

3.1.6 The Oxygen Analyzer

The oxygen analyzer was used to measure the amount of oxygen present in the system. As the experiments had to be conducted at high temperatures, creation of an inert environment was necessary to avoid the corrosion of metals being tested. This prompted the inclusion of an oxygen analyzer. The system after assembly was purged with nitrogen gas and the levels of oxygen was continuously monitored. During this process the temperature of the system was maintained at room temperature. The Oxygen analyzer used was an Omega 2016 model with a temperature measurement range of -40 to 70°C and oxygen measurement range of 5 to 21%. When the percentage of oxygen was less than 5 % the power supply into the system was turned on and the oxygen analyzer was disconnected. This was done in order to prevent hazardous Cu-Cl fumes from getting inside the analyzers pump.

Fig. 3.10 The Oxygen Analyzer

3.1.7 Hanging and Lifting Mechanism

The hanging and lifting mechanism is a special mechanism for suspending the samples inside the immersion test vessel. It consisted of two plates parallel to each other separated by a set of bolts and nuts to hold the plates in place. The samples to be immersed were suspended from the top plate and the crucibles containing the Cu-Cl were placed on the bottom plate of this mechanism. A long vertical rod was also bolted to the upper plate and this rod was used to lift the upper plate during the experimental work. The sole purpose of this mechanism was to immerse the samples in molten copper chloride and lift them before turning off the power supply. This would prevent the samples from getting fused along with the solidified Cu-Cl when the power supply was turned off. The long rod was extended above the immersion test vessel lid and was enclosed by the pipe that was bolted on the lid opening meant for gas entry and lifting of this mechanism.

Fig. 3.11 Hanging and Lifting Mechanism

3.1.8 Gas Flowmeter

The flowmeter used in this setup was a Dwyer model flowmeter which had a measurement range of 30-240 cc/min. It was important to maintain the flow rate of nitrogen gas at 200 cc/min in order to avoid any seepage of oxygen into the system. The inlet of the flowmeter was connected to the nitrogen gas cylinder inlet though a rubber hose and the exit of the flowmeter was connected to the gas inlet opening of the immersion test vessel through a set of hoses and metal tubes. The gas cylinders used in these experiments had a gas volume of 6.33 m^3 at a pressure of 15,168 kPa at 21°C.

Fig. 3.12 Gas Flowmeter

3.1.9 Sealants

High temperature sealants were an integral part of this experimental and played a major role in ensuring that the environment inside the setup remained inert. High temperature stove and furnace cements were used which could work at 1000 to 1500 ^{o}C. Kwik seal was used for sealing the joints and it had a working temperature almost close to room temperature.

3.1.10 Gasket Material

Fibre glass gaskets were used for sealing in all the experiments that were carried out. Fibre glass gaskets are low cost material that can withstand temperatures of up to 1000^{0}C. It was initially tested under harsh conditions and results showed that it was very effective at high temperatures even in the presence of toxic and chemically reactive fumes. Sealants were the main cause of damage to gaskets. Sealants had to be applied on the top and bottom portions of the gaskets and this resulted in the breaking of the gaskets laterally into 2 halves after every experiment. Thus there was a need to replace the gaskets after every experiment.

3.1.11 SEM/EDX Equipment

SEM and EDX analysis was performed at the University of Toronto, at the Center of Advanced Coating Technology (CACT) laboratory. TM-3000 Hitachi with wide magnification range of 15X – 30,000X was employed for scanning electron microscopy. Energy dispersion x-ray spectroscopy was performed on a variable pressure scanning electron microscope (Hitachi SU1510) along with EDX spectrometer (Bruker QUANTAX 100). The samples were cut to shape by using the BUEHLER Isomet 5000 Linear Precision saw and were subsequently polished by using the Buehler Ecomet 300 polishing machine. The cut portions of the samples were ultrasonically cleaned with ethanol in a 3510 BRANSON machine.

3.1.12 Fumehood

Any experiment involving the use of harmful or hazardous chemicals must be conducted inside a fumehood. The fumehood is basically a ventilating device that continuously exhausts the harmful gases emanating from within its area and replenishes its environment with fresh air. At high temperatures the fumes emanating from the molten Cu-Cl are harmful. Moreover the molten Cu-Cl may react with other metals within the setup to form other hazardous and flammable products. It is thus imperative to conduct experiments inside the fumehood.

3.1.13 Assembled setup

Figure 3.15 depicts a picture of the entire setup during the experimental process. The heating immersion test vessel, condenser and the scrubber were connected to each other through connecting rods and hoses. Gas Flowmeters were added in order to regulate the amount of purge gas, in this case nitrogen and maintain the system at a positive pressure. This would prevent any seepage of oxygen gas into the system. An oxygen analyzer was also installed initially to monitor the levels of oxygen. Thermo-couples and temperature controllers measured and maintained the temperatures at the desired level. A tripod stand was included to support the pipe through which the inert gas entered into the system. The same opening was also used to support the lifting mechanism. The experiments were carried out in a fume hood in order to ensure safe operations.

Fig. 3.13 Assembled Setup

3.2 Experimental Procedure

The following subsections provide a step by step procedure for the immersion tests being conducted. The methodology for the immersion tests was adapted from ASTM-G-31-72 standards. All experiments were conducted with utmost adherence to the safety procedures and protocols. The preliminary stages of sample preparation, coating and equipment preparation has been highlighted before stating the steps for the immersion test procedure.

3.2.1 Sol-gel Coating Method

The sol-gel coating method was employed to coat the samples with coatings such as Alumina and YSZ. Specifically, the dip coating method option was selected for this purpose. The synthesis of alumina was performed by adding 500 g of powdered aluminium isopropoxide into a boiling solution of 2.25 liters of deionized water and 5ml of concentrated nitric acid. The solution was stirred vigorously until the total volume of the solution was reduced to 1 liter. The solution was then subsequently cooled to room temperature. Upon cooling, a solidified and colourless gel was obtained which is depicted in the Figure 3.14

Fig. 3.14 (a) Solution preparation (b) Heating and Stirring of the solution (c) Formation of a solidified and colourless gel upon cooling.

An appropriate solution to deposit coatings with 10% Al2O3 was prepared by mixing the original gel with water in suitable ratios.

The synthesis of YSZ was performed in three stages. Firstly, 142.85 ml of Zirconium (IV) propoxide ($Zr(OPr)_4$) solution was added to 26.2 ml of Acetyl-acetone in 1-propanol under constant stirring in order to obtain $Zr(OPr)_4$ in 1-propanol. The quantities were derived such that the molar ratio of the modifier and Zirconium (IV) propoxide ($Zr(OPr)_4$) solution was maintained at 0.8. Secondly, 25 gms of Yttrium (III) nitrate hexa-hydrate was mixed under constant stirring with 130 ml of 1-propanol solution so as to obtain a yttrium concentration of 0.5 mol/L in 1-propanol. A mixture of 18 ml of water with 100 ml of 1-propanol under constant stirring was also prepared in order to avoid local concentration of water in the solution with $Zr(OPr)_4$. This quantity was selected such that the molar concentration of water in 1-propanol was 10 mol/L. Finally all the 3 solutions

were mixed together under constant stirring to obtain a high viscous gel of YSZ. Figure 3.17 depicts the synthesis of YSZ

Fig. 3.15 Synthesis of YSZ

The sol-gel coatings were performed using the dip coating method technique with a custom made dip coating machine. The sample was hung by a rope which was wound around a shaft connected to a motor through gears. A constant linear velocity of 1mm/sec was maintained for dipping the sample into the corresponding solution. Each cycle of dipping and lifting of the sample was controlled manually by changing the motor rotational direction. A total of 60 cycles was carried out on each sample and the same was performed in 3 different sets. The samples were allowed to cool between each set. Finally the samples were cured in a furnace at 600^0C for 1 hour in order to obtain a uniform, strong sol-gel coating.

Fig. 3.16 Sol-gel coating by Dip coating Method

3.2.2 Pre-immersion tests

Before conducting the actual immersion test experiments, a trial run was performed with the setup and molten copper chloride. The set up was run for about 8 hours under close monitoring in order to

note issues that may have to be resolved before conducting the actual immersion test experiments. This blind experiment was carried out at a temperature of 500 ^{0}C by increasing the temperature in increments of 50^{0}C. Electrical conductivity of the molten copper chloride was determined. The thermal expansions of the lifting and handling mechanism and other metal portions were also checked in order to ensure no damage was made to the immersion test vessel. Joints connecting the condenser, connecting tube and the immersion test vessel were also checked for any undue strains. The system was also fed with nominal amounts of nitrogen gas to check for potential leaks within the system. An oxygen analyzer was also installed to evaluate the presence of oxygen. The apparatus was sealed properly before purging it with nitrogen gas. The oxygen analyzer was installed at the condenser as it could not withstand the high temperatures from the furnace. A gas sample from the condenser was fed into the oxygen analyzer's inlet and the exit from the analyzer was sent back to the condenser. As the ITV, the condenser and the scrubber were connected in a series, the sample for oxygen testing could be taken from any of these components. It was also ensured that all the fumes emanating from the setup were exhausted inside the fumehood and were safely let out.

Bare samples were also tested without the presence of Cu-Cl and nitrogen gas to mainly ensure the smooth functioning of the lifting and handling mechanism. The set-up was assembled and was heated to a temperature of 500 ^{0}C again by increasing the temperature in increments of 50^{0}C. At 500^{0}C, the lifting and handling mechanism was operated easily by using proper techniques and PPE. The samples were found to corrode after the test. Black deposits were obtained all over the sample. The samples were weighed before and after the test and an obvious reduction in weight was noticed due to corrosion.

3.2.3 Immersion Tests

The samples that were tested were mild carbon steel and stainless steel 304. Initially the samples to be tested were cleaned thoroughly with ethanol to render them free of any debris. They were then measured for their weight and diameter and these parameters were recorded. The immersion test vessel and its lid were washed thoroughly with distilled water to get rid of the debris from previous experiments. The samples were then hung in the hanging and lifting mechanism and were immersed in crucibles containing 25 to 30 g of Cu-Cl. The shape of the samples didn't play a major role in the experiments being conducted as the materials were only being tested for the copper deposits .The hanging and lifting mechanism along with the samples and the crucibles containing Cu-Cl were then placed inside the immersion test vessel. Next the entire setup was sealed to a tight seal and was

purged with nitrogen gas until the oxygen levels displayed by the oxygen analyzer was found to be very low. The heating system was then turned on and the temperature was raised in intervals of 50^{o}C until the temperature inside the vessel reached 500^{o}C. Upon completion of the test duration the samples were lifted using the lifting mechanism and were suspended for about 2 hours above the crucibles containing the Cu-Cl. This was done to ensure that the molten Cu-Cl deposits on the sample would drop back into the crucible. Once the apparatus was cooled, the top lid of the immersion test vessel was opened and the samples were inspected for their changes. The samples were then cleaned with EDTA solution at 80^{o}C and weighed again to determine the final changes in its geometry. For the SEM/EDX analysis, the samples had to be placed in fixtures containing epoxy for about 8 hours. Upon solidification of the epoxy, the samples were cut in regions meant for observations. Next the samples were polished to mirror finish and cleaned ultrasonically with ethanol. Finally the surface analysis was performed using SEM/EDX options.

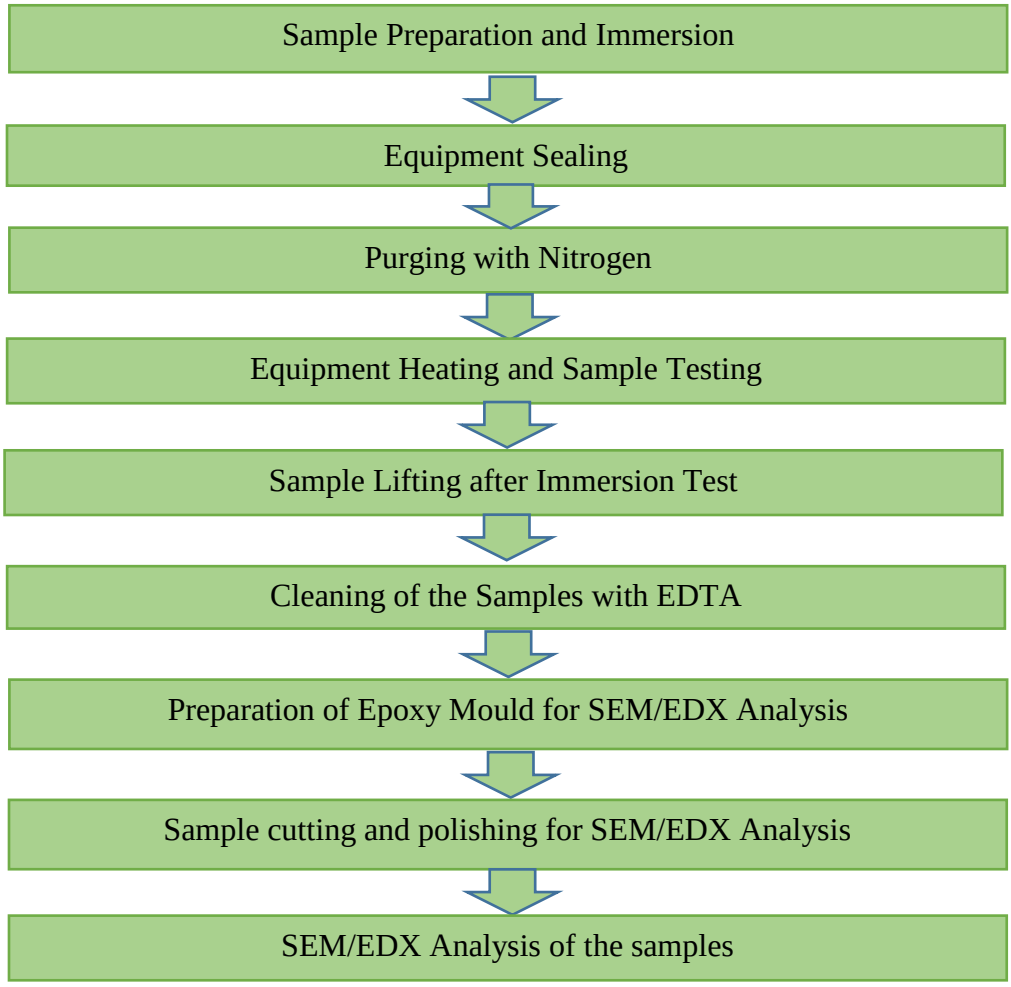

Fig. 3.17 Immersion Test Procedure

The Figure 3.17 provides a flow chart indicating a step by step procedure for conducting the immersion tests. The methodology for the immersion tests was adapted from the ASTM standards. Overall, the entire experiment consisted of coating the samples by sol-gel method (in a few selected tests), immersion test, post immersion cleaning, preparation of sample molds in epoxy, mold cutting, sample polishing by using grit papers of different sized, SEM and EDX analysis.

The total process is of considerable length with the total duration for each sample spanning a couple of months depending on the duration of the immersion test. The detailed procedure for the immersion tests is discussed as follows:

3.2.3.1 Sample Preparation and Immersion

Samples were prepared in accordance with ASTM standards while sample geometry was modified to bullet shape geometry with only one end rounded as just one half was proposed to be immersed inside the crucible.

Some of the samples were coated using the Sol-gel method of coating. This was done to observe the properties such as corrosion resistance and strength of the sol-gel coatings. Some samples were uncoated and were tested for their ability to form copper deposits. The coated quality was evaluated based on porosity, bond strength, oxide content and surface roughness.

Preparation for immersion test consists of cleaning and washing of the apparatus which includes the ITV, lifting mechanism and other accessories with deionized or distilled water. It is highly recommended to clean ITV with a wet cloth to clean out all the deposits and other debris left over from the previous tests. Lifting and hanging mechanism had to be cleaned with a scrapper. Scrapper was better option to clean out all the dust, Cu-Cl flakes and other deposits from the tests conducted previously. Record the geometrical parameters of the samples and take pictures before inserting the sample in to the immersion test vessel.

Take 25g Cu-Cl in a crucible and immerse sample as shown in Figure 3.18. New screws have to be used at the start at every test since it isn’t possible to use the screws from previous tests due to corrosion and pitting. The sample should be carefully immersed in molten Cu-Cl and ensured that atleast half of the sample is buried in it. If crucibles are not available, then small boro-silicate beakers can be used for the same purpose.

Fig. 3.18 Crucible containing Cu-Cl and sample (Adapted from Shuja 2016)

This screw should be hung from the hanging and lifting mechanism with the support of another anchor screw as shown in Figure 3.18. It is not possible to unscrew after every test as unscrewing causes undue strain in the fused screws which may lead to cracking of the coatings. It is therefore very important to use the hanging and lifting mechanism for handling the samples. The second screw is just to ensure that the original sample screw remains in its original position. A maximum of three samples can be hung together during one particular test.

Fig. 3.19 Lifting mechanism screws (Adapted from Shuja 2016)

Figure 3.20 is shown to give an idea how the samples can be hung with the hanging and lifting mechanism. The two horizontal platforms observed are plates of aluminium which are light, easy to handle and also effective. The top plate is used to support the hanging samples while the bottom plate is meant to support the crucibles containing Cu-Cl. Once the samples are hung, this entire mechanism is carefully inserted into the immersion test vessel.

Fig. 3.20 Hanging and lifting mechanism

3.2.3.2 Equipment Sealing

The next step is sealing which is an integral part of the experiment. Sealants are responsible for keeping the atmosphere inside the setup inert and free from oxygen. WD-40 spray is applied on the vessel before application of sealant to ensure that the sealant and the gaskets will detach easily after immersion test. High temperature sealant is then pasted on ITV flange using a plastic scrapper. Surgical gloves must be worn while the sealant is being applied. Caulking gun can be used to inject the sealant uniformly onto the vessel flange. Once a layer of sealant is injected on ITV flange, the glass fiber gasket is firmly placed on it with force acting downwards to ensure that no gap persists between the flange and the gasket. Next inject another layer of sealant on top of the gasket with the caulking gun and then close the top lid cover with lifting rod passing through the lid's opening again with a strong downward force. Finally more sealant is injected in order fill in the gaps between the gasket, flange and the top lid.. Care should be taken to ensure that no pin holes are formed on or around the joint. The presence of pin holes will cause a leak and hence no bubble formation will be obtained in the scrubber. Finally the immersion test vessel is clamped with paper clips. Insert thermocouples in the opening meant for the thermocouples. In this case a J type thermocouple was used with its plugged end connected to the temperature controller. Fix the connecting tube, nitrogen gas pipe and seal all the joints with kwik seal. Let the system cure for 30 to 50 minutes.

Once the sealants are solidified, start purging the system with nitrogen gas by slowly increasing the flowrate all the while keeping an eye on the scrubber. There should be formation of bubbles. If the bubble formation is not observed, that is an indication that the system hasn't been sealed well and the leaks must be detected and repaired. Check the system again for possible leaks using the soap solution method. Identify, repair and then try again.

There are two possible locations to fit the oxygen analyzer. The first one is to install it in condenser opening. Analyzer will draw in gas samples at regular intervals and will keep returning the samples back to the condenser. The temperature in condenser noted was not more than 30 ^{o}C. With respect to temperature it was safe to operate analyzer in condenser. However it was noticed that an increase in temperature may lead to Cu-Cl fumes entering the condenser. Therefore it was decided to purge the apparatus with nitrogen while monitoring oxygen level and then dismantle oxygen analyzer before starting the heating equipment.

The second option is to install analyzer at the exit of scrubber. This position is safer for the analyzer to operate as it is low a temperature zone and the Cu-Cl fumes will already be neutralized by the scrubber. Leave the analyzer on recording mode with appropriate sample rate, depending upon the length of experiment.

3.2.3.3 Purging with Nitrogen

Purging with nitrogen gas takes about half an hour. The flow rate will have to be gradually increased up to a point when bubbles are observed in the scrubber. If proper sealing is provided, a very low gas flow rate of around 50 to 80cc/min may be required, else a higher flow rate of around 150 to 250 cm^3/min will have to be maintained. If the flow rate exceeds 200 cm^3/min, it can be deduced that the seal is a weak seal. However it must be noted that it is very tedious to limit the leak to a minimum value. The oxygen analyzer must be observed and it must be ensured that the oxygen levels in the system start to decrease. The alarm in the oxygen analyzer will be set off when the oxygen levels in the system fall below 5%. Once the minimum level of oxygen is reached, the experiment may be commenced.

3.2.3.4 Equipment Heating and Sample Testing

Next the heating system must be turned on in order to heat the Cu-Cl to its melting temperature. The temperature increase must be performed at intervals of 50^0C in order to avoid any damage due to sudden heating. The Glas-Col temperature controller was used to increase and regulate the temperature of the setup. As the temperature in the system reaches the set temperature of the controller, the controller automatically shuts off power supply. The temperature must be increased until the final temperature of the system reaches 500^0C. As the thermocouple is inserted inside the heating vessel, the difference in temperature of the Cu-Cl and that mentioned on the controller will be infinitesimally small.

A tag must to be placed inside the fumehood in front of the apparatus stating that a high temperature experiment is in progress and also stating the continuous supply of nitrogen gas into the system. Emergency contact details and safety measures will have to be set in place if any abnormalities are observed. If an abnormality is observed the system will have to be first turned off followed by a shut off of nitrogen gas supply

The apparatus and more specifically the heating mantle should not be touched while the experiment is in progress. Gloves, breathing apparatus and other appropriate PPE must be worn while handling the apparatus and Cu-Cl. The apparatus must be inspected at regular intervals. It may not be possible to continuously monitor the state of the apparatus throughout the course of the experiment. However frequent visits must be made in order to ensure the presence of bubbles within the scrubber. If bubbles are not observed, the gas flow rate must be adjusted accordingly. Further the temperature of the system must also be maintained around the set temperature of the controller.

3.2.3.5 Sample Lifting

Upon completion of the test duration the samples must be lifted up from the Cu-Cl crucibles by lifting the hanging and lifting mechanism rod. This must be done at least 4 hours before turning off the heating mantle. It is necessary to ensure that all of the Cu-Cl drops off the sample before turning off the heat. This will avoid solid chunks of Cu-Cl from adhering to the surface of the sample when cooled. Shut off power supply once the duration of the experiment has been met and wait until the system reaches the room temperature. It takes approximately 2 to 3 hours for the system to cool down to the room temperature. Once the system temperature drops to the room temperature, dismantle the seals and open the top lid to observe the conditions of the samples. Necessary pictures of the sample must be taken.

3.2.3.6 Cleaning of the samples with EDTA

After every test, deposits of Cu-Cl will be present on the sample and the same must be cleaned before the sample can be analyzed. The samples can be cleaned chemically in a solution of EDTA. 1 liter of water must be taken in a beaker with 2 gms of EDTA powder added to it. The solution must be heated to 80 ^{o}C while stirring continuously at 75 rpm using a magnetic stirrer. The samples should not be inserted into the solution until the solution temperature reaches 80^{0}C. Once the required temperature is reached, insert the samples to be cleaned in the solution while keeping the solution stirred. A change in the colour of the solution will be observed. Now prepare another solution and immerse sample in it. This process must be repeated until the colour of the EDTA solution remains unchanged. At this point it may be deduced that the sample is free from Cu-Cl deposits. Care should be taken to ensure that the sample is not placed very close to the magnetic stirrer. Dry the sample by placing it in a furnace set at 80^{0}C for about 20 minutes. Store the samples in a contaminant free bag or plastic container in order to keep it safe from corrosion due to atmosphere.

3.2.3.7 Preparation of Epoxy Mould for SEM/EDX Analysis

The next step is to cut the samples perpendicular to its axis in order to observe its cross section. However cutting damages the coating of the samples. To avoid damage to the coatings, first enclose the samples in a hardened epoxy mould. Preparation of the epoxy mould takes a few minutes. Combine epoxy and hardener in a ratio of 5:1 by weight and mix them thoroughly until a uniform mix is obtained. Release agent must be applied on the walls of the mould container in order to ensure easy removal once the epoxy is hardened

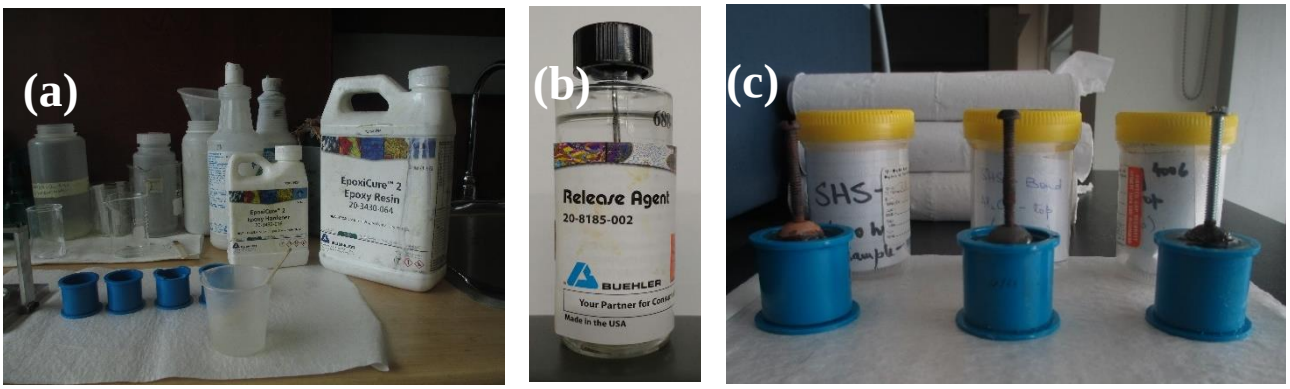

Fig. 3.17 (a) Epoxy preparation (b) Release agent (c) Samples dipped in epoxy (Adapted from Shuja 2016).

Dip the samples in the mould and leave it for approximately 8 hours. Check the status of the mould upon completion of the soaking time. If the mould has turned into a solid block, then the entire mould must be removed by opening the bottom lid of the mould container. Light hammer strokes may be applied to assist with the mould removal. If the mould is still soft, then it has to be cured for more hours until the required hardness level is reached. The blocks should look like the way shown in Figure 3.18.

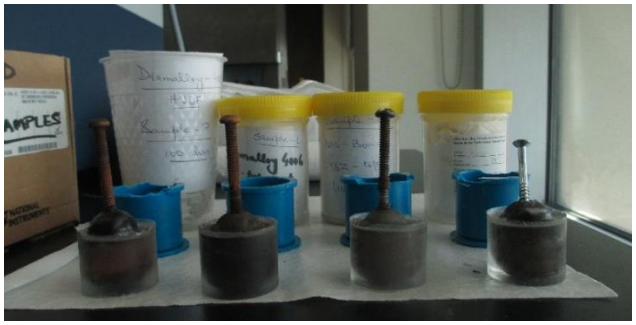

Fig. 3.18 Samples after the solidification of epoxy (Adapted from Shuja 2016)

3.2.3.8 Sample Cutting and polishing for SEM/EDX Testing

Cutting the sample becomes easy when it is mounted in epoxy. Set feed rate of 2 mm/min and fit the sample in auto-cutting machine as shown in the Figure 3.19. It takes around 15 minutes to cut a single sample. A lubricant jet must be sprayed continuously on the diamond cutter to ensure that the temperature of the cutter and the sample are within acceptable limits.

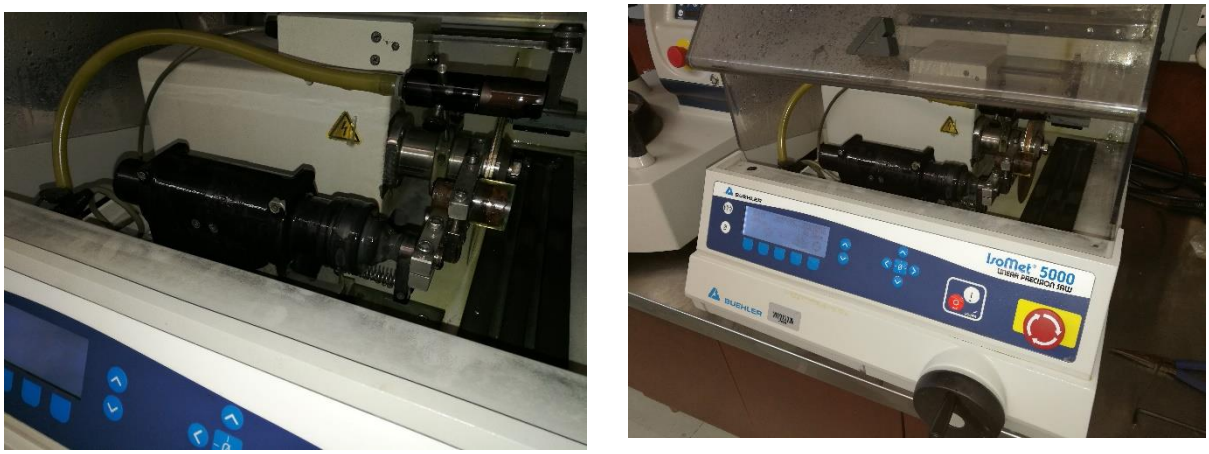

Fig. 3.19 Sample cutting process

The next step will be polishing of the samples. This step is very important as it helps improve the visibility of the microstructure and this ensures a clear view of the samples in the SEM. This process will take around 20 minutes to complete per sample as the grit papers have to be changed to refined levels sequentially. Start polishing with lower grit then refine it with higher grit until the surface structure produced by the previous grit paper is completely removed. Grit papers were used in the flowing series: Grit 320, 400, 600 and 1200

Fig. 3.24 Samples being polished

The samples must be polished to mirror finish at the end of the polishing step. The next step is to clean the samples ultrasonically in ethanol in order to ensure that no debris from the sample enters the SEM while testing. This is done by placing the sample in a beaker containing ethanol and placing this beaker in an ultrasonic machine filled with water. Each sample was cleaned for 5 minutes to ensure all debris was removed. Upon cleaning all the samples were dried with compressed air and covered in order to avoid attack from the outside environment.

Fig. 3.25 Samples being cleaned ultrasonically with Ethanol

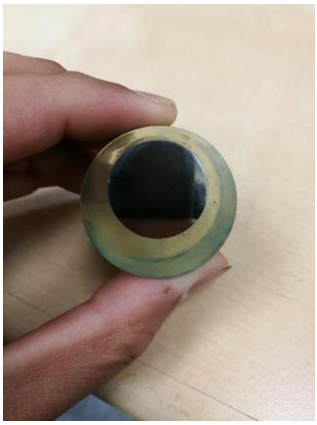

Fig. 3.26 Sample cleaned and polished

3.2.3.9 SEM/EDX Analysis of the Samples

Scanning Electron Microscopy was performed on the samples with a TM-3000 Hitachi machine at the University of Toronto. The machine operates with its own software and it has inbuilt features for aligning, zooming and moving the sample to the desired position. The machine initially vacuumizes its inner atmosphere with an inner suction pump in order to ensure clarity of the images obtained.

The entire duration for testing of each sample i.e right from position the sample, vacuumizing the inner atmosphere, analyzing the surface and performing an EDX takes about 20 minutes.

The Energy Dispersion X-ray spectroscopy indicates the presence of the elements deposited on the sample. The specimen under consideration may be mapped across a particular area and can be analyzed for the different elements present across that area. The elements may be described based on their weight percentage or quantity. In addition to a particular area, elements across a particular section may be also detected by simply drawing a line across the section to be analyzed using the software. The elements across the line will be indicated by graphs which show a peak when it detects the presence of a particular element of interest.

3.2.4 Physical behavior of Cu-Cl

Copper (I) Chloride is a white solid which turns light green due to the presence of oxidized impurities and copper (II) chloride. It melts at a temperature of 426^{o}C and is sparingly soluble in water. It is highly corrosive in nature and the integrity of most metals are affected by it. Molten copper chloride is dark black in colour, however it turns light green upon solidification. Molten copper chloride was photographed after the blind test was conducted. The hard chunk of Cu-Cl was later cleaned by using a 2M solution of HCl. A respirator, a wind shield, high temperature gloves and a coverall are mandatory safety requirements during this exercise.

Fig. 3.20 Solidified Cu-Cl after heating

3.3 Health and Safety considerations

It is very important to follow safety protocols to ensure safe working of self and fellow colleagues working in a laboratory. The purpose of this section is to outline the safety measures involved and identify the potential risks and hazards that may occur in the workplace.

3.3.1 Personal Protective Equipment (PPEs)

It is always imperative to use the right PPE during any kind of mechanical activity. A high temperature protection set should always be worn during the immersion tests. The protection set consists of a respirator, safety goggles, fiber glass high temperature gloves, a face shield and latex gloves.

During the immersion test, the condenser, the connecting tube and the scrubber are cool enough and can be touched with the bare hands. As the heating mantle has good insulation around it, it doesn't get hot enough to cause any hazard. However it is better to stay away from the heating mantle during an experiment in order to avoid any burns. The lid of the immersion test vessel is not equipped with any kind of insulation, and if it is steel, it will be at the same temperature as indicated by the heat controller. The top cover lid may be handled only with high temperature gloves. During operations nitrogen gas and Cu-Cl fumes will be released from the pipe containing the lifting mechanism. Therefore high temperature gloves and a breathing apparatus must also be worn while operating the lifting and handling mechanism. Toxic and hazardous gases can easily be avoided by using a fume hood. It is always a safe practice to place the apparatus inside the fume hood.

Personal protective equipment must be used during the entire experimental work. While dealing with chemicals the use of surgical gloves, coveralls, a fume hood and a safety mask are highly recommended for safe operation. Even during fabrication operations like drilling, filing, cutting, tapping etc. it is very important to wear safety gloves and goggles. This will reduce the hazard of dangerous metal chips entering the eyes and will also reduce the possibility of cuts and burnsMost of the experimental work in this research requires use of personal protective equipment be it at high or low temperatures. The main processes where the use of PPE is a mandate is as follows:

- Scrubber solution preparation.
- Sealing the scrubber.
- Sealing of ITV and condenser.
- Filling of powder Cu-Cl in crucibles.
- Opening of ITV lid after experiment.
- Cleaning of crucibles by concentrated HCl
- EDTA solution preparation.

It is definitely not a good practice to handle high temperature equipment without gloves and lab coats. During the experiment process, warning signs or sticky notes must be placed in and around the equipment to alert others about the running equipment.

Drying the samples post immersion and cleaning requires a high temperature of around 80^0C. High temperature gloves are mandatory to carry and insert the samples in to the furnace. Similarly as the EDTA solution is prepared at 80^oC proper high temperature gloves are also mandatory. Samples will produce harmful chemical bi-products in EDTA solution which might be harmful for human skin and must be handled with care.

Washing of the apparatus like immersion test vessel, condenser, scrubber etc must be done by wearing safety gloves. Cu-Cl sticks on the hands and get into the through respiration. It is a very harmful compound and hence special care should be taken while handling new and used Cu-Cl.

3.3.2 Risk assessment

As most of the tests involved in this research are long term experiments a potential risk assessment has to be prepared outlining the risks involved and methods to combat them. The following are the risks involved with long time experiments.

The primary source of danger in the experiment is the immersion test vessel containing the samples as it has heating wires and the electrical supply running directly through it. The ITV is made up of fused quartz with a high melting temperature. However as the setup has to be maintained at a temperature of 500^0C and as overheating has to be avoided, it is very important to connect the ITV to the temperature controller. Accidental connections of the ITV with the external power supply will lead to melting of the vessel and may cause a potential fire hazard. To avoid the ITV from tipping over it is always important to fix it in place using certain fixtures. In the event of an emergency the main power supply must be turned off. Smoke detectors must be present around the immersion test vessel which will sound an alarm if any smoke is detected. Table 3.1 provides an indication of the risks involved with long time experiments.

Table 3.1 Risk assessment register

Incident	Cause	Mitigation Measures	Response	Impact	Likelihood
Fire	1. Overheating of the Immersion Test Vessel 2. Contact with an unstable substance	1. Fire extinguisher placed in the room. 2. As far as possible no flammable materials must be placed near the experiment	1. Extinguish fire 2. Inform Fire personnel/ security	High 1. Damage to surrounding 2. Water on ground due to dousing	Low
ITV temperature overshoots limit	1. Broken Limiter (temperature controller). 2. Human error (connecting the ITV to the external power supply rather than the temperature controller)	1. The internal temperature must be visible on the screen beside the experiment. 2. An emergency power shut-off to turn off the setup when the temperature overshoots critical limit	1. Furnace limiter will shut off the ITV zone as fail safe 2. Inform designated personnel.	High 1. Damage to the setup and the surroundings	Fair
ITV tripping over	ITV not secured firmly prior to the start	ITV must be bolted to the ground must be held firmly in place using fixtures	1. Shut off ITV and monitor area for any spills and signs of fire 2. Report the incident to safety personnel	Medium Damage to the surrounding	Low

Internal temperature out of operating range	Fault in the ITV or thermocouples	Controller will be set to a desired temperature and will be shut off to prevent increase in temperature	1. Temperature limited will shut off power. 2. Inform designated personnel	Low Experiment will shut off	Low
Major Leaks from the equipment	Equipment not sealed	1. Conduct the experiment inside the fumehood 2. Use an air monitor to monitor the conditions around the setup	Turn off the setup and try to arrest the leak before continuing	Low Experiment will be shut off and have to be restarted	

3.3.3 Fire alarm response

The primary risk associated with the experiment is a fire. If the experiment causes a fire, the same will be detected by the smoke detectors places near the setup. A display in the hallway of the clean energy research building would indicate the location of the alarm. Efforts must be made to ensure that no flammable materials are placed near the apparatus during the experiment in order to make sure that the fire doesn't grow. In the event of a fire in the building the UOIT fire protocol will be followed and the campus security will deal will deal with the fire. If the cause of the fire was the experiment, the first step will be to render the room safe for use with fire extinguishers, water and cutting off power supply to the room. The power distribution panels are located in room 109 in the main hallway of the CERL. The circuit breaker for the room, is located in the electrical room so power would be shut off in order to allow for proper dousing of fire. Carrying out the experiment inside the fume hood will thus ensure extra safety and will cut out the possibilities of fire by three quarters.

3.3.4 Material safety data sheets

It is always a safe practice to refer the material safety data sheets before using any materials in the lab. Handling of chemicals , particular types of sealants, lubricants may vary and hence it becomes very important to refer to the data sheets in order to know the proper handling, storing and disposal

procedures for each type of material. Proper PPE must also be worn while handling any material bound to create a hazard. The material safety data sheets are present in every room of the CERL building near any of the entry or exit points.

3.3.5 Closing remarks

The experiments were performed at various intervals of time, the longest being 90 hours. It was conducted as per the methods described in the previous chapter. No hindrances were encountered during any of the experiments. The safety system is entirely automated which makes the operation even more feasible. A bulk of the risk is handled by the temperature controller, hence it would be a safe option to monitor the controller during the initial stages of the experiment and confirm that the power supply is cut off when the temperature in the ITV reaches the set temperature. As it is not possible to be with the setup throughout the course of the experiments, campus security may be asked to simply confirm that the setup is operating in a safe manner.

CHAPTER 4: RESULTS AND DISCUSSION

This section discusses the results obtained from the tests involving immersion of steel samples in molten Cu-Cl for various durations. Some tests involved the testing of bare samples while others involved samples coated via the Sol-gel method. The sample analysis post immersion test was performed using scanning electron microscopy and Energy dispersive X-ray technique

4.1 Carbon Steel (CS) samples dipped in molten Cu-Cl for 50 hours

Two CS samples were tested for 50 hours in molten Cu-Cl inside the ITV. A gas flow rate of 120 cm^3/min was set and continuous formations of bubbles were noticed inside the scrubber. Bullet shaped samples were selected with only one end rounded. After the experiments it was observed that both the samples were embedded with shiny deposits of copper.

Fig. 4.1 CS samples (a) Before Immersion test (b) after immersion test (c) after cleaning with EDTA solution

Upon completion of the test duration, the samples were lifted above the molten Cu-Cl using the hanging and lifting mechanism and were suspended above the crucibles for about two hours. It was observed that some portions of the molten Cu-Cl deposits were still left on the sample and were removed only after cleaning with EDTA solution. This prompted for an increase in the time for suspending the samples above the crucibles upon completion of the test duration. One of the samples was cleaned with EDTA solution. It was observed that layer of copper deposited was weak and flaky as all of the deposits were washed off from the surface and into the EDTA solution.

The diameters and weights of the samples before and after the immersion test have been listed in Table 4.1. A clear reduction in the weight and diameter of the sample is observed after the immersion test.

Table 4.1 Sample Parameters for Carbon steel samples dipped in molten Cu-Cl for 50 hrs.

Initial weight of the sample-1	100.4 g
Initial weight of the sample-2	100.41 g
Weight of Sample-1 after the immersion test	105.2 g
Weight of Sample-2 after the immersion test	105.6 g
Weight of sample-2 after cleaning with EDTA solution	99.03 g

One of the samples (sample-1) was not cleaned with EDTA solution in order to enable testing of the shiny deposits. The sample-2 was washed with EDTA solution at 80^{o}C until the solution changed in colour. This occurred in two separate cycles. During the first washing cycle, the weight of the sample-2 was reduced from 105.6 g to 103.35 g and during the second, the weight reduced to 99.03 g. The cleaned sample was placed in an oven for drying before its final weight was measured. There was also an appreciable drop in the diameter which indicated that the base metal was reacting with the molten Cu-Cl.

The images obtained from the optical microscope indicated that a layer of copper was observed on the surface of the samples. This layer was non uniform in thickness in sample-1but had a constant thickness in sample-2. The layer was also observed to be continuous in some portions of sample-2 and discontinuous in others.

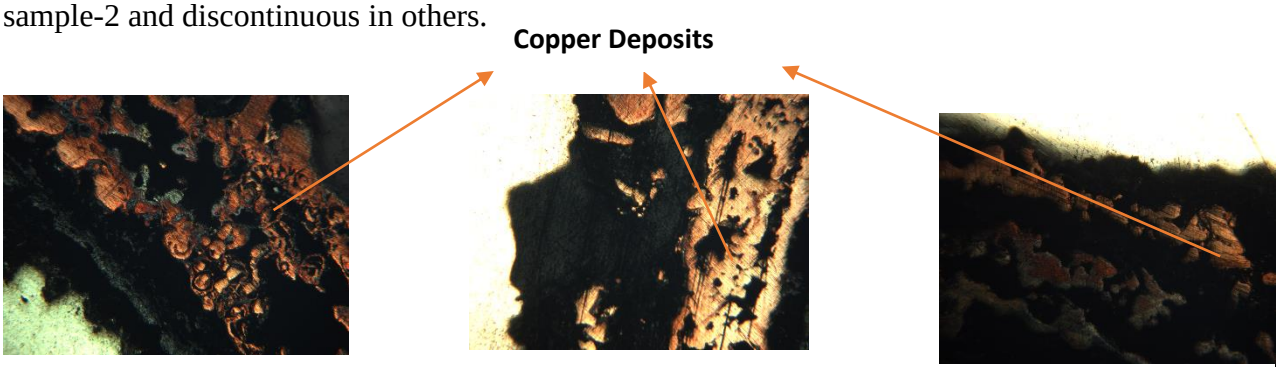

Fig. 4.2 Optical Microscopy images from Sample-1 after the immersion test.

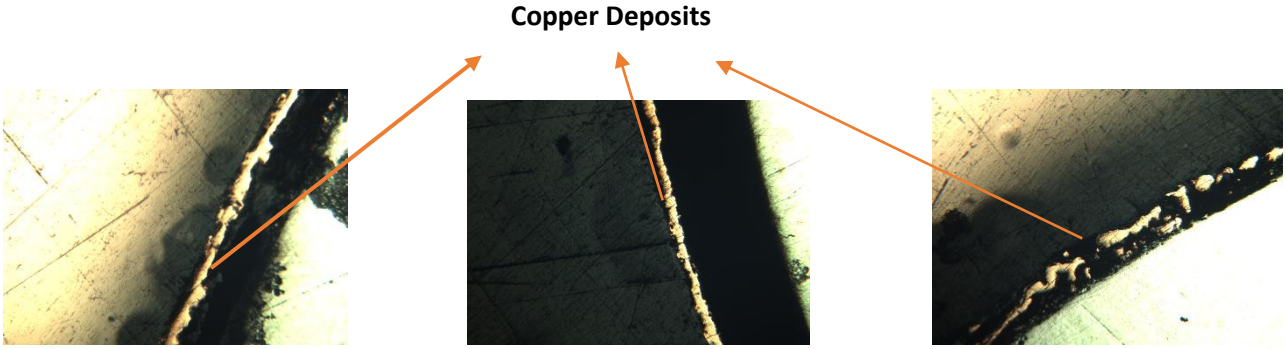

Fig. 4.3 Optical Microscopy images from Sample-2 after cleaning with EDTA

The SEM and the EDX results for sample-2 confirmed the presence of a continuous but weak layer of copper in some regions and a discontinuous layer of copper on other regions of the surface.

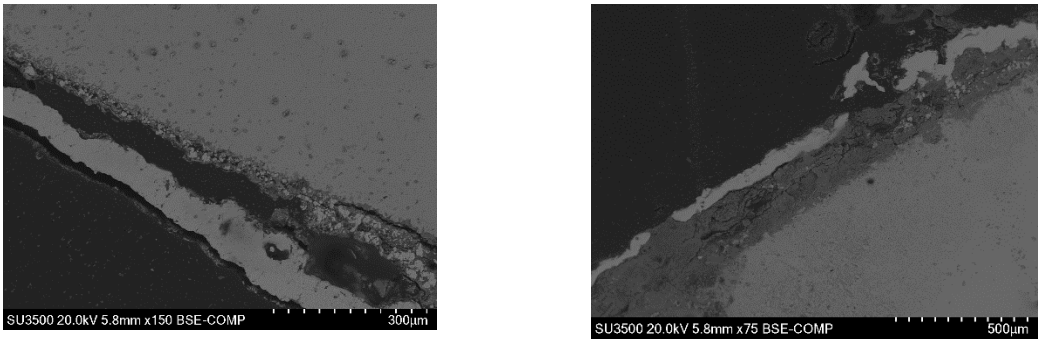

Fig. 4.4 EDX images of the sample-2

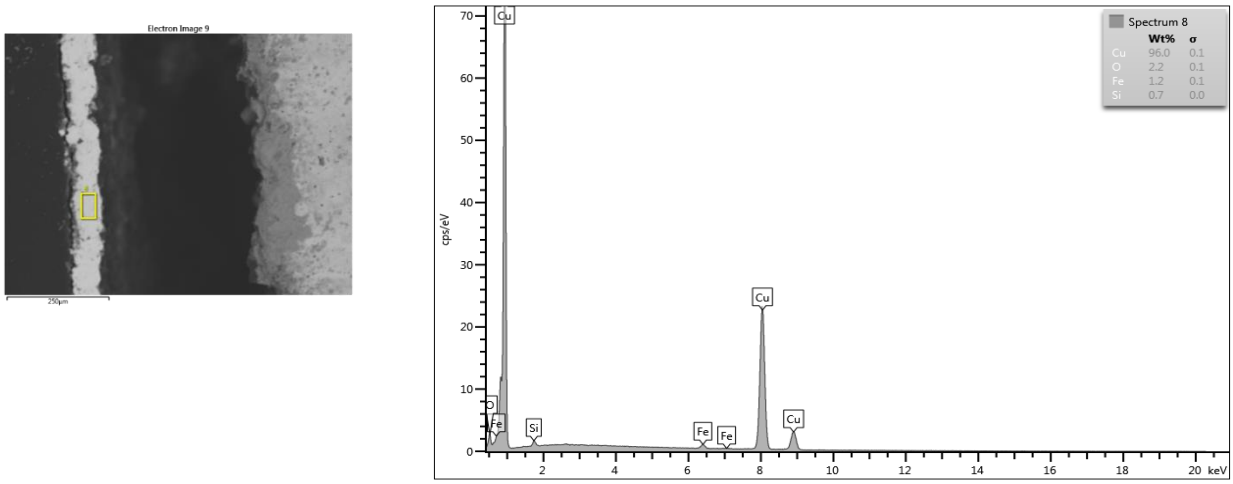

Fig. 4.5 Elemental Analysis of the Sample-2

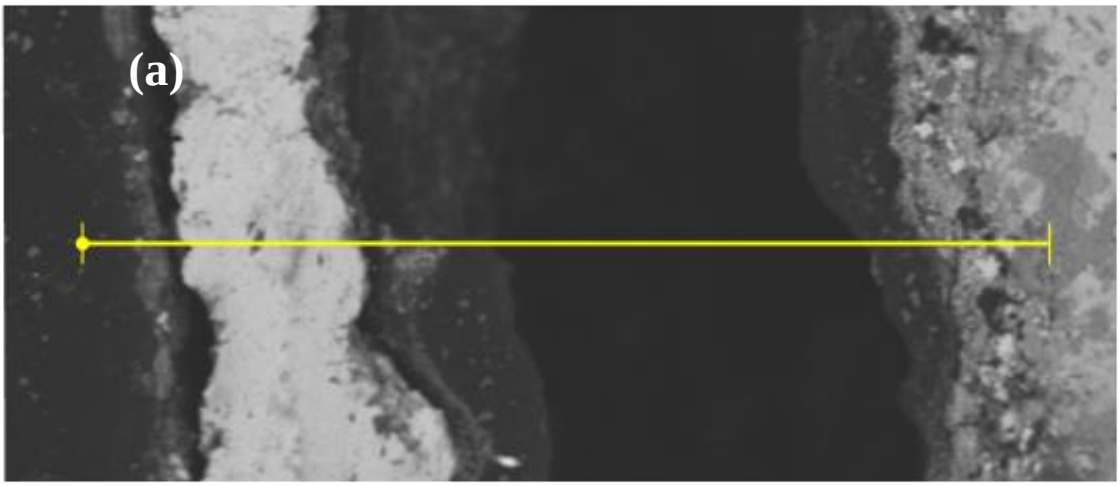

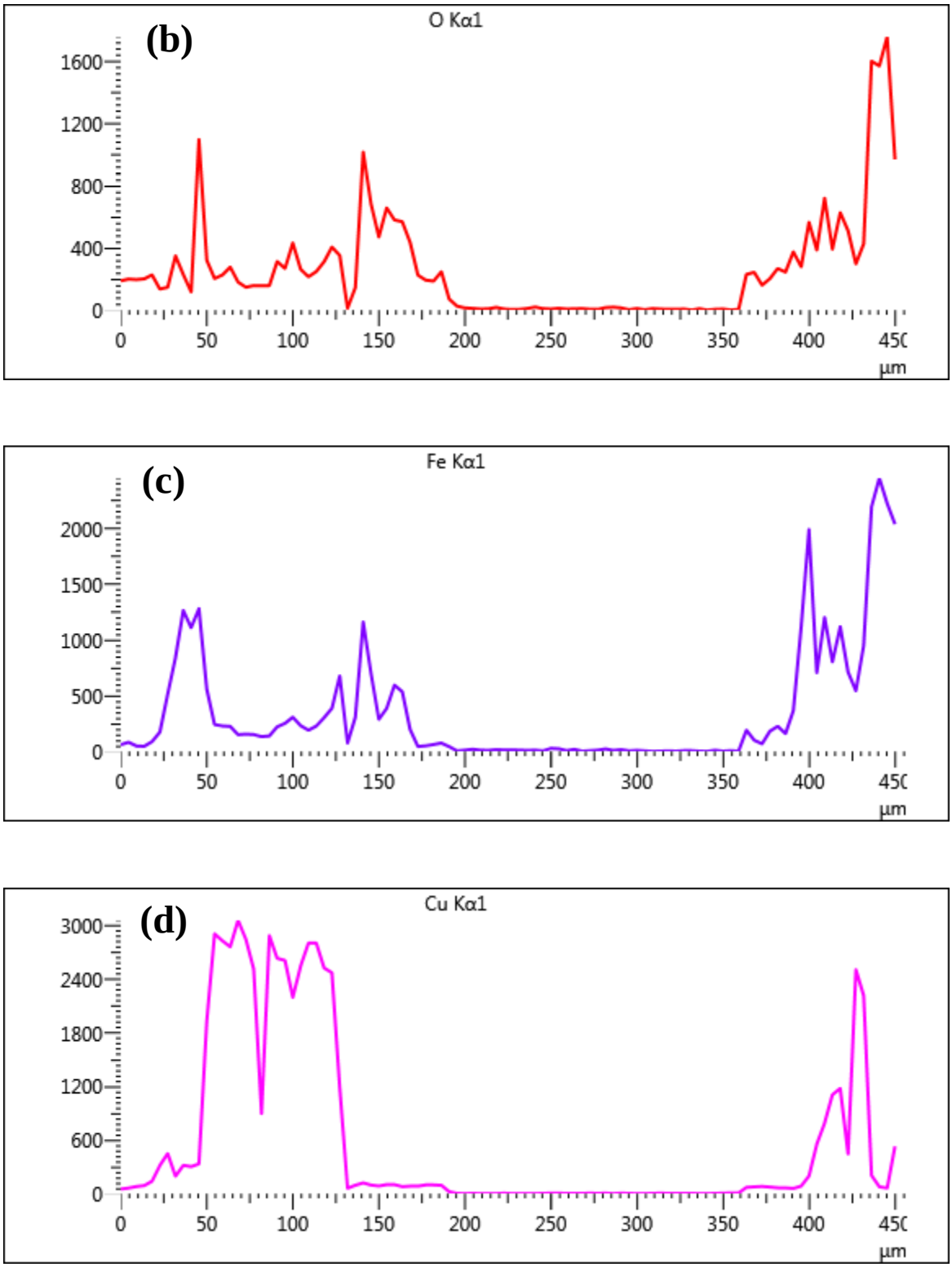

Fig. 4.6 EDX line analysis of the CS sample (a) Sample section considered (b) presence of oxygen along the section (c) presence of iron along the section (d) presence of copper along the section.

From the above analysis, the clear presence of copper was confirmed. However the copper coating though thick, was found to be discontinuous and flaky. The EDX sectional analysis also indicated the presence of an empty space between the layer of copper and the substrate material indicating attack of the molten salt with the substrate. The layer of copper present in the different regions of the substrate appear to be uniform. The synthesis of Sol-gel coatings on carbon steel samples was found to be ineffective as the synthesis required the presence of acids which were corrosive to carbon steel.

4.2 Carbon Steel samples dipped in molten Cu-Cl for 90 hours

Upon completion of the 50 hour test, it was observed that a portion of the copper wire protruding out of the mantle and into the junction box had a burn spot due to cramming of the wires thus leading to undue stress and electron concentration at that point. Hence it was decided to use a bigger mantle filled with insulation to enclose the heating vessel (immersion test vessel). The following apparatus was used to conduct the 90 hour test with carbon steel samples dipped in molten Cu-Cl.

Fig. 4.7 Immersion test apparatus utilizing an enlarged mantle

The geometric parameters of the samples were recorded before the immersion test. The set up was re-assembled and checked for leaks before the start of the experiment. A higher nitrogen gas flow rate of 220 cm^3/min was maintained in the setup. During the course of the experiment it was observed that the formation of bubbles inside the scrubber subsided which prompted an increase in the gas flow rate. It was also concluded that oxygen might have crept into the system during the course of the experiment. Results showed that both the samples had corroded after the experiment with obvious reductions in weight.


Fig. 4.8 CS sample images after the immersion test


Fig. 4.9 Solidified Cu-Cl in crucibles

The weights of the sample before and after the immersion test are listed in the Table 4.2. There is a clear indication of loss of material after the tests as indicated by reductions in weight and diameter.

Table 4.2 Sample Parameters for Carbon steel samples dipped in molten Cu-Cl for 90 hrs

Initial weight of the sample -1	100.98 g
Final weight of the sample-1 after cleaning with EDTA	100.06 g
Initial weight of the sample-2	100.16 g
Final weight of the sample-2 after cleaning with EDTA	99.28 g

4.3 Carbon steel samples dipped in molten Cu-Cl for 20 hours

As the results obtained from previous two tests had drastic variations, it was decided to test the samples for a shorter duration. This would eliminate the fact that the CS samples degraded due to the increase in immersion times in molten copper chloride. As per procedure the geometric parameters of the samples were recorded before the immersion test. The set up was re-assembled and checked for leaks before the start of the experiment. The scrubber solution was monitored for the formation of gas bubbles by varying the gas flow rate and subsequently a nitrogen gas flow rate of 200 cm^3/min was maintained in the setup. It was decided to immerse one sample into the copper chloride solution and suspend the other above it. Upon completion of the test it was again observed

that the bubbles in the scrubber solution arising from the inert gas flow were damped which indicated that there was some obvious oxygen leaks into the system. The results again confirmed this theory as both the samples were corroded and also reduced in weight.

Fig. 4.10 CS sample images after immersion test

It was observed that the sample that the sample which was immersed in copper chloride was corroded due to the corrosive nature of Cu-Cl which was deduced from the brownish layers found on the surface of the sample. The suspended sample however was found to have turned black which indicated that the sample had oxidized due to the presence of oxygen in the air.The weights of the samples before and after the immersion test are listed in Table 4.3.

Table 4.3 Sample Parameters for Carbon steel samples dipped in molten Cu-Cl for 20 hrs.

Initial weight of the sample-1 (immersed in copper chloride)	100.14 g
Final weight of the sample-1 after washing it with EDTA	100.02 g
Initial weight of sample-2 (suspended above copper chloride)	99.6 g
Final weight of sample-2 after washing with EDTA solution	99.54 g

After a thorough examination of the ITV it was observed that the ITV had developed a few cracks due to continuous heating and cooling cycles. This was rectified by covering the cracks with a layer of cement. As the copper deposits developed during previous research works was more prominent in stainless steel samples and also as carrying out sol-gel analysis on CS samples was not an option, it was decided to shift focus from CS to SS samples.

4.4 Stainless Steel and Carbon Steel sample dipped in molten Cu-Cl for 8 hours

Previous research performed by Shuja (2016) showed that, when stainless steel samples coated with different coating materials were immersed in molten copper chloride for about 50 hours, the coating

material was replaced with a smooth layer of copper which remained on the surface even after the samples were cleaned with EDTA. It was observed that the corrosion resistant coating layers were unable to survive the tests but was replaced with a dense, smooth and continuous layer of copper. It was assumed that, upon displacement of the corrosion resistant coatings, molten copper chloride reacted with the host metal to form copper. It was decided to test this phenomenon with a single SS sample at varying time periods.

In this test an SS sample and a test CS sample were taken and mounted on the hanging and lifting mechanism. The stainless steel sample was immersed inside the molten copper chloride while the carbon steel sample was suspended above it. The set up was sealed and the gas flow rate was set to 220 cm^3/min. The scrubber solution was observed for the formation of gas bubbles and efforts were being made to ensure that the gas bubbles were noticed in the scrubber throughout the course of the experiment. This guaranteed the presence of an inert environment, free from oxygen inside the setup.

Results from this experiment showed that both the samples were left unreacted and upper portions of the samples were covered with an irregular deposit of copper. This was probably due to the reactions occurring out of the copper chloride fumes. Moreover an interesting phenomenon was observed in this case. The copper chloride which was initially green turned muddy brown towards the end of the experiment. This indicated that the copper chloride did not melt during the course of the experiment. It was later deduced that the anhydrous copper chloride which is a brownish muddy form of copper chloride was formed within the vessel. This occurred as the cement layer within the vessel absorbed the moisture from the copper chloride powder.

Upon placing in the fume hood the anhydrous copper chloride converted back into the copper chloride by re-absorbing the moisture from the atmosphere and turning its colour back to light green. It was also detected that the thermocouple which was being used had malfunctioned, thus displaying irregular values of the temperature. These matters were rectified before the start of the next experiment.

The parameters of the sample before and after the immersion test are listed in Table 4.4. Hence it was observed that the weight and the diameter of the stainless steel sample increased after the immersion test. This was probably due to the formation of a copper coating resulting from its reaction with the copper chloride fumes.

Fig. 4.11 SS sample images before and after immersion test

.

Table 4.4 Sample Parameters for Stainless Steel and Carbon steel samples dipped in molten Cu-Cl for 8 hrs.

Weight of the SS sample before the experiment	130.35 g
Weight of the SS sample after the immersion test and after cleaning with EDTA solution	130.48 g
Diameter of the SS sample before the immersion test	19.10 mm
Diameter of the SS sample after the immersion test and after cleaning with EDTA solution	19.15 mm

4.5 Stainless Steel sample dipped in molten Cu-Cl for 12 hours.

Before initiating test 5, the stainless steel sample was checked for any irregularities and was cleaned with ethanol. The geometric parameters were then recorded and the sample was mounted on the hanging and lifting mechanism and placed inside the ITV. The set up was assembled and sealed to ensure that no leaks were present. The scrubber solution was observed for the formation of gas bubbles by varying the gas flow rate and a nitrogen gas flow rate of 220 cm^3/min was maintained in the setup. It was observed that the bubbles in the scrubber were present throughout the duration of the experiment which gave impetus to the fact that an inert environment was maintained in the setup throughout the duration of the experiment.

Upon completion of the experiment it was observed that the portion of the Stainless steel sample immersed in copper chloride was blackish which was washed away upon cleaning with EDTA solution. It was observed that a layer of copper was formed on the surface which was rigid even after the sample was washed with EDTA solution.

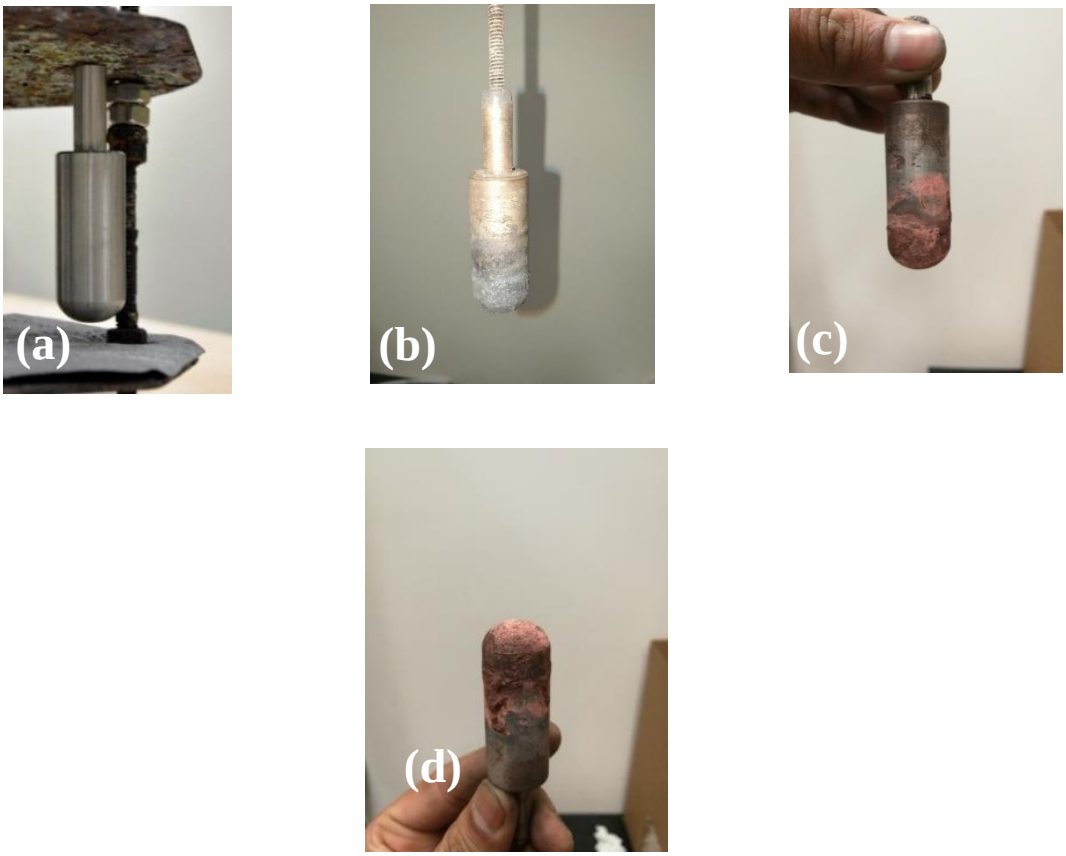

Fig. 4.12 (a) SS Sample before immersion test (b) SS sample after immersion test (c) and (d) SS sample after immersion test cleaned with EDTA solution

Table 4.5 Sample Parameters for Stainless steel samples dipped in molten Cu-Cl for 12 hrs.

Weight of the sample before the experiment	129.42 g
Diameter of the sample before the test	19.3 mm
Weight of the sample after the experiment and cleaned with EDTA	129.32 g
Diameter of the sample after the test	19.35 mm

The parameters of the sample before and after the immersion test have been listed in Table 4.5.Through these details, it was deduced that the molten copper chloride reacted with the base metal resulting in loss of metal. The copper deposit however was not sufficient to compensate for the loss of metal. An increase of 0.05 mm was observed in the diameter of the base metal.

The images obtained from the optical microscope indicated an obvious deposit of copper layer around the stainless steel sample. Though this layer was found to be rigid, it was not found to

be continuous. Since the images obtained from the optical microscope were of a relatively lower magnitude, the results had to be validated using the EDX/SEM equipment.

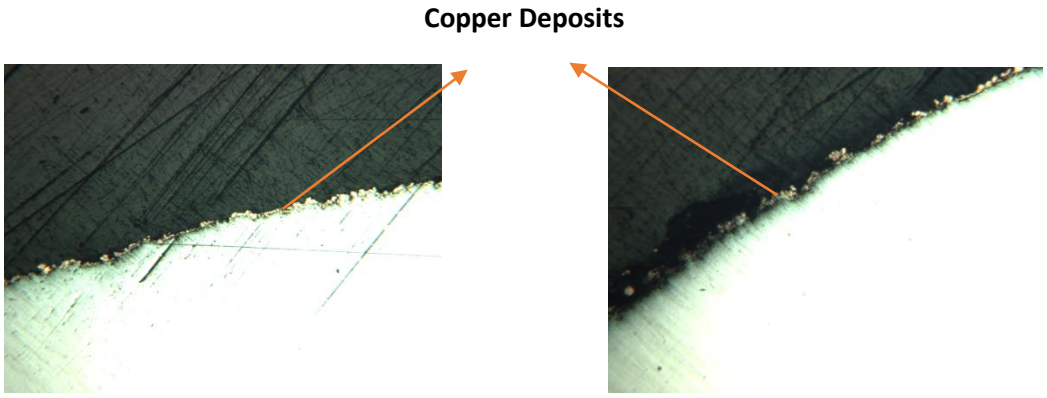

Fig. 4.13 Optical microscopy images of SS sample immersed in Cu-Cl for 12 hours

The SEM and EDX analysis performed on the sample confirmed the presence of copper on the surface. The layer was found to be continuous along certain portions of the substrate but however was not uniform in thickness along the surface. The SEM and EDX images obtained for the sample are mentioned in Figure 4.14 and the sectional line analysis is mentioned in Figure 4.15.

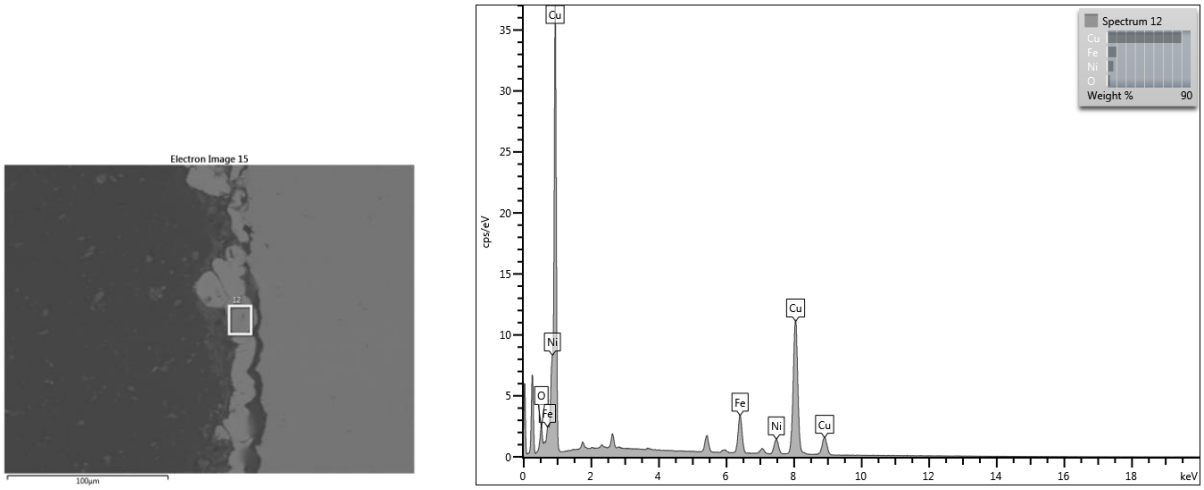

Fig. 4.14 Elemental analysis of the section under consideration

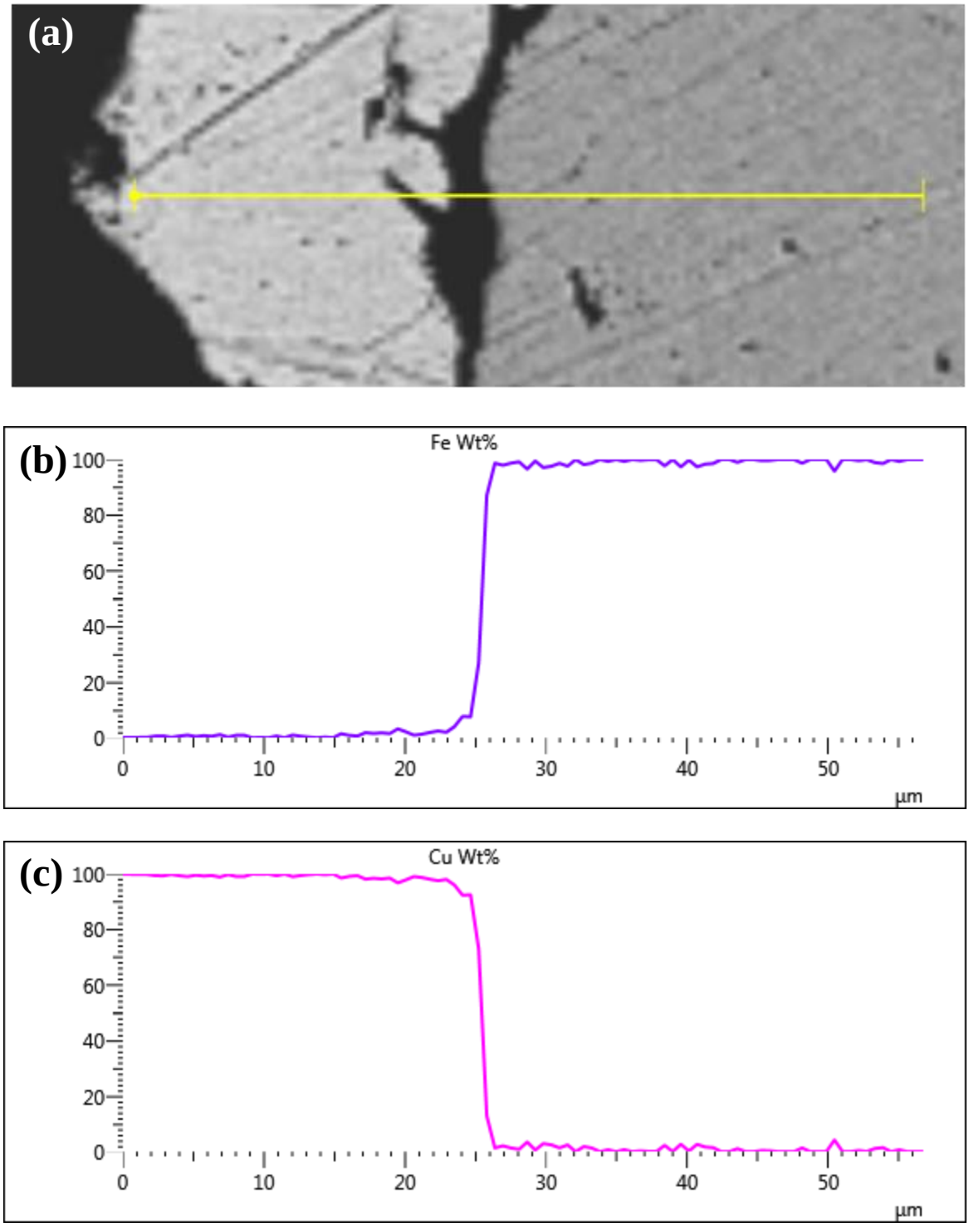

Fig. 4.15 EDX line analysis of the SS sample (a) Sample section considered (b) Elemental analysis of the portion of the substrate thus validating the presence of iron (c) presence of copper deposit along the section of consideration.

Elemental analyis of the portion under consideration confirmed the presence of a thick and continuous layer of copper. It was also observed that the copper layer and the substrate were separated by an opening which reduced the adhesiveness of the copper layer formed. Hence, the images obatained from the SEM and EDX analysis indicated that layer of copper was found to be thick, continuous and uniform along certain regions of the subsrate but was not continuous all along the periphery of the sample. It was thus proposed to increase the duration of the experiments in order to understand the changes in the deposit and the effect of time on the sample.

4.6 Stainless Steel sample dipped in molten Cu-Cl for 20 hours.

The set up was cleaned for any old debris before commencing the experiment. The old sealant deposits were cleaned and the old fibre glass gasket was replaced. The stainless steel sample to be tested had a coating of YSZ which was applied using the phase vapour deposition method . It was decided to test the sample along with the coating for a longer duration. The set up was sealed and gas flow rate was set to 220 cm^3/min to observe gas bubbles inside the scrubber. Upon completion it was observed that the entire sample was surrounded by a layer of copper which seemed to be peeling off. The top half of the sample not immersed in molten Cu-Cl was also found to be coated with copper deposits seemingly from the Cu-Cl vapours.

Fig. 4.16 SS sample immersed in Cu-Cl for 20 hours and cleaned with EDTA

It was also observed that while the material was being cleaned with EDTA solution , the colour of the solution turned maroon everytime the temperature of the EDTA solution crossed 80^0C. it was thus deduced that layers of copper were disintegrating from the surface into the solution. This process was repeated twice and during both cases the colour of the EDTA solution turned maroon when the temperature of the solution crossed 80^0C.

Table 4.6 Sample Parameters for stainless steel samples dipped in molten Cu-Cl for 20 hrs.

Initial Weight of the sample before testing	129.89 g
Initial Diameter of the sample before testing	19.2 mm
Final Weight of the sample after washing with EDTA solution	131.75 g
Final Diameter of the sample after washing with EDTA solution	19.75 mm

The parameters of the sample before and after the immersion test are listed in Table 4.6.It was observed that the weight and the diameter of the sample increased by a considerable amount. It was speculated that chunks of Cu-Cl may have remained on the surface of the sample which was not possible to be washed. The images obtained from the optical microscope spectroscopy showed that a fair amount of copper was deposited on the surface. This layer was found to be rigid but not continuous.

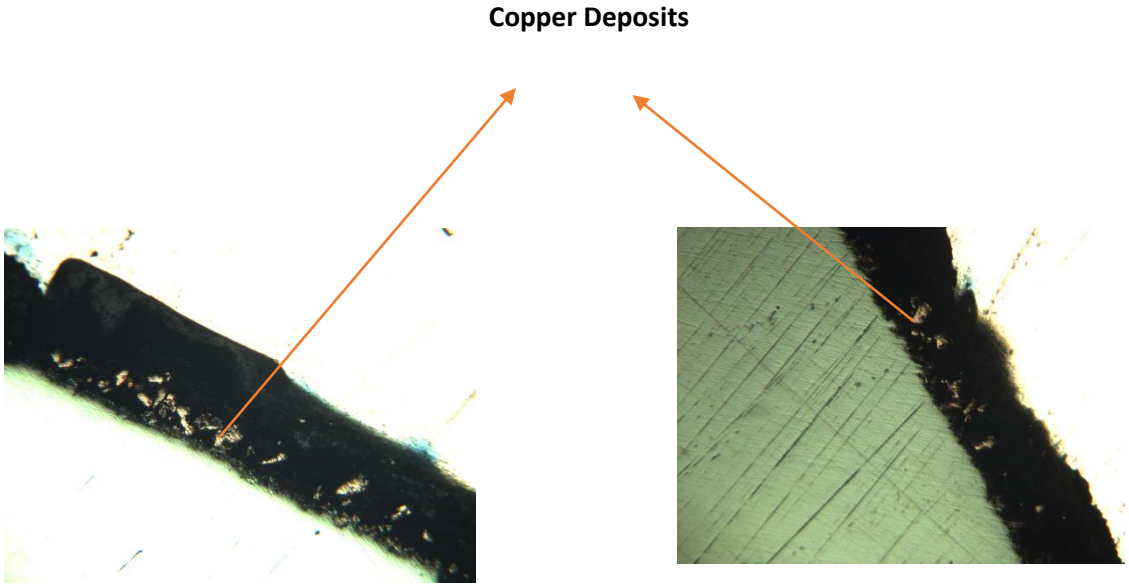

Fig. 4.17 Optical microscopy images of SS sample immersed in Cu-Cl for 20 hours

As observed from the images above the copper layer observed in this case was not continuous. However since the optical microscope had a fairly low magnification range (400 X) a lot could not be deduced from this image. An SEM and EDX analysis was also done of the samples

The SEM and the EDX analysis of the sample confirmed the formation of copper on the sample. It was also observed that the YSZ coating layer was maintained along a portion of the periphery. A strong presence of chlorine was also detected which resulted in the formation of a delicate and irregular deposit of copper.

(a)

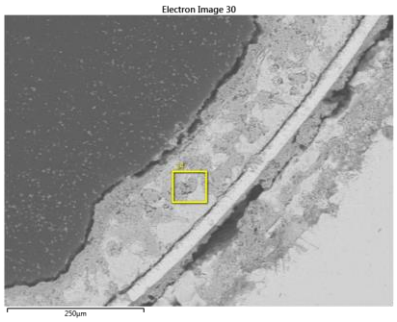
Electron Image 30
250µm

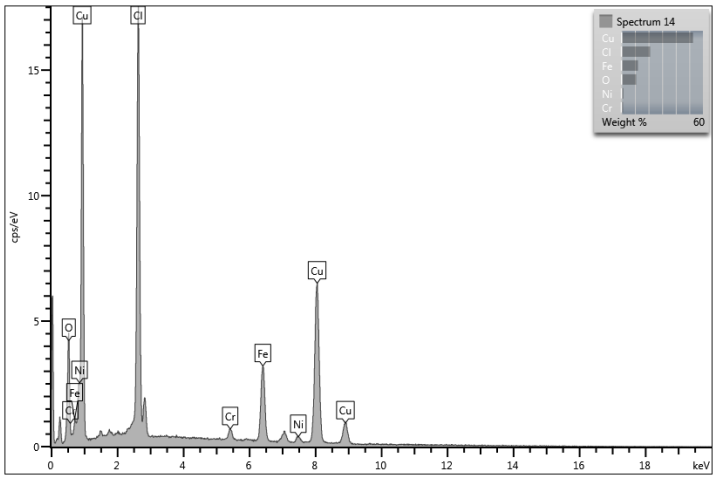
Spectrum 14
Cu
Cl
Fe
O
Ni
Cr
Weight %
60
cps/eV
keV

(b)

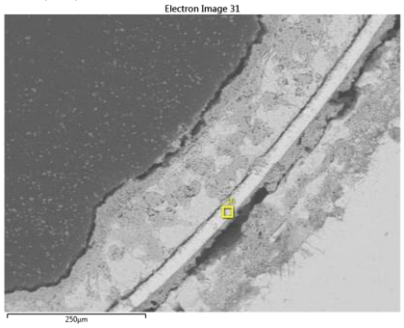
Electron Image 31
250µm

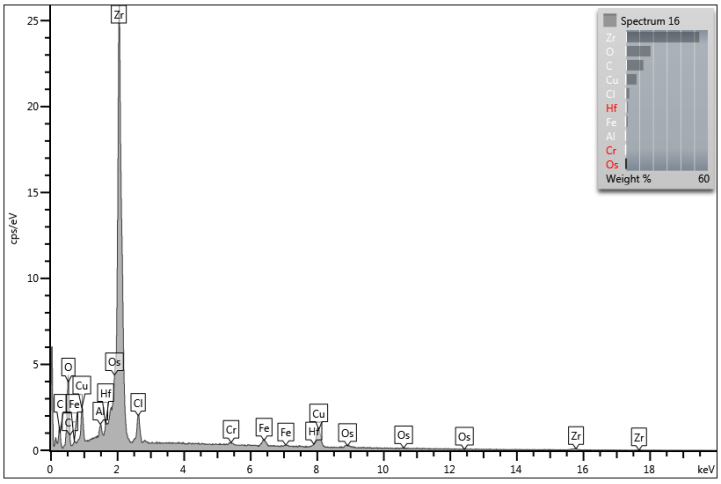
Spectrum 16
Zr
O
C
Cu
Cl
Hf
Fe
Al
Cr
Os
Weight %
60
cps/eV
keV

(c)

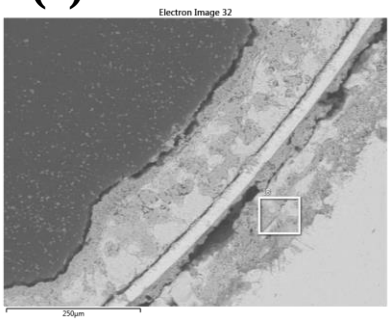
Electron Image 32
250µm

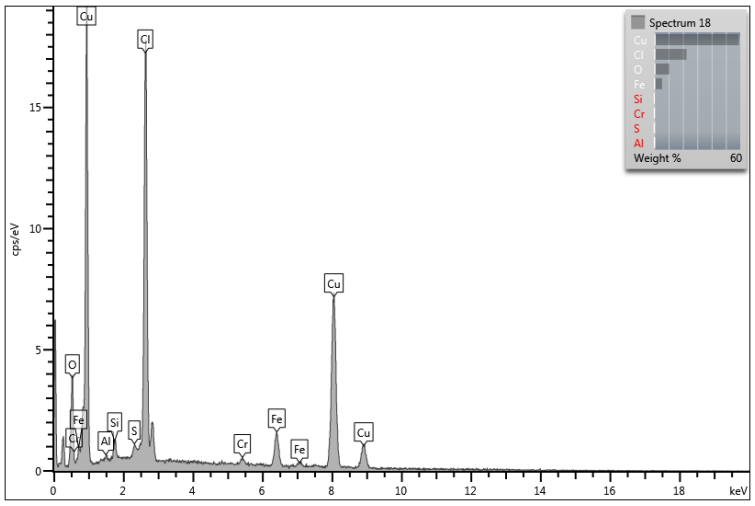
Spectrum 18
Cu
Cl
O
Fe
Si
Cr
S
Al
Weight %
60
cps/eV
keV

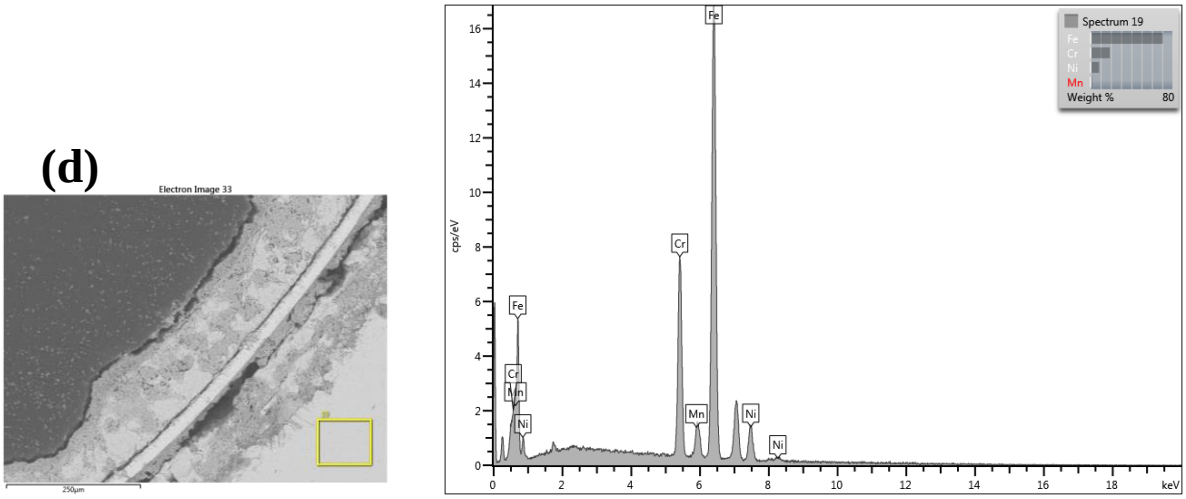

Fig. 4.18 Elemental analysis of a portion of the sample (a) presence of copper and chlorine deposits (b) remnants of the YSZ deposit (c) presence of copper and chlorine deposits (d) portion of the substrate indicated by the presence of iron.

Figure 4.19 indicates the discontinuity in the YSZ layer. The YSZ layer was unable to adhere to the substrate due to high porosity in the coatings. It was observed that the copper layer formed in this case was the weakest due to the presence of chlorine.

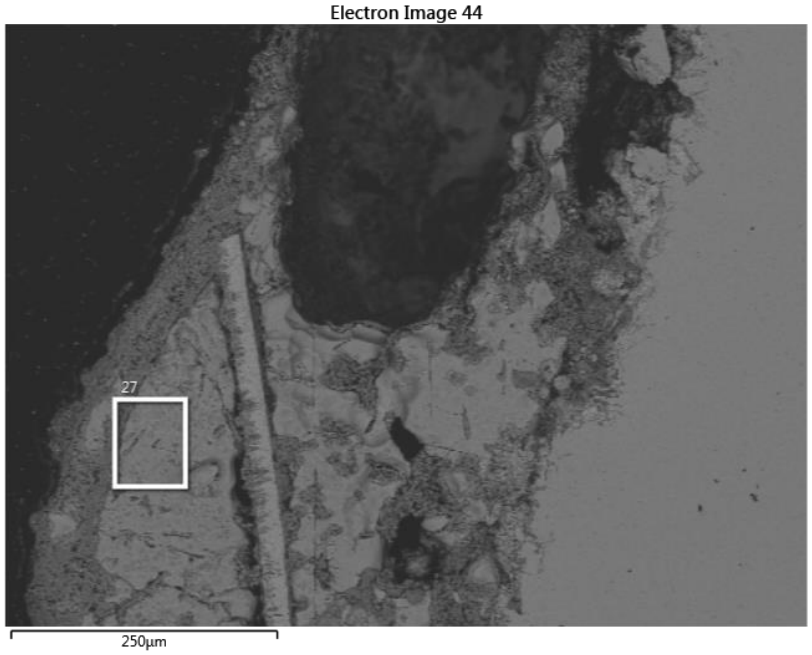

Fig. 4.19 Region of YSZ coating discontinuity

As observed from Figure 4.19, the layer of YSZ is appeared to be shielded by copper which appear to be distributed unevenly across the surface of the substrate.

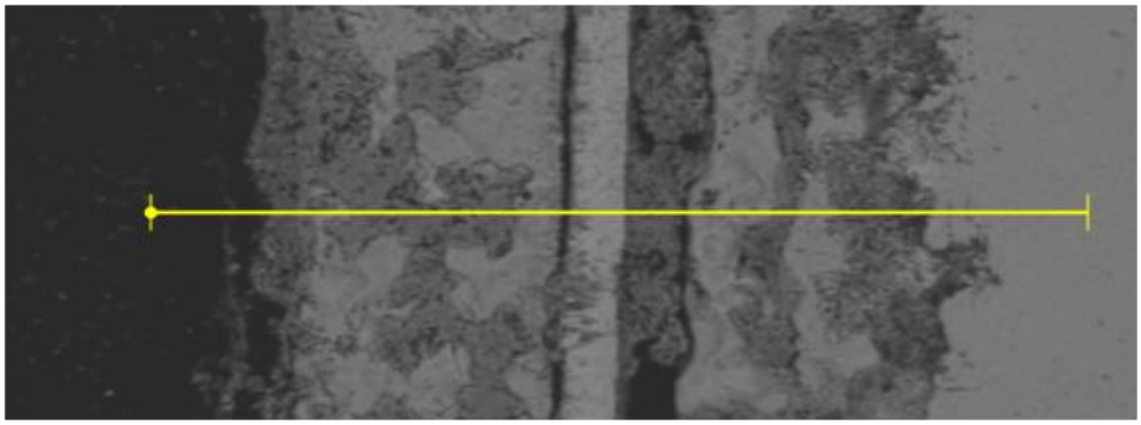

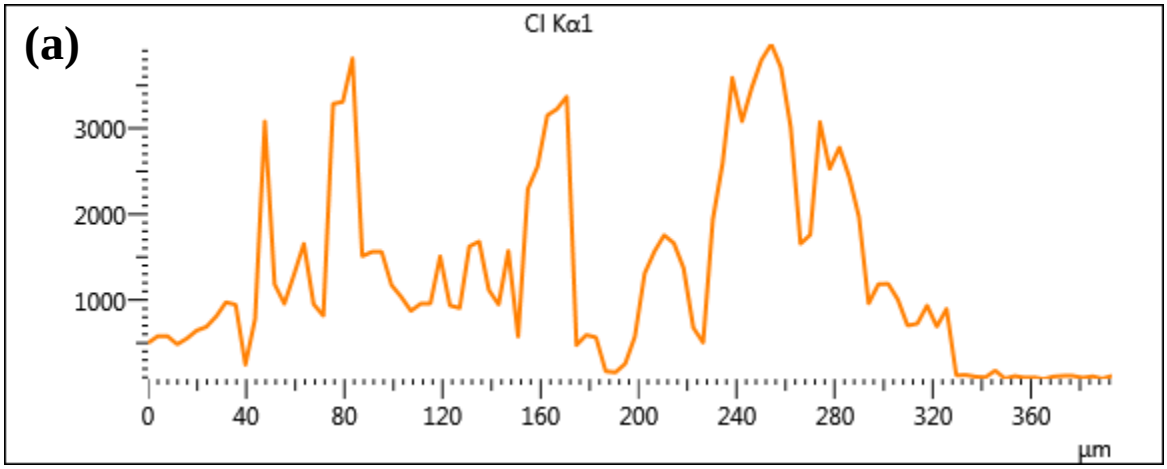
(a)
Cl Kα1
3000
2000
1000
0
40
80
120
160
200
240
280
320
360
µm

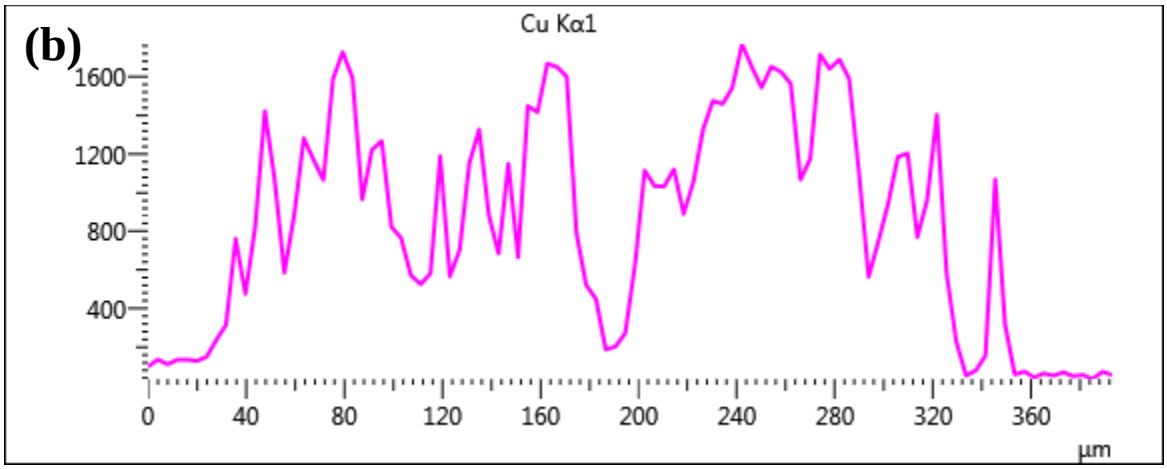
(b)
Cu Kα1
1600
1200
800
400
0
40
80
120
160
200
240
280
320
360
µm

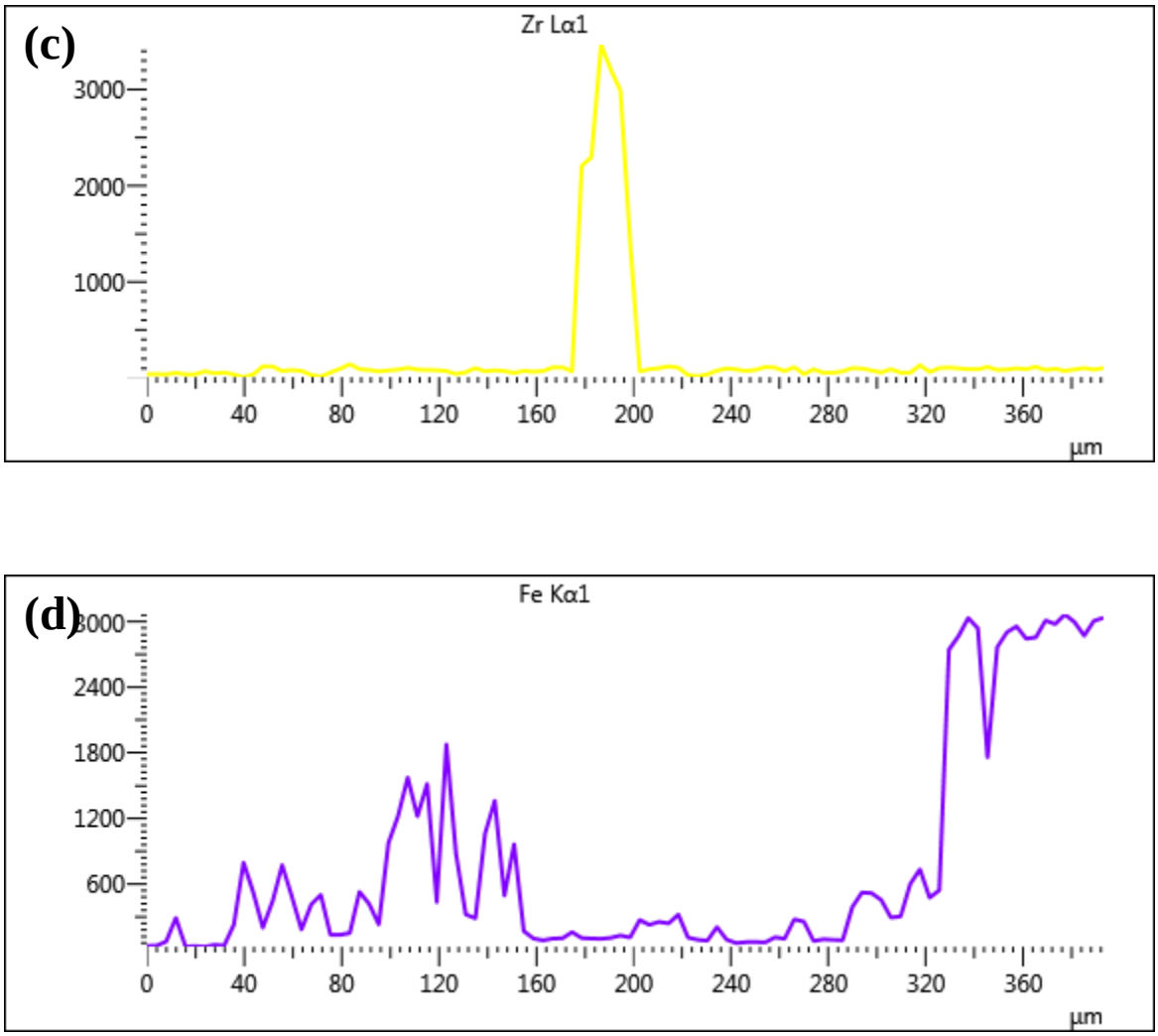

Fig. 4.20 Elemental analysis of a portion of the sample (a) traces of chlorine deposits throughout the section (b) deposits of copper across the section (c) remnant of the YSZ layer (d) portion of the substrate indicated by the presence of iron.

The images obatined from the SEM and EDX analysis indicated that the layer of copper formed along the surface began to disintegrate along some portions of the sample leading to a rigid but discontinuous layer. The layer of YSZ that was observed along few portions of the substrate appeared to be shielded by the copper layer deposition from other sections of the sample. The non-uniformity in the copper layer provided an indication that the layer was weakening thus integrating with other elements to form a non uniform coating. It was proposed to have a 50 hr test to determine the effects of time on the integrity of the coatings.

4.7 Stainless Steel sample dipped in molten Cu-Cl for 50 hours.

As the entire sample immersed in copper chloride for 20 hours was covered with layers of copper, it became imperative to test the stainless steel sample for longer durations and thus it was decided to carry out a 50 hour test in order to study the layer of copper deposits formed on the stainless steel samples and the changes that it brought about on its metallographic structure. The old gasket was replaced and the setup was sealed to ensure no leaks were present. As the duration of the experiment was scheduled to be longer, efforts were being made to reduce even the minute of leaks in the setup. Additional elastic clamps were used and were mounted around the immersion test vessel to ensure a tight seal. Thin rubber sheets were utilized to avoid any contacts of the clamps with the immersion test vessel. Additional Caulking was performed in order to avoid any minute leaks in the setup. The gas bubbles in the scrubber were noticed at flow rates as low as 100 cm^3/min.

Results showed that, as in the case of the 20 hour test, the sample was covered entirely with flakes of copper. The sample was then washed with EDTA at 80^0C and for any copper chloride remnants. It was also observed that there was no change in colour of the solution to maroon and no copper flakes were washed out from the surface. However a drastic change in diameter was observed at the tip of the sample.

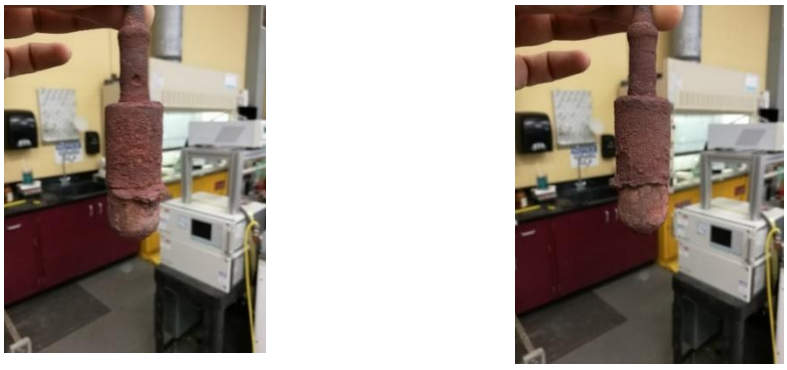

Fig. 4.21 SS sample immersed in Cu-Cl for 50 hours and cleaned with EDTA

As observed from Figure 4.21, a discontinuous surface structure of the stainless steel sample was observed after the test. Although there was definite reduction in the diameter of the sample , an increase in its weight was observed. Observance was made of the fact that an increase in weight was observed for all tests with larger durations owing to the increase in copper deposition.

The parameters of the sample before and after the immersion test are listed in Table 4.7. It was observed that the weight of the samples increased after the tests while the diameters reduced.

Table 4.7 Sample Parameters for stainless steel samples dipped in molten Cu-Cl for 50 hrs.

Weight of the sample before testing	129.25 g
Diameter of the sample before testing	19.3 mm
Weight of the sample after testing and washing with EDTA solution	135.29 g
Diamter of the sample after testing and cleaing with EDTA solution	19.25 mm

The increase in weight was attributed to the layers of copper formed on the top surface of the samples which wasn't immersed in molten Cu-Cl due to the strong Cu-Cl vapours.

The results obtained from images taken using the optical microscope showed the presence of a dense and continuous layer of copper on some portions of the sample but showed an irregular and discontinuous layer on the others. Some areas of periphery also lacked a coating of copper which gave rise to speculations about disintegration of the already formed copper.

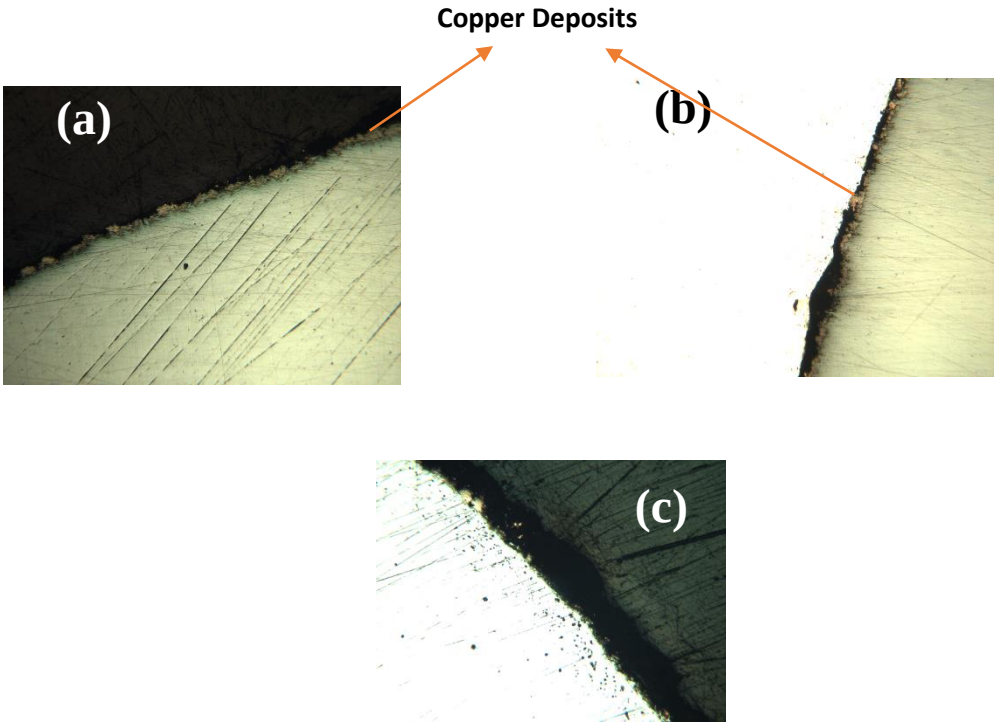

Fig. 4.22 (a) and (b) regions in the sample containing a dense and continuous layer of copper; (c) region where-in the presence of a copper layer is not observed.

An SEM and EDX analysis was performed in order to validate the results obtained from the optical microscope. The layer of copper obtained was observed for its uniformity and strength under prolonged durations

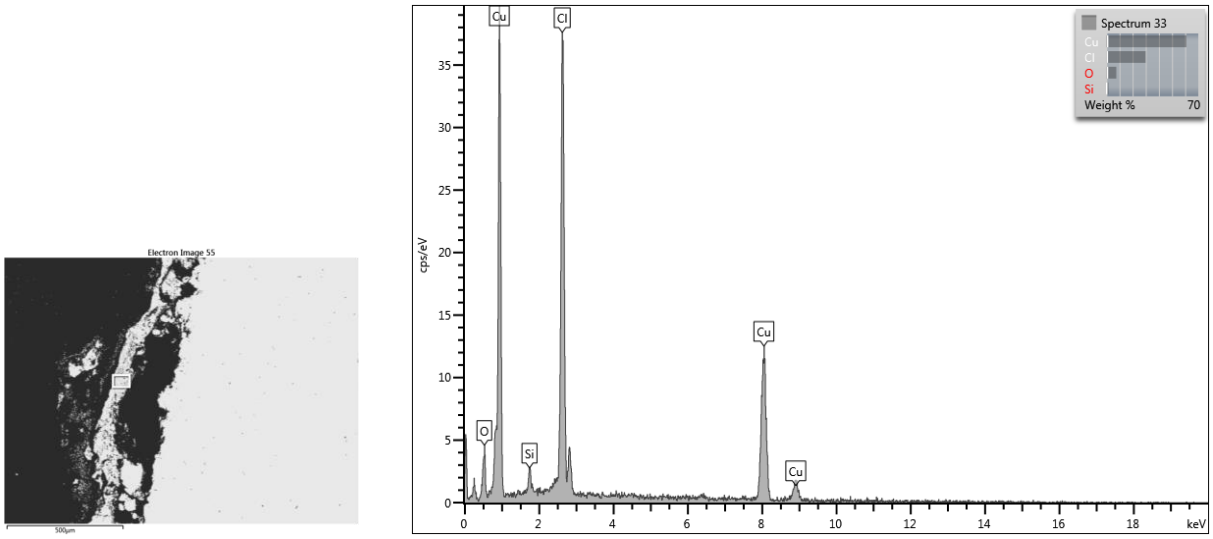

Fig. 4.23 Copper layer observed on the surface of the substrate

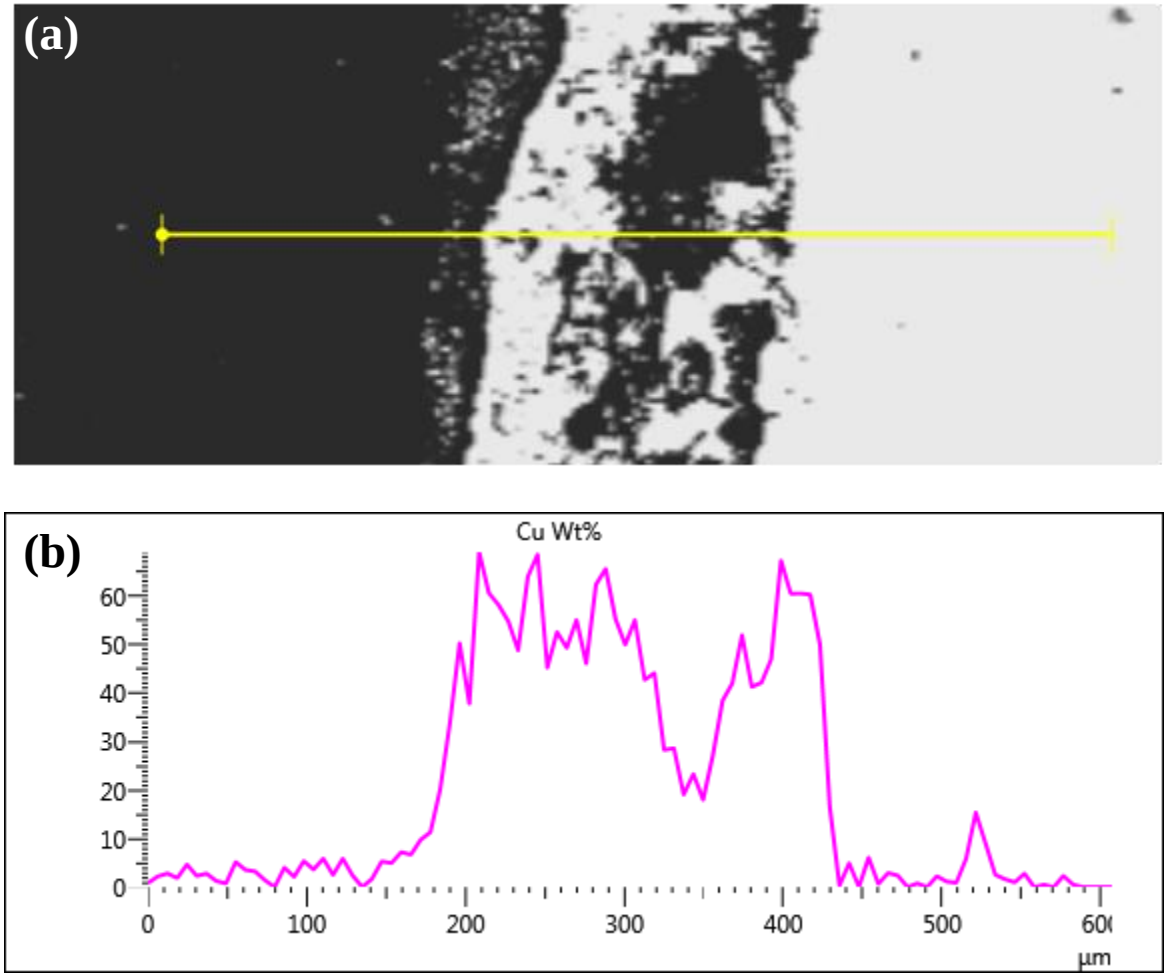

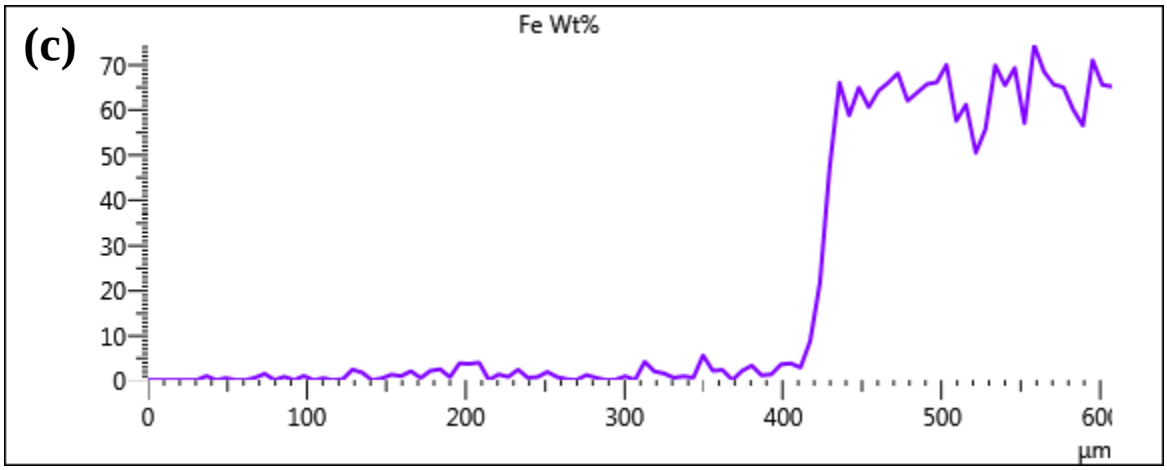

Fig. 4.24 (a) Section of the sample under consideration (b) deposits of copper across the section (c) portion of the substrate indicated by the presence of iron.

The SEM analysis of the sample indicated the presence of an open space between the copper layer and the substrate. Moreover the presence of chlorine was also observed in this case. It was thus inferred that the layer of copper obtained was weak and not sustainable. The EDX sectional analysis obtained for the sample indicated that the layer of copper obtained was non uniform along the section of the sample. The layer degraded and thus was inferred to be non-suitable as a protective coating layer.

The diamters of the stainless steel substrates subjected to the 12, 20 and 50 hour tests were measured for their variation in sizes as compared to their original size. It was observed that the diameter of the samples reduced with increase in immersion duration indicating that the substrate was undergoing corrosion . Table 4.8 depicts the reduction in the substrate diamaters.

Table 4.8 Diameters of the SS substrates after immersion test.

Sl.No	**Immersion Test Duration**	**Average Diameter (Inches)**
1	12	0.760
2	20	0.757
3	50	0.748

As the integrity of the substrate was being compromised, focus was shifted towards protective coating of the substrate, specifically sol-gel coatings.

4.8 SS sample coated with YSZ via sol-gel method and dipped in molten Cu-Cl for 15 hours

The setup was cleaned for any debris from the previous experiments and the gasket was replaced. The sample was coated via the sol-gel method and its parameters were recorded. The gas flow rate throughout the experiment was maintained at 150 cm^3/min as fairly efficient sealing was obtained. Gas bubbles were observed in the scrubber throughout the course of this experiment. The test was carried out for 15 hours.

Results showed that the sol-gel coating was unable to withstand the attack from the Cu-Cl. Blackish deposits were observed upon completion of the experiment which was washed away in the EDTA solution. The sol-gel coating throughout the sample was replaced with copper. The parameters of the sample before and after the immersion test are listed in Table 4.9.

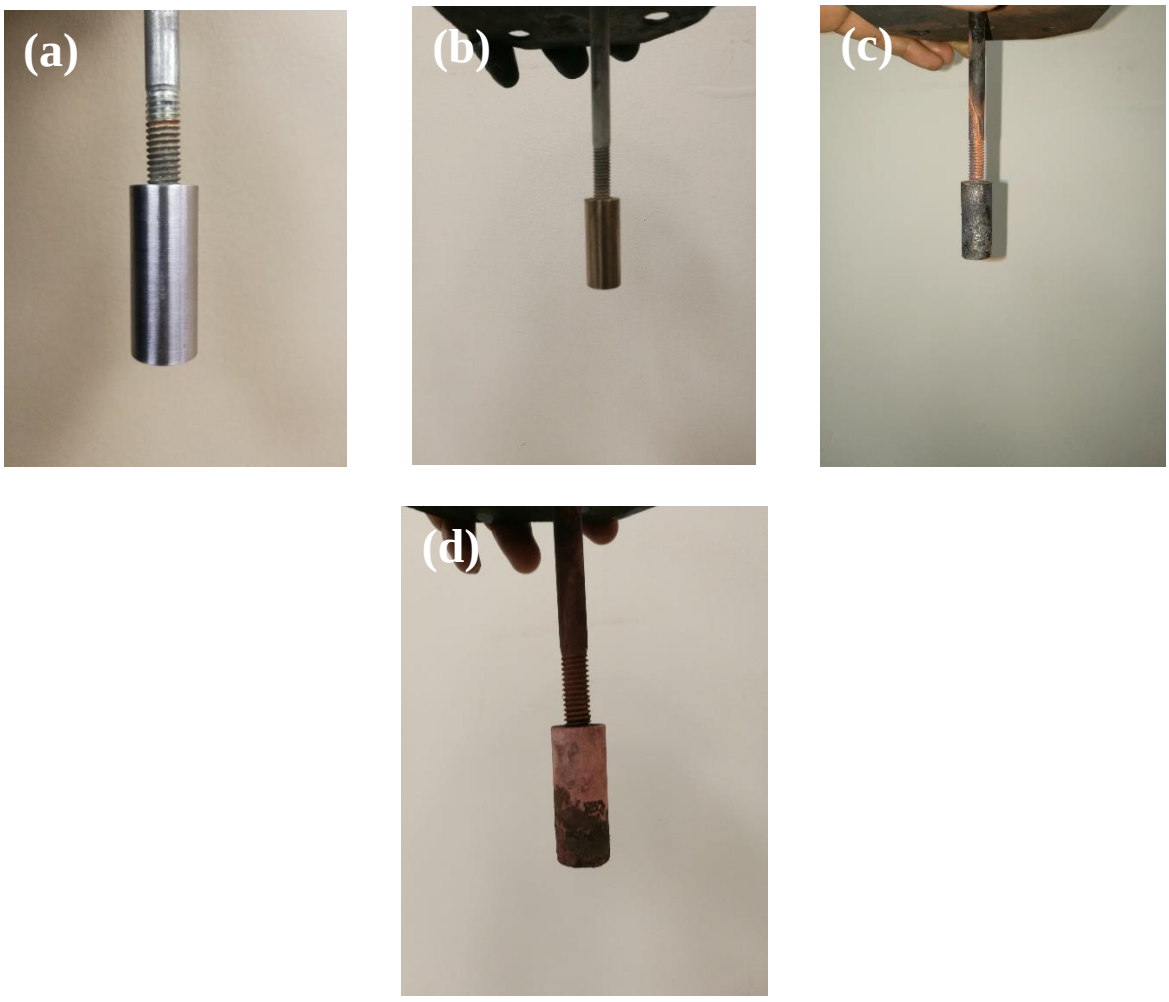

Fig. 4.25 (a) SS Sample before immersion test (b) SS sample after coating with YSZ via sol-gel method (c) SS Sample after the immersion test (d) SS sample after immersion test cleaned with EDTA solution.

Table 4.9 Sample Parameters for stainless steel samples coated with YSZ via sol-gel method and dipped in molten Cu-Cl for 15 hrs.

Weight of the sample before testing	58.11 g
Diameter of the sample before testing	15.2 mm
Weight of the sample after testing and washing with EDTA solution	57.67 g
Diamter of the sample after testing and cleaing with EDTA solution	15.4 mm

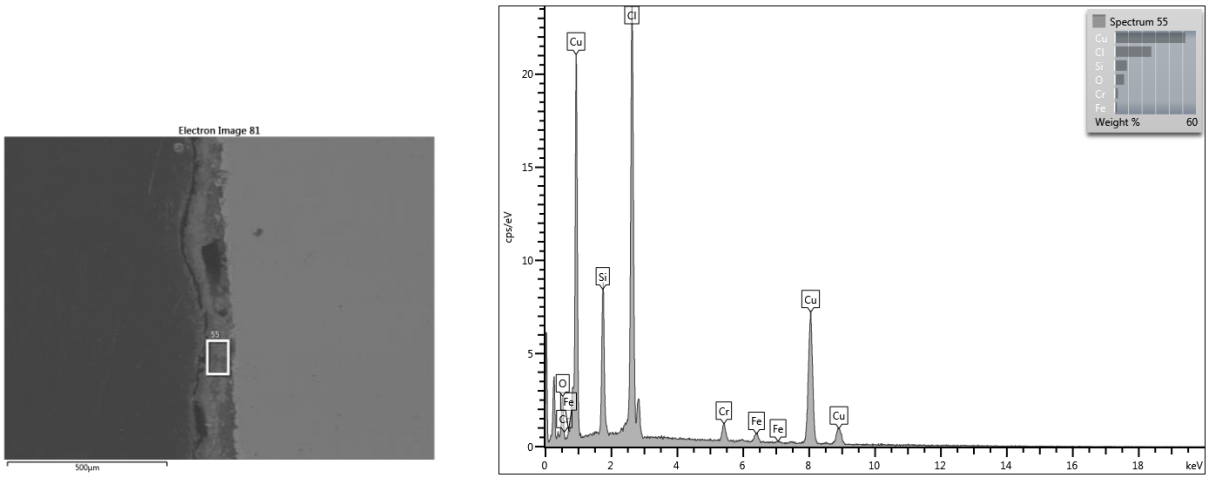

Fig. 4.26 Thick but discontinuous layer of copper observed on the surface of the substrate

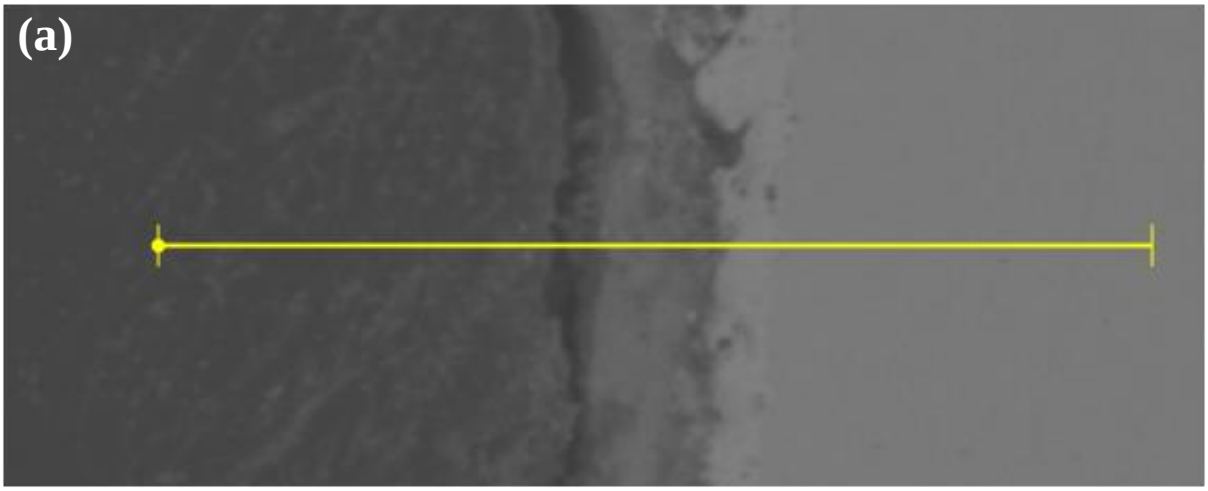

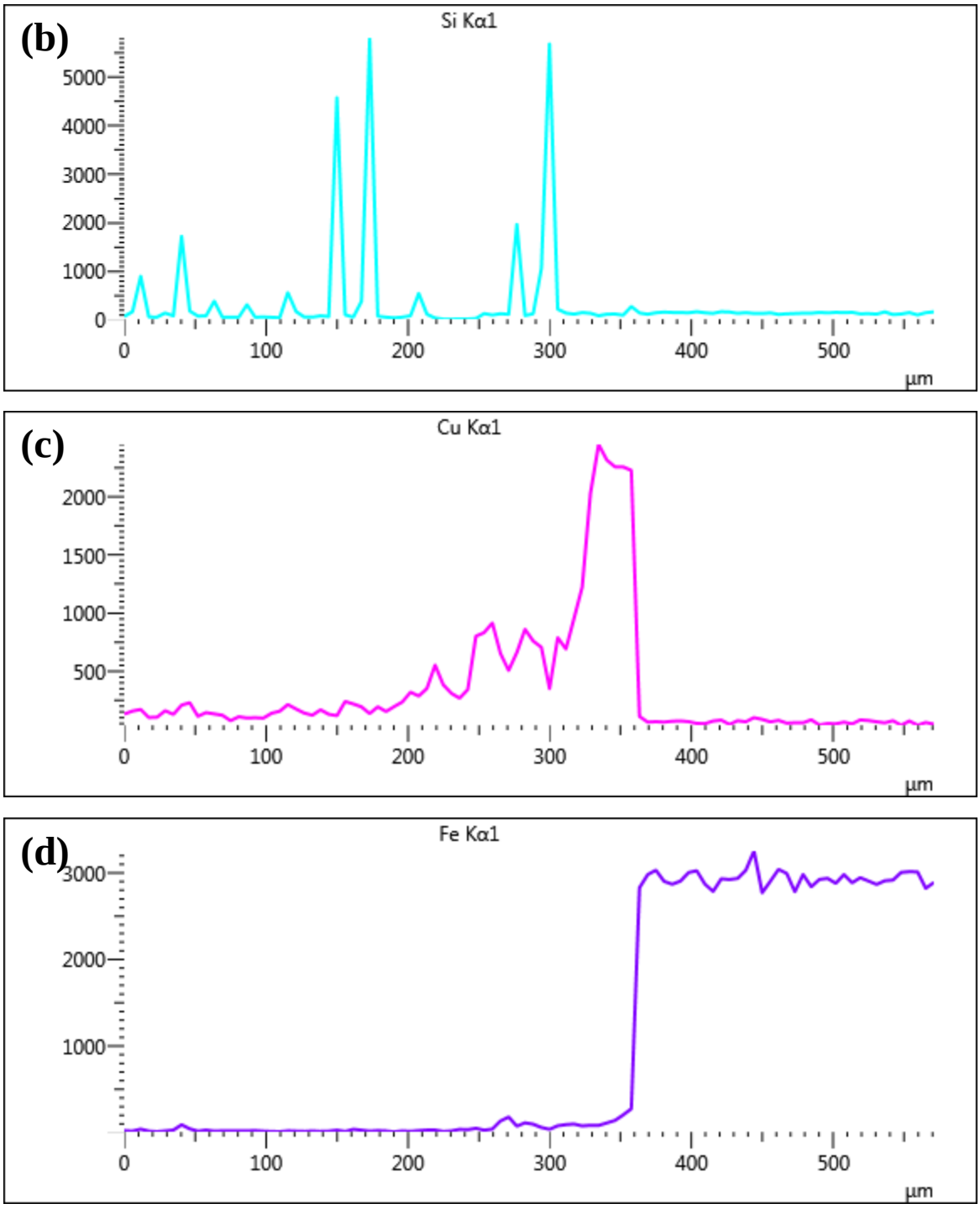

Fig. 4.27 (a) Section of the sample under consideration (b) deposits of silicon across the section (c) deposits of copper along the section (d) portion of the substrate indicated by the presence of iron .

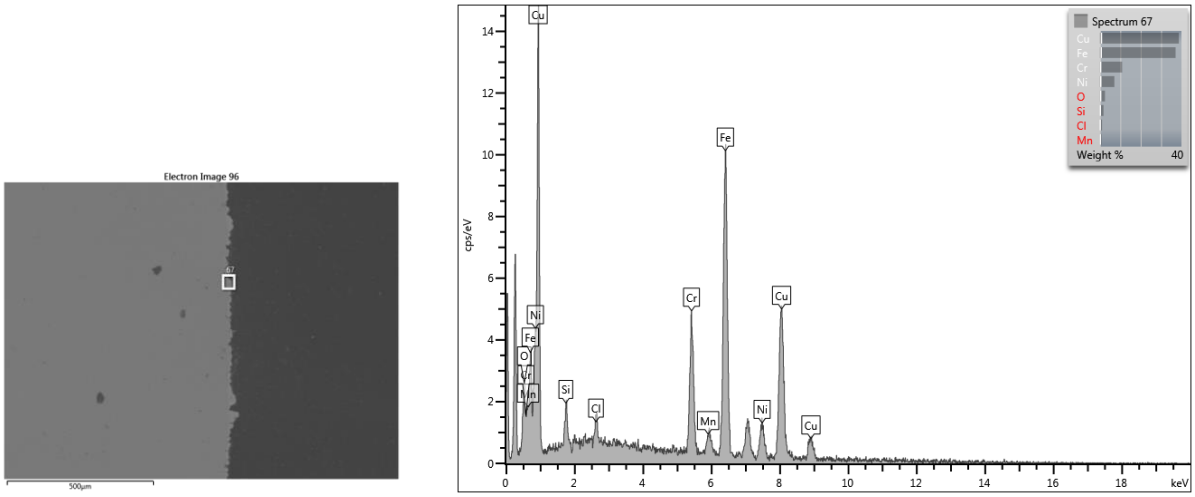

Fig. 4.28 Formation of thick and continuous deposits of copper

The EDX analysis indicated the presence of a smooth copper layer on some portions of the sample and a thick but discontinuous layer of copper on other portions. The layer was also found to be weak and embedded with air gaps. There were no traces of the YSZ coating throughout the sample periphery which indicated that the YSZ coating applied was highly porous. Traces of silicon were obtained throughout the circumference of the cross section under consideration.From the analysis it was inferred that a stronger and more dense layer of YSZ must be prepared in order to obtain corrosion resistance.

4.9 SS sample coated with Al_2O_3 via sol-gel method and dipped in molten Cu-Cl for 20 hours

The setup was prepared as necessary and all seals and gaskets were replaced. The sample was coated with alumina via the sol-gel coating method. Its parametres were recorded before mounting it in the hanging and lifting mechanism. A nitrogen gas flow rate of 150 cm^3/min was maintained during the experiment and bubbles in the scrubber were observed throughout its course ensuring an inert environment within the setup.

The results show that, as in the case of the YSZ coatings, the alumina coatings were also unable to survive the attacks of molten Cu-Cl. However, the performance of alumina coatings was found to be better than the YSZ coatings. It was observed that patches of alumina coatings remained on the surface of the samples even in areas as low as the sample tip. The regions where-in which the alumina was unable to adhere to the substrate were replaced with copper coatings.

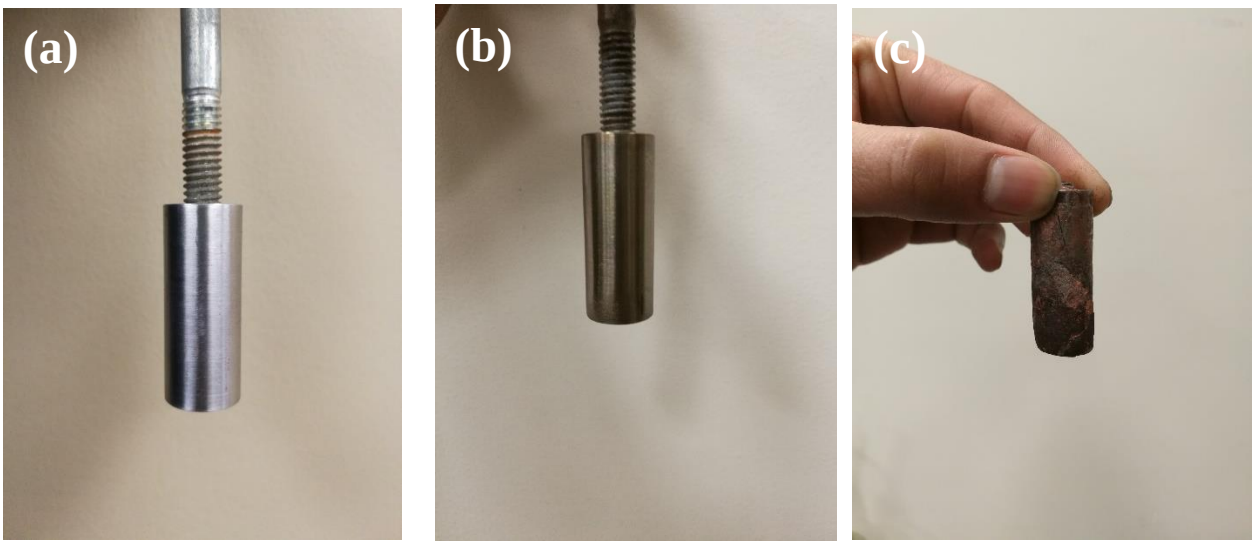

Fig. 4.29 (a) SS Sample before immersion test (b) SS sample after coating with Al_2O_3 via sol-gel method (c) SS sample after immersion test cleaned with EDTA solution.

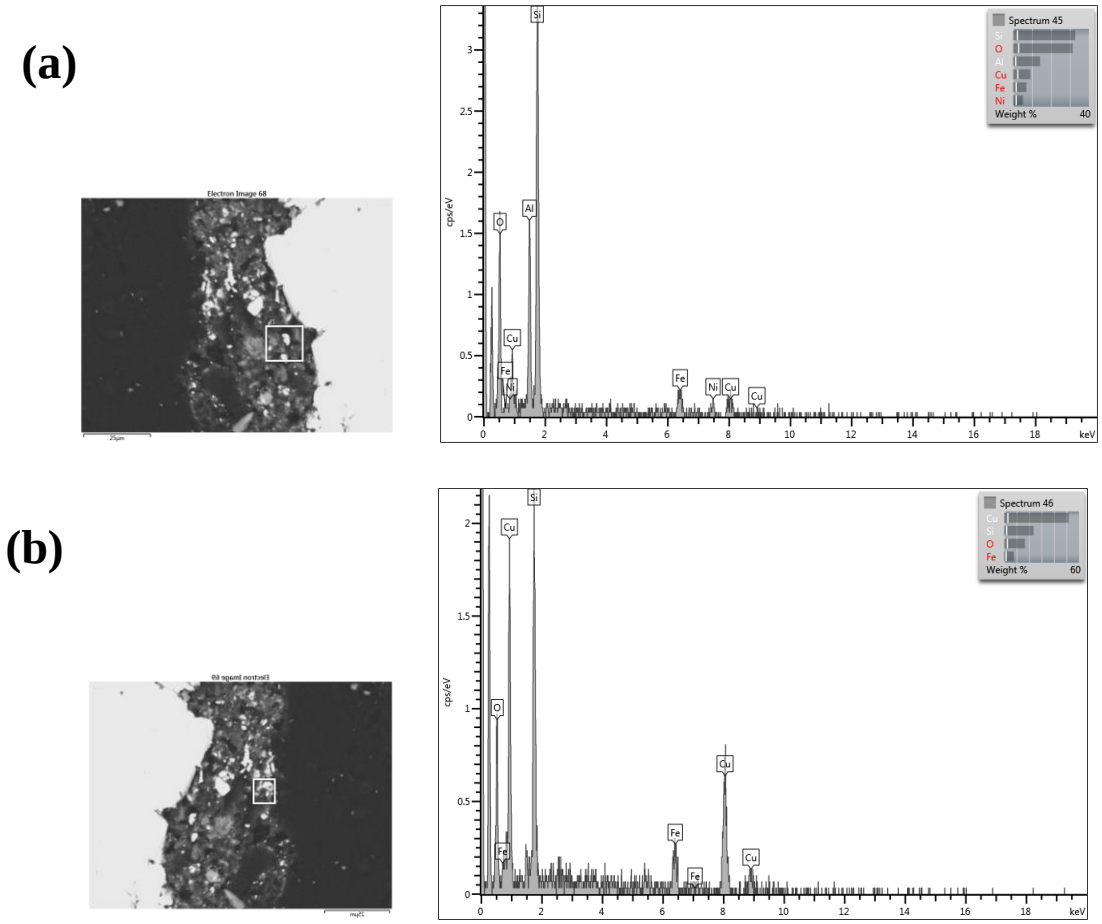

Fig. 4.30 (a) Presence of silicon across the sample periphery (b) Traces of copper deposits along the periphery

The parameters of the sample before and after the immersion test are listed in Table 4.10. As in the case with other samples it was observed that the weight increased with the duration of the samples owing to the increase in the deposition rate of copper with time

Table 4.10 Sample Parameters for stainless steel samples coated with Al_2O_3 via sol-gel method and dipped in molten Cu-Cl for 20 hrs.

Weight of the sample before testing	59.16 g
Diameter of the sample before testing	15.25 mm
Weight of the sample after testing and washing with EDTA solution	59.58 g
Diamter of the sample after testing and cleaing with EDTA solution	15 mm

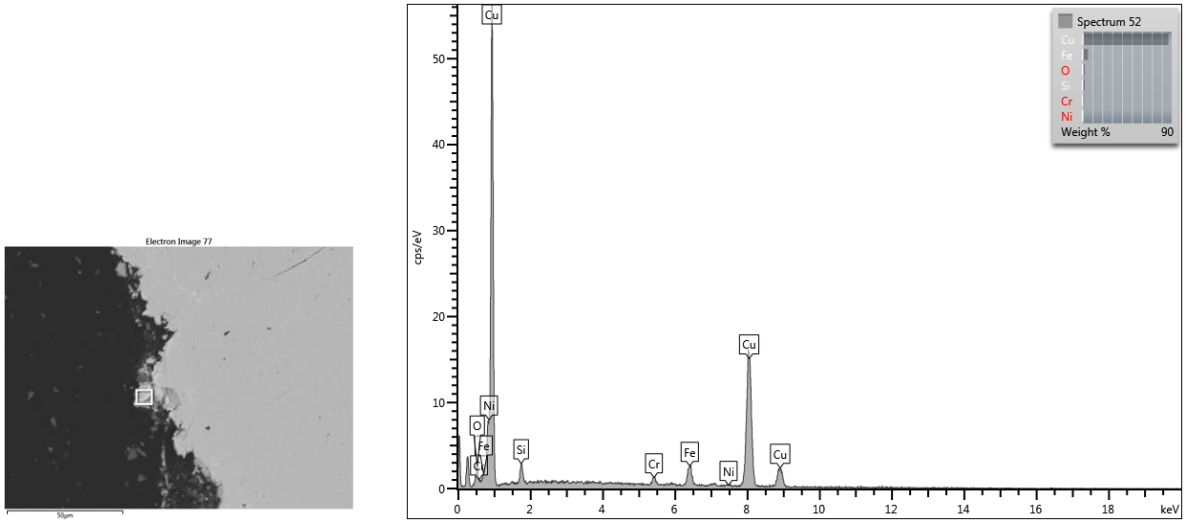

Fig. 4.31 Copper deposits across the sample periphery

The EDX results for the samples coated with alumina portrayed the presence of silicon in large portions across the sample periphery. It was observed that copper deposits were only present in traces. However some portions of the sample coatings were dominated by the presence of copper. Alumina coating was found adhered to the sample across major portions and the same was indicated by the SEM analysis. It was also observed that the protective ability of the sol-gel coatings was meagre, as the substrate was found to be disintegrated across major portions of its periphery.SEM/EDX results indicated that the alumina coatings performed better than the YSZ coatings. However, the presence of copper was detected more when the samples were coated with YSZ.

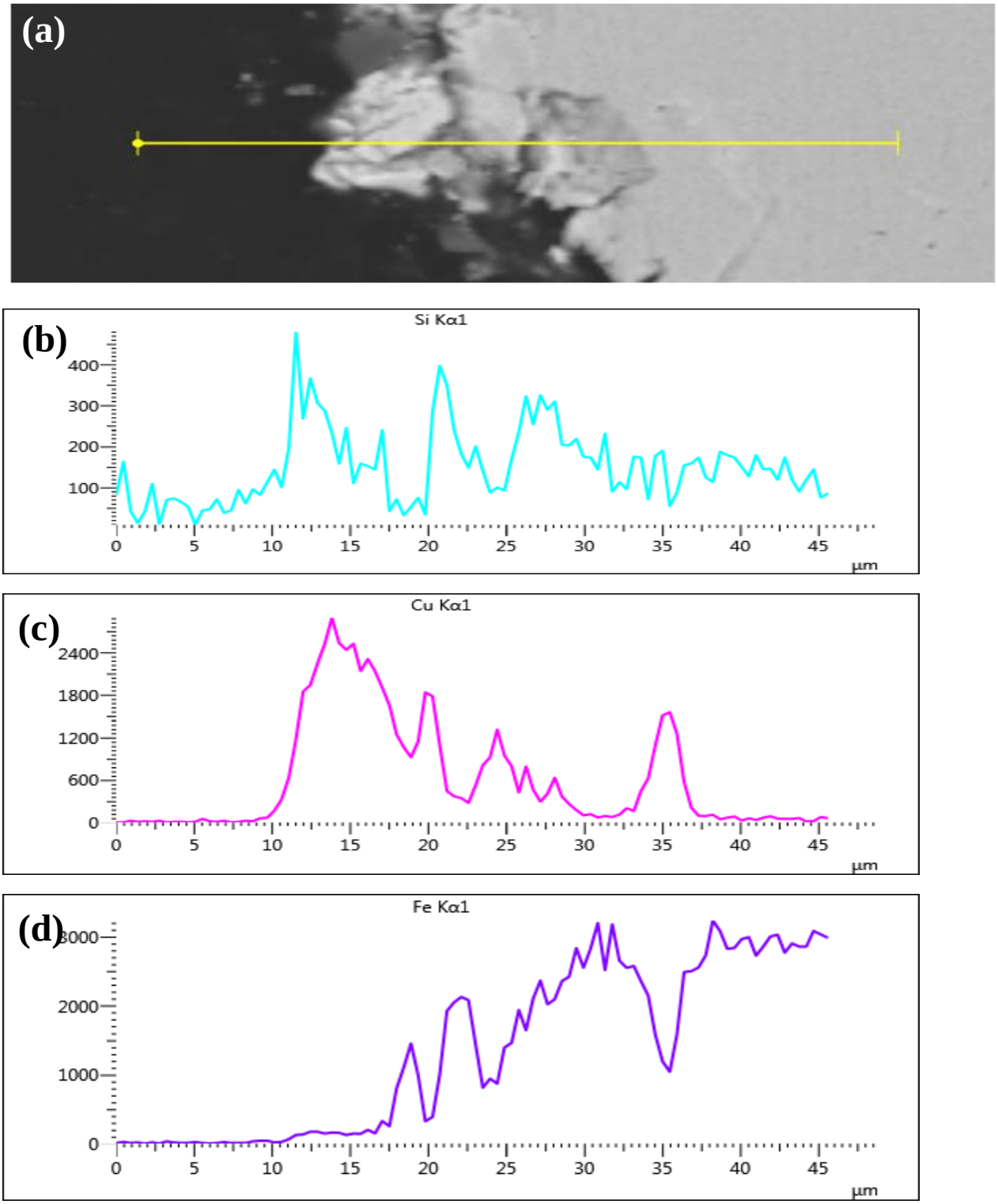

Fig. 4.32 (a) Section of the sample under consideration (b) deposits of silicon across the section (c) deposits of copper along the section (d) portion of the substrate indicated by the presence of iron.

CHAPTER 5: CONCLUSIONS AND RECOMMENDATIONS

In this chapter, the main outcomes obtained in this research have been briefly explained and summarized in a concise manner. Further, recommendations have also been presented based on the findings derived.

5.1 Conclusions

Iron reacts with copper chloride to form a layer of copper on its surface. In this research the phenomenon of copper depositing on steel is studied and the possibility of having a protective copper coating has been investigated. CS and SS samples of different shapes and sizes were tested in molten copper chloride at 500^0C. Alumina and YSZ coatings were coated on the samples via the sol-gel coating method and were tested for their ability to withstand the molten Cu-Cl environment. As previous coating methods namely HVOF, thermal spray coating, air plasma spray coating and phase vapour deposition coating had failed the molten Cu-Cl tests, the sol-gel coating method was tried as a coating option in this research.

The main findings of this thesis can be summarized as follows:

- Upon completion of all tests, CS samples were coated with a continuous but delicate layer of copper. The SS sample tested for shorter duration i.e 10 hours was found to be coated with an adherent but discontinuous layer of copper. The weight of the sample in this case had reduced drastically. The SS samples tested for longer durations were found to have a comparatively weaker and discontinuous layers of copper near its tip. These samples inherited a reduction in the cross sectional area but however increased in weight owing to the increase in copper deposition rate on the surfaces away from its tip.
- The samples coated with alumina and YSZ via the sol-gel coating method were found to lose their coatings due to the harsh attack of molten copper chloride. The coatings were replaced with copper deposits which were found to be weak and discontinuous.
- The phenomenon of copper depositing on steel was inferred to be likely due to the reaction between iron in the sample and chlorine within the solution. Iron most likely reacted with chlorine forming iron chloride thus leading to the formation of copper which was reduced on the sample surface

- The formation of a continuous and strong layer of copper on the surface of the steel substrate without the substrate being involved in the reaction which was observed earlier by Shuja (2016) was most likely due to the presence of the bond coat namely MCrAlY coating (where M indicates Ni).
- The formation of the smooth copper layer obtained in the samples tested by Shuja (2016) was probably due to reaction between nickel and chlorine. Nickle from the coatings presumably reacted with the chlorine in the solution to form nickel chloride, thus leading to the reduction of copper on the surface of steel.
- The phenomenon that iron and nickel have more electrochemical affinity towards chlorine than copper, most likely caused reduction of copper which deposited on the surface of stainless steel samples. This deposited layer of copper was found to degrade with time and hence cannot be construed as a protective layer.

5.2 Recommendations

This thesis investigates the behavior of corrosion resistant coatings in molten Cu-Cl. In order to expand the study to a wider perspective and increase the utilization opportunities, the following recommendations are listed:

- Better coating methods with porosities less than 1% should be tested in order to shield the substrate from the harsh Cu-Cl environment.
- Existing coating methods such as HVOF, APS and PVD should be improved to reduce porosity in order to obtain a uniform and dense coating.
- Alternate material options should be tested for their corrosion resistance capabilities.

REFERENCES

Acar C, Dincer I. Comparative assessment of hydrogen production methods from renewable and non-renewable sources. Int J Hydrogen Energy 2014.

Afgan, N.H., Al-Gobaisi, D., Carvalho, M.G. and Cumoc, M. "Sustainable energy development". Renewable and Sustainable Energy Reviews, Vol.2, 1998, 235-286.

Afgan, N.H. and Carvalho, M.G. "Sustainability assessment of hydrogen energy systems". International Journal of Hydrogen Energy, Vol. 29, 2004, 1327-1342.

AGA (2001). "Purging Principles and practices." American Gas Association, 3rd Edition, Washington DC, USA.

Aghahosseini, S., Dincer, I., Naterer, G.F. (2013). Process integration of hydrolysis and electrolysis processes in the Cu-Cl cycle of hydrogen production, International Journal of Hydrogen Energy.

"Alternate fuels data centre – US Department of Energy" https://www.afdc.energy.gov/fuels/hydrogen_basics.html.

Atanu Banerjee , Rakesh Kumar , Monojit Dutta , Sandip Bysakhb, Anil K. Bhowmick , Tapas Laha "Microstructural evolution in Cu–Sn coatings deposited on steel substrate and its effect on interfacial adhesion" Surface & Coatings Technology 262 (2015).

Awad AH, Veziroglu TN. Hydrogen vs. synthetic fossil fuels. Int J Hydrogen Energy 1984.

Azarbaijani K., G. Rizvi, F. Foroutan (2016a). "Evaluating effects of immersion test in molten copper chloride salts on corrosion resistant coatings." International Journal of Hydrogen Energy 41.

Azarbaijani K., G. Rizvi, F. Foroutan (2016b). "System development for evaluating performance of corrosion resistant coatings exposed to molten copper chloride salts." International Journal of Hydrogen Energy 41.

Azarbayjani K (2014). "System for Evaluating Effects of Immersion in Molten Copper Chloride Salts on Corrosion Resistant Coatings". MASc Thesis, UOIT, Oshawa, Ontario.

Baretto, L., Makihira, A., and Riahi, K. "The hydrogen economy in the 21st century: a sustainable development scenario". International Journal of Hydrogen Energy, Vol. 28, 2003.

Balashov, V., Schatz, R.S., Chalkova, E., Akinfiev, N., Fedkin, M., Lvov, S.N. (2011). Cu-Cl electrolysis for hydrogen production in the Cu–Cl thermochemical cycle, Journal of Electrochemical Society 158.

Brinker. G. J, Scherer. G. W, Sol-Gel Science: The Physics and Chemistry of Sol-Gel Processing, Academic Press, San Diego, 1990.

Callister W. D (2007). "Materials Science and Engineering: An Introduction." 7th Edition. John Wiley and Sons, New York.

Chen. Y, Wang. X. H, Li. J, Lu. J. L, Wang “Polyaniline for corrosion prevention of mild steel coupled with copper” Electrochimica Acta 52 (2007).

CNIE (2001). Hydrogen: Technology and Policy, Washington, D.C: The Committee for the National Institute for the Environment, Congressional Research Service. Report for Congress.

Conte, M., Iacobazzi, A., Ronchetti, M., Vellone, R. "Hydrogen economy for a sustainable development: state-of the-art and technological perspectives". Journal of Power Sources, Vol.100, 001.

Do Sacramento EM, De Lima LC, Oliviera CJ, Veziroglu TN. A hydrogen energy system and prospects for reducing emissions of fossil fuels pollutants in the Ceara state e Brazil. International Journal of Hydrogen Energy 2008.

De Jong W. Sustainable hydrogen production by thermochemical biomass processing. In: Gupta RB, editor. Hydrogen fuel: production, transport and storage. CRC Press; 2009.

Dincer.I, Canan Acar “A review on clean energy solutions for better sustainability “International journal of energy research Volume 39, Issue 5 April 2015.

Dincer I. Green methods for hydrogen production. Int J Hydrogen Energy 2012.

Dincer I. Potential options to greenize energy systems. Sixth International Green Energy Conference, Eskisehir, Turkey; 2011. June 5-9, Keynote Lecture

Dincer, I., and Rosen, M.A., "A worldwide perspective on energy, environment and sustainable development". International Journal of Energy Research, Vol. 22, No. 15, 1998.

Dincer, I. "Technical, environmental and exergetic aspects of hydrogen energy systems". International Journal of Hydrogen Energy, Vol. 27, 2002.

Dincer, I. and Rosen, M.A., "Thermodynamic aspects of renewable and sustainable development". Renewable and Sustainable Energy Reviews, Vol. 9, No.2, 2005.

Dragica, Lj.S., Milica P. M., Sofija, P. S., Šćepan, S. M. (2003). Hydrogen generation from water electrolysis—possibilities of energy saving, Journal of Power Sources 118.

Duhua Wang, Gordon. P. Bierwagen, “Sol–gel coatings on metals for corrosion protection”. Progress in Organic Coatings 64 (2009).

Edwards, P.P., Kuznetsov, V., David, W.I.F, Brandon, N. Hydrogen and fuel cells: towards a sustainable energy future. Mini Energy Project, Foresight; 2006.

Ferrandon M.S., M.A. Lewis, D.F. Tatterson, A. Gross, D. Doizi, L. Croize, V. Dauvois, J.L. Roujou, Y. Zanella, P. Carles (2010). “Hydrogen production by the Cu–Cl thermochemical cycle:

Hammond, G.P.," Towards sustainability: energy efficiency, thermodynamic analysis, and the ‘two cultures". Energy Policy, Vol. 32, 2004,.

Hirata T., S. Ota, T. Morimoto (2003). “Influence of impurities in Al2O3 ceramics on hot corrosion resistance against molten salt.” Journal of the European Ceramic Society 23.

Holladay JD, Hu J, King DL, Wang Y. An overview of hydrogen production technologies. Catal Today 2009.

Hopwood, B. Mellor, M. and O’Brien, G. "Sustainable development: mapping different approaches". Sustainable Development, Vol. 13, 2005.

Hui, S. C. M., "From renewable energy to sustainability: the challenge for Hong Kong". POLMET '97 Conference, Hong Kong, 1997.

Hydrogen production-thermochemical water splitting – Office of energy efficiency and renewable energy https://energy.gov/eere/fuelcells/hydrogen-production-thermochemical-water-splitting.

Investigation of the key step of hydrolysing CuCl2 to Cu2OCl2 and HCl using a spray reactor.” International Journal of Hydrogen Energy 35.

Kablan, M.M., "Energy conservation projects implementation at Jordan’s industrial sector: a total quality management approach". Energy, Vol.28 2003.

Lee H., K. Baik (2009). “Comparison of corrosion resistance between Al2O3 and YSZ coatings against high temperature LiCl-Li2O molten salt.” Metals and Materials International 15.

Levin DB, Chahine R. Challenges for renewable hydrogen production from biomass. Int J Hydrogen Energy 2010.

Lewis M.A., J.G. Masin (2009). “The evaluation of alternative thermochemical cycles – part II: the down-selection process.” International Journal of Hydrogen Energy 34.

Lodhi MAK. Hydrogen production from renewable sources of Energy. Int J Hydrogen Energy 1987

Marsal. A, Ansart. F, Turq, Bonino.J . P, Sobrino. J. M, Chen. Y. M, Garcia .J, Mechanical properties and tribological behavior of a silica or/and alumina coating prepared by sol-gel route on stainless steel, Surface & coatings Technology 237 (2013).

Masalskia. J, Gluszeka. J, Zabrzeskia. J, Nitschb. K, Gluszeka. P “Improvement in corrosion resistance of the 316l stainless steel by means of Al2O3 coatings deposited by the sol-gel method” Thin Solid Films 349 (1999).

McQuillan B.W., L.C. Brown, G.E Besenbruch, R. Tolman, T. Cramer, B.E Russ. B.A. Vermillion et al. (2002). “High efficiency generation of hydrogen fuels using solar thermochemical splitting of water.” Annual Report. GA-A24972, General Atomics, San Dieogo, CA.

Mills D.J., D. Nuttall (2013). “Eurocorr 2012: ‘Safer world through better corrosion control’ - part 2.” Corrosion Engineering, Science and Technology 48.

Midilli, A., Ay, M., Dincer, I. and Rosen, M.A. "On hydrogen and hydrogen energy strategies-I-current status and needs". Renewable and Sustainable Energy Reviews
Vol.9, No.3, 2005a.

Midilli, A., Ay, M., Dincer, I. and Rosen, M.A. (2005b). "On hydrogen and hydrogen energy strategies-II: future projections affecting global stability and unrest", Renewable and Sustainable Energy Reviews, Vol. 9, No.3, 2005.

Miltner A, Wukovitz W, Proll T, Friedl A. Renewable hydrogen production: a technical evaluation based on process simulation. J Clean Prod 2010.

Muradov NZ, Veziroglu TN. From hydrocarbon to hydrogencarbon to hydrogen economy. Int J Hydrogen Energy 2005.

Norwitz George (1954) “Deposition of copper by immersion” (Patented June 8, 1954 OFFICE DEPOSITION OF COPPER BY IMMERSION George Norwitz, Philadelphia, Pa.).

Ozbilen, A., Dincer, I., Rosen, M.A. (2016). Development of a four –step Cu-Cl cycle for hydrogen production-Part I: Exergoeconomic and exergoenvironmental analyses, International Journal of Hydrogen Energy 41.

Omega (2016). “Portable Oxygen Monitor and Data Logger.” Omega Engineering, Laval, Quebec, Canada. http://www.omega.ca/pptst_eng/HHAQ-104.html.

Roberge P.R. (2012). “Handbook of corrosion engineering.” 2nd Edition. McGraw Hill, New York.

Shuja A (2016) “Evaluation of the effects of Molten Cu-Cl on Corrosion Resistant Coatings” MASc Thesis, UOIT, Oshawa, Ontario.

Siantar E (2012). "Study of the Effect of Molten Cu-Cl Immersion Test on Alloys with High Ni-Content with and without Surface Coatings". MASc Thesis, UOIT, Oshawa, Ontario.

Spath P.L. and M.K. Mann. (2001) Life cycle assessment of hydrogen production via natural gas steam reforming. National Renewable Energy Laboratory, Report No NREL/TP-570-27637. U.S. Department of Energy Laboratory.

Srinivasan. K. N, Shamugam. N. V, Selvam. M and John. S “immersion copper coating of steel” Central Electrochemical Research Institute, (1987).

Szklarska-SÂmiaowska. Z, Pitting Corrosion of Metals, National Association of Corrosion Engineers, Houston, TX, 1986.

Veziroglu TN. A fresh look at energy systems and hydrogen energy. International Journal of Hydrogen Energy 1994

Viazzi.C J.P. Bonino, F. Ansart “Synthesis by sol-gel route and characterization of Yttria Stabilized Zirconia coatings for thermal barrier applications” Surface & Coatings Technology 201 (2006).

Winter C-J. Hydrogen energy e abundant, efficient, clean:a debate over the energy-system-of-change. International Journal of Hydrogen Energy 2009

Zamfirescu C, Naterer GF, Dincer I. Progress of international consortium on nuclear hydrogen production with the Cu-Cl cycle. Progress of Cryogenics and Isotopes Separation 2011.

Zhong X.H., Y.M. Wang, Z.H. Xu, Y.F. Zhang, J.F. Zhang, X.Q. Cao (2010). "Hot-corrosion behaviors of overlay-clad yttria-stabilized zirconia coatings in contact with vanadate–sulfate salts." Journal of the European Ceramic Society 30.